

Alma Mater Studiorum – Università di Bologna

**DOTTORATO DI RICERCA IN
SCIENZE DELLA TERRA**

Ciclo XXV

Settore Concorsuale di afferenza: 04/A2

Settore Scientifico disciplinare: GEO/02

**LATE QUATERNARY GEOLOGICAL EVOLUTION OF THE
MONTENEGRO AND NORTHERN ALBANIA CONTINENTAL
MARGINS**

Presentata da: Fabrizio Del Bianco

Coordinatore Dottorato
Prof. Vincenzo Picotti

Relatore
Luca Gasperini

Correlatori
Mariangela Ravaioli
Federico Giglio
Giovanni Bortoluzzi

Esame finale anno 2014

INDEX

ABSTRACT	5
RIASSUNTO	7
PREFACE	9
CHAPTER 1 - Introduction	13
1.1 The Montenegro and Northern Albania continental margins in the Mediterranean Sea.....	14
1.2 Late Quaternary sea level changes, the last glacial-interglacial transition and its stratigraphic signature in the Adriatic Sea.....	17
1.3 Physiography of continental margins	20
<i>References</i>	23
CHAPTER 2 - The study area	27
2.1 Morphology and oceanographic setting of the Adriatic Sea	28
2.2 Geodynamic and structural setting of Montenegro and Northern Albania continental margins.....	30
<i>References</i>	36
CHAPTER 3 - Morphology, present-day sediment dispersal system, and Late Quaternary depositional sequences along the Montenegro/N. Albania continental margin	39
3.1 Introduction to scientific papers	40
3.2 Seafloor morphologies of the Montenegro / Northern Albania continental margin.....	43
Figures with caption	59
<i>References</i>	69
3.3 Stratigraphic architecture of the Montenegro / Northern Albania continental margin	73
Figures with caption	90
<i>References</i>	101
3.4 Present-day sedimentation patterns along the Montenegro / N. Albania continental margin.....	109
Figures with caption	116
<i>References</i>	121
CHAPTER 4 – Discussion and conclusions	125
4.1 Discussion	126
4.2 Conclusions.....	131
<i>References</i>	135
APPENDIX	137
A.1 Abstract published on CIESM	138
A.2 Some concepts about physics of sound in water media	141
A.3 Multibeam bathymetry	144
A.4 The “Chirp” sub-bottom profiler	147
<i>References</i>	149

ABSTRACT

The object of this work has been the analysis of natural processes controlling the geological evolution of the Montenegro and Northern Albania Continental Margin (MACM) during the Late Quaternary. These include the modern sediment dispersal system and oceanographic regime, the building and shaping of the shelf margin at the scale of 100 kyr and relative to the most recent transition between glacial and interglacial periods.

A preliminary bibliographic research on these subjects has revealed the scarcity of marine geological/geophysical data in this sector of the Mediterranean, in contrast with the large amount of recent scientific works carried out on the western counterpart of the Adriatic Sea, e.g., the Italian coasts. Subsequently, acquisition and processing of data collected during several oceanographic cruises led us to obtain a high-resolution morphobathymetric map of the margin, which allowed us to carry out a morphological analysis of the region and to identify different physiographic domains. The presence of peculiar morphologies was suggestive of recent changes in the paleo-oceanographic condition, compared to the present-day regime. The following step was the combined interpretation of multibeam and high-resolution seismic reflection data to describe the MACM shelf-slope system. We observed that it is formed by a suite of physiographic elements, including: (1) an inner and an outer continental shelf of variable length, separated by two tectonically-controlled morphological highs (the *Bar* and *Kotor* ridges); (2) a lobated drowned mid-shelf paleodelta, formed during the last sea level fall and low stand; (3) an upper continental slope, affected by gravity-driven instability and a system of extensional faults with surficial displacement, featuring an orientation coherent with the regional tectonics.

At this stage, an acoustic characterization of the seafloor, ground-truthed by the analysis of seafloor sediments sampled at several stations, was attempted. It was then possible to subdivide the MACM seafloor types into four classes (low, medium, medium-to-high and high reflectivity areas), based on reflectivity, grain-size analysis of seafloor sediments and characterization of the acoustic facies. We observed that accumulation of low reflectivity deposit is limited to two sectors in the inner shelf and the upper slope, while the remaining areas, lacking of fine-grained sediments, show high reflectivity, suggesting that they are presently site of non-deposition/erosion. This preliminary phase was necessary due to the large amount of marine geophysical data collected within the ADRICOSM-STAR project, and the wide extent of the study-area, that called for identification of representative sectors where focusing our analysis.

The stratigraphic study of the shelf-slope system benefitted from the availability of high-resolution seismic reflection profiles, AMS ^{14}C datings, $^{210}\text{Pb}/^{210}\text{Po}$ curves, and the study macrofossils

associations sampled at key gravity core stations. In this way, we observed a clear correspondence between the Late Pleistocene/Holocene mud-wedge and the low reflectivity sectors of the inner shelf, which represent the most important depositional areas during the present-day sea level highstand phase. Conversely, most of the outer shelf and part of the continental slope expose deposits from the last sea level low stand (*Lowstand Systems Tract*), featuring a general condition of lack in sedimentation or the presence of localized thin post glacial sediment cover.

In term of vertical movements, the MACM shows uplift in correspondence of the *Kotor* and *Bar* ridges, and subsidence in the outer shelf and upper slope sectors, as suggested by the analysis of the LGM paleoshoreline. In fact, seaward of these uplifting tectonic ridges, we observed a continuous stacking of stratigraphic sequences controlled by sea level fluctuations. Four sequences, interpreted as forced regression deposits, were identify, corresponding to the last four main glacial maxima, starting from Marine Isotopic Stage (MIS) 10. In this way, the MACM records the 100 kyr scale sea level fluctuations on its seismo-stratigraphic architecture over the last 350 kyr. Over such time range, encompassing MIS 10.2, 8.2, 6.2, 2.2, we estimated an average subsidence rate of about 1.2 mm/yr.

Finally, a preliminary analysis of geochemical proxy (C, N, $\delta^{13}\text{C}$) confirmed the sediment distribution inferred on the basis of geophysical and sedimentological analysis, and suggest that the particles input from Buna/Bojana River are displaced towards SE-NW along the Montenegro coasts by longshore currents.

RIASSUNTO

L'obiettivo di questo lavoro è stato quello di analizzare i processi naturali che hanno controllato l'evoluzione del Margine Continentale del Montenegro e dell'Albania Settentrionale (MACM) durante il tardo Quaternario. Tali processi includono il sistema attuale di dispersione del sedimento ed il regime oceanografico, la formazione ed il modellamento del margine alla scala dei 100 ka e relativamente all'ultimo periodo di transizione dal glaciale all'interglaciale.

Inizialmente il lavoro ha previsto una fase conoscitiva della zona attraverso la ricerca bibliografica dello scarso materiale scientifico disponibile e pubblicato. Successivamente, dopo una prima fase di acquisizione, *processing* ed unione dei dati delle diverse campagne oceanografiche, sono state prodotte le mappe batimetriche ad alta risoluzione alla scala dell'intero margine per poter effettuare un'analisi morfologica mirata all'individuazione dei differenti domini fisiografici. Successivamente, l'interpretazione combinata dei dati *multibeam* e di quelli di sismica a riflessione ad alta risoluzione ha permesso di osservare che il MACM è un sistema piattaforma-scarpata caratterizzato da: (1) una piattaforma interna ed una esterna a larghezza variabile dove sono presenti due alti morfologici a controllo tettonico, i *ridges* di Bar e di Kotor; (2) un delta trilobato relitto attribuito all'ultima fase di caduta del livello marino e (3) una scarpata continentale superiore affetta da processi gravitativi superficiali e da sistemi di faglie estensionali a rigetto superficiale che mostrano un'orientazione coerente con la tettonica regionale.

La seconda fase del lavoro è stata finalizzata alla caratterizzazione acustica del fondale marino, calibrata con le analisi granulometriche dei sedimenti superficiali. Questa caratterizzazione ha permesso di suddividere il MACM in quattro principali classi acustiche (*low, medium, medium to high and high reflectivity areas*) evidenziando la variabilità nella distribuzione dei depositi superficiali, e mostrando la presenza di depositi a bassa riflettività confinati in due bacini lungo la piattaforma interna ed in parte della scarpata superiore. Le altre zone, prive di sedimenti fini, appaiono altamente riflettenti e suggeriscono la presenza di processi di erosione o di non deposizione. Data l'enorme mole di dati geofisici marini acquisiti grazie al progetto ADRICOSM-STAR, questa seconda fase è stata fondamentale perché ha permesso di individuare le zone di indagine dove successivamente sono state analizzate le geometrie interne dei corpi sedimentari superficiali.

In questa terza ed ultima fase del lavoro di dottorato, avvalendosi dei dati di sismica a riflessione, delle datazioni del radiocarbonio, delle analisi del $^{210}\text{Pb}/^{210}\text{Po}$ e dello studio delle associazioni dei macrofossili, è stato osservato che il cuneo fangoso tardo Pleistocenico-Olocenico corrisponde alle zone a bassa riflettività individuate sulla piattaforma interna e che risulta delimitato verso mare da alti strutturali. La piattaforma esterna e parte della scarpata continentale mostrano

sedimenti più antichi attribuibili alla fase dell'ultimo stazionamento basso del livello marino (ultimo *Lowstand Systems Tract* - LST), risultando generalmente prive di sedimentazione attuale o localmente ricoperte da sottili strati di sedimenti postglaciali. In corrispondenza dei *ridges* di Kotor e Bar, a controllo tettonico, il margine mostra un comportamento di stazionarietà verticale o di sollevamento localizzato, come suggerito dall'analisi geomorfologica effettuata sull'attuale profondità della paleo-linea di costa riferita all'ultimo massimo glaciale, che attraversa il *ridge* di Bar. All'esterno di questi *ridges* tettonici, entro le profondità osservate attraverso i profili *sparker*, si nota la presenza di una sovrapposizione continua di sequenze stratigrafiche controllate principalmente dalle variazioni del livello marino. Infatti, sono state identificate quattro sequenze attribuibili a depositi di regressione forzata formati durante le ultime quattro principali glaciazioni, a partire dallo stadio marino isotopico 10 (MIS 10). Il MACM registra quindi le variazioni del livello marino alla scala dei 100 ka nella sua architettura stratigrafica, durante gli ultimi ~350 ka. In questo intervallo temporale, attraverso l'individuazione della profondità delle paleo-linee di costa attribuibili al picco delle ultime 4 glaciazioni (MIS 10.2, 8.2, 6.2, 2.2) è stata effettuata una stima approssimativa del tasso di subsidenza secondo un modello di regressione lineare semplice che mostra valori di circa 1,2 mm/a.

Ulteriori studi basati su un approccio geochimico (C, N, $\delta^{13}\text{C}$) confermano la distribuzione sedimentaria osservata nei depositi di piattaforma interna e suggeriscono che gli apporti del fiume Buna/Bojana vengano dispersi in direzione SE-NO lungo la costa del Montenegro in accordo con l'andamento dell'attuale regime oceanografico.

PREFACE

The continental margins of the Mediterranean Sea have been the subject of intensive studies during the last decades, following the developments of geological and geophysical techniques applied to the marine environment. In such studies, the combined analysis of high-resolution morphobathymetric data, seismic reflection profiles and sediment samples has proved to be very effective to unraveling the complex interplay between sea level changes, sediment supply, and accommodation driven by tectonic processes. In the Adriatic Sea case, although the western shelf was extensively investigated by marine geological and oceanographic cruises, its eastern side, and in particular the southeastern sector, remains poorly covered by high-quality marine geological data. The Montenegro/Northern Albania Continental Margin (MACM) is part of this sector, and do not constitutes an exception, because the knowledge of its morphology, stratigraphy and tectonic processes is still very limited. A recent acquisition of marine geological/geophysical and biogeochemical data partially fills this gap. In fact, from 2008 to 2010 several oceanographic cruises, organized by the Italian National Research Council (CNR) – Institute of Marine Science (ISMAR) Section of Marine Geology in Bologna onboard of CNR research vessels, investigated the MACM. The analysis of this set of data constitutes the subject of the present PhD thesis.

The geological analysis of the MACM started with the collection of the few literature available for the study area. It appeared that most of the available work is based on unpublished multichannel seismic lines, collected for industrial purpose and not available to the wider audience, if we exclude few sections and line drawings used to describe the deep-seated geological structures. Typical marine geological studies are lacking in this area, including analyses of geological processes that led to the reconstruction of the present-day oceanographic setting and sediment dispersal as well as the Late Pleistocene/Holocene stratigraphic architecture. Thus, we decided to follow a multidisciplinary approach that included the analysis of multibeam-based morphobathymetric maps, seismic reflection profiles at different degrees of penetration, and sediment samples to address the reconstruction of the recent geological evolution of the margin.

The first part of the work during this PhD thesis was focused on the acquisition and processing of bathymetric and seismic reflection high-resolution data, and included participation to five oceanographic cruises aboard R/V Mariagrazia (MNG02, 2009) and R/V Urania (ADR02, 2008; MNG01, 2009; MNG03, 2010 and MNG04, 2010), both part of the CNR research facilities. Geophysical data collected during those expeditions, i.e. multibeam swath bathymetry and seismic reflection profiles, were used to study the physiography of the margin, and the distribution of Late Quaternary sediments, as well as the geometries of depositional basins as result of several geological

processes. These data were integrated with the analysis of bottom and sub-bottom sediments carried out through box- and gravity-corer, collected in different sectors of the MACM. After collection of magnetic susceptibility, logs and x-ray imaging, the cores were described and sub-sampled for porosity, grain size, and ^{14}C - ^{210}Pb radiometric analyses.

The dataset used in this work constitutes the first example of this type in the area, and was collected in the frame of the ADRICOSM-STAR Project (ADRIatic sea integrated CoaStal and river basin Management system: Montenegro coaStal ARea and Bojana River catchment) with the financial support of the Italian Ministry for the Environment, Land and Sea and coordinated by *Istituto Nazionale di Geofisica e Vulcanologia* (INGV) and *Centro Euro-Mediterraneo sui Cambiamenti Climatici* (CMCC). In this project, ISMAR provided geological-geophysical and biogeochemical data in support of sustainable coastal management and sedimentary dynamics/physical oceanography modeling. In addition, by reconstructing the Late Quaternary to present-day sediment distribution along the margin, it was possible to obtain an independent evidence to test and validate model results by the other project's partner.

This PhD thesis is based on a series of scientific papers (2 already submitted and 1 in preparation), which address specific aspects of the recent geological evolution of the MACM, such as the morphology, evidenced by multibeam data collected on the shelf and upper slope, the Late Quaternary stratigraphy, as well as an analysis of the present-day sediment dispersal system based on geochemical tracers. These interrelated subjects are discussed in the frame of the geodynamic setting of the study area and within a specific chapter ("Discussion and Conclusions"), which highlights the main findings of the analytical work.

In more detail, this work is organized according to the following sequence:

- (i) a first chapter (CHAPTER 1 – Introduction), aimed to introduce the scientific rationale of the work;
- (ii) a second chapter (CHAPTER 2 – The study area), in which an analysis of the geology of the study area is presented; this chapter includes information about geodynamic/structural setting and oceanography available on literature;
- (iii) a third chapter (CHAPTER 3 - Morphology, present-day sediment dispersal system, and Late Quaternary depositional sequences along the Montenegro/N. Albania Continental Margin) including two scientific papers already submitted to international journals, and one in preparation: 1)- "Seafloor morphologies along the Montenegro/N. Albania Continental Margin (Adriatic Sea - Central Mediterranean)" submitted to the *Geomorphology*, which

- encompasses all aspects of the large-scale morphologies and shapes along the bottom analyzed; 2)- "Stratigraphic architecture of the Montenegro/N. Albania Continental Margin (Adriatic Sea - Central Mediterranean) " submitted to *Marine Geology*, which includes stratigraphic studies carried out on the MACM; 3)- "Present-day sedimentation patterns along the Montenegro/N. Albania Continental Margin from geochemical analysis (Adriatic Sea - Central Mediterranean)", in preparation which dealing with the study of the present-day sediment dispersal system through the use of geochemical tracers;
- (iv) a fourth chapter (CHAPTER 4 – Discussion and Conclusions) integrating discussion of the various topics analyzed and their mutual connections with a final conclusions;
 - (v) a final appendix containing a conference abstract developed during the first stage of the PhD and the description of the geophysical techniques and methods used in the thesis work.

CHAPTER 1
--
INTRODUCTION

1.1 The Montenegro/Northern Albania Continental Margin in the Mediterranean Sea

The geological evolution of the continental margins reflects the interaction of natural processes at different scales. The most significant among them are type and amount of sediment inputs, relative sea level changes and oceanographic regime that redistribute sediments along different physiographic domains. Each process is controlled over different time-scales by regional tectonics that could cause uplift or subsidence in different sectors, creating space for sedimentary sequence to be preserved.

Due to their complex geological evolution, the continental margins along the Mediterranean Sea show a wide variety of geological and geodynamic settings. The presence of fold-and-thrust orogenic belts, extensional basins, and remnants of old oceanic crust, almost entirely subducted below the continent, lead to the presence of a wide variety of margin types, separated one to each other by relatively short distances.

The Montenegro/Northern Albania Continental Margin (MACM, Fig.1.1) constitutes a peculiarity among the peri-Mediterranean margins, because it lacks of high quality marine geological/geophysical data. This area is located in the southeastern sector of the Adriatic Sea and includes the entire Montenegro and the Northern Albania coastlines. It is limited to the N by the political boundary between Montenegro and Croatia, located immediately northwest of the Bokakotorska Bay, and to the S, in Albania, by the Cape Rodonit and the outflow of the Drini River (Fig. 1.1).

From the point of view of geodynamics, the MACM is a convergent margin formed at the front of the Dinarides fold-and-thrusts system belt, whose tectonic structure encompasses the shelf and the continental slope. A preliminary neotectonic study based on the analysis of both, newly collected and published data in Del Bianco et al. (2010) suggests that some of the shallow deformations observed along the MACM are related to the compressive regime along the more external Dinaric thrusts and to transpressive faults located near the Montenegro/Albania boundary. This hypothesis, although in agreement with seismological studies (Anderson and Jackson, 1987; Pondrelli et al., 2002; Hunstad et al., 2003), is supported by the analysis of shallow seismic reflection images only, and should be confirmed by deeper structural data.

Historical catalogues (ANSS 1963-2009) and instrumental records (Pondrelli et al., 2006) show that this region is one of the coastal zones in the Central Mediterranean more prone to seismic hazard. The list of large earthquakes occurred in the near past include (i) the $M=7$ Dubrovnik event (April 6 1667), (ii) the $M=6.5$ of June 13, 1593 event with epicenter close to Kotor, and (iii) the destructive June 1, 1905 event, close to Skadar. The most recent large magnitude (M_w 7.1) earthquake occurred on April 15, 1979 offshore Montenegro, between Bar and Ulcinj. The hypocentre of the

1979 mainshock was located along a shallow (7 km deep), low angle (14°) thrust fault, parallel to the coastline and dipping to the NE (Benetatos et al., 2006). This latest event highlighted the importance of marine geological studies along the MACM to understand how deformations originating from deep-seated seismogenic structures reflect on the uppermost sedimentary sequence, and could eventually affect the seafloor morphology.

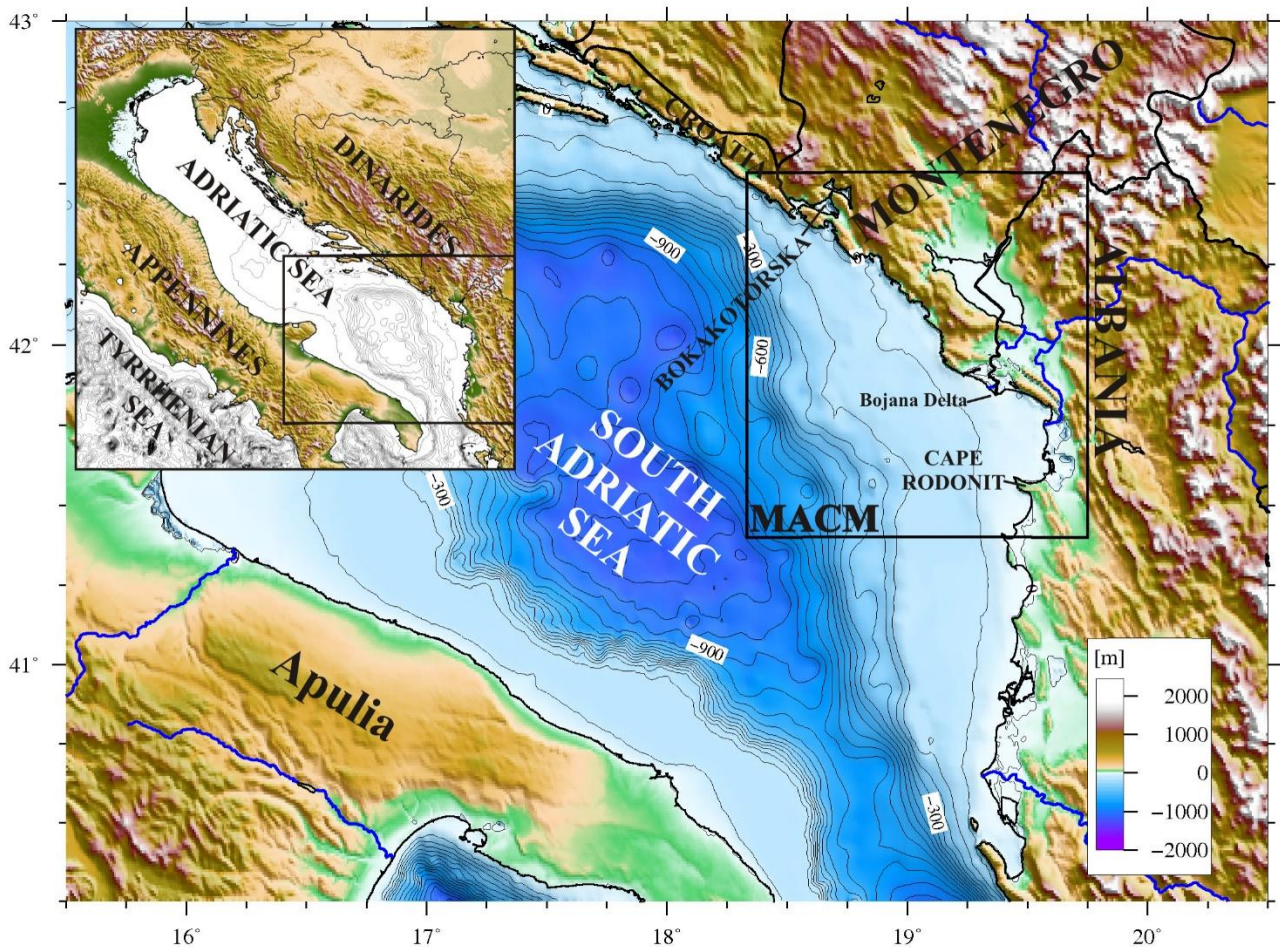


Fig.1.1. Geographical setting of Montenegro/N.Albania Continental Margin (MACM).

Regarding available marine geological/geophysical data, the closest example is a set of multichannel seismic reflection profiles acquired along the Albania offshore (Argnani et al., 1996) which, however, do not reach the MACM. Data acquired by the oil companies starting from the '70, potentially useful to study relationships between shallow and deep geological structures, are not currently available except for a few examples (Dragasevic, 1974, 1983; Oluic et al., 1982; Aliaj et al., 2004; Aliaj, 2008).

Although there is no information about stratigraphic architecture of the MACM, we could use

as a reference the well-studied western Adriatic margin. Here, it has been shown that since the Middle Pleistocene, the high-frequency glacio-eustatic fluctuations are the primary controlling factor for the cyclical deposition of sedimentary units (Trincardi and Correggiari, 2000; Ridente and Trincardi, 2002). This effect, combined with a progressive tilting of the shelf due to regional subsidence, allowed for preservation of a relatively expanded sedimentary sequence. This includes deposits from all different stages of the climate cycles, such as the Highstand (HST), the Falling-stage (FSST), the Lowstand (LST) and the Transgressive (TST) systems tract, differently preserved and widely recovered and studied in the Adriatic Sea and in other Mediterranean margins (e.g. Tesson et al., 1990; Trincardi and Field, 1991; Piper and Aksu, 1992; Gensous and Tesson, 1996; Chiocci et al., 1997; Bernè et al., 1998; Skene et al., 1998; Somoza et al., 1998; Ridente and Trincardi, 2002; Maselli et al., 2011).

The eastern and western Adriatic shelves are characterized by similar geodynamic settings and a common history of Late Quaternary paleogeographic changes, culminated ~21 kyr in the last episode of glacio-eustatic low stand (-120 m below the present-day datum; Clark et al., 2009). In its northern part, the western Adriatic is characterized by high accommodation related to the constant and relatively high subsidence rate at the front of the Apennine Chain. South of the Mid Adriatic Depression (central Adriatic Sea), compressive deformations reach the uppermost part of the stratigraphic sequence (Ridente and Trincardi, 2006), as well as in other areas where the Apennine Chain front intersects the coastline. In such zones, subsidence is highly variable, and sediments are locally affected by incipient tectonic deformations. Recently, Maselli et al. (2001) presented a compilation of subsidence rate estimates from several sources, in different sectors of the western Adriatic margin; these rates range from 1.2 mm/yr in the Northern, and 0.3 mm/yr in the Central Adriatic. Conversely, the Southern Adriatic shelf in correspondence of the Apulia swell is uplifting at rates in the order of 0.2-0.3 mm/yr.

However, the main factors that control the depositional sequences of the latest sea level cycles along the eastern Adriatic shelf, and an estimate of the vertical movement that characterizes the margin and creates accommodation for these sequences to be preserved, is not studied to date.

Unlike the few existing published work on the MACM that deal mainly with seismology or the description of deep tectonic structures, this work represents the first analysis of high-resolution morphobathymetric and seismic reflection data to study the geological evolution at the scale of the Late Quaternary. It thus represents a first marine geological description of the MACM, which includes a reconstruction of its morphology, an analysis of sediment distribution along the margin and its evolution in time during the Late Pleistocene-Holocene, as well as an estimate of the subsidence rate at the shelf-break based on combined seismo-stratigraphic and chrono-stratigraphic

analysis of selected sediment samples. Furthermore, a preliminary analysis of the relationships between deep tectonic structures and their expression at the shallow seafloor is presented. A final, not completely developed aspect concerns the analysis of modern distribution of sediments through a geochemical approach, which constitutes the main objective of the EC ADRICOSM-STAR project, the reference framework for data acquisition in this area.

The topics analyzed in this work are important for the comprehensive knowledge of the Adriatic Sea basin, and to determine the main geological factors that control the physiography and distribution of Late Quaternary sediments along a seismically active margin, such as the MACM, that develops above the outer tectonic structures related to the Dinarides Chain. Being the first work of its kind conducted in the MACM, it will also lay the groundwork for future research in more depth.

The following introductory paragraphs provide an overview on sea level changes during the Late Quaternary and an introduction to the physiography of the continental margins in convergent geodynamic settings.

1.2 Late Quaternary sea level changes, the last glacial-interglacial transition and its stratigraphic signature in the Adriatic Sea

As previously mentioned, the glacio-eustatic sea level fluctuations during the Late Quaternary have played a key role in controlling the deposition of sedimentary units in the Adriatic Sea. For this reason, we will briefly summarize the studies about global sea level changes during this period.

At time scales of thousands of years, climate is characterized by important cyclic variations, linked to changes in Earth orbital parameters and axis tilting, which lead to variations in the effects of solar radiation in the two hemispheres of our Planet; this causes important climatic oscillation called “Milankovitch cycles”: (i) the eccentricity (the shape of the orbit and consequently the Earth-Sun distance) characterized by a period of ca. 100 kyr, (ii) the obliquity (the tilting of the Earth rotational axis) with a period of about 40 kyr and (iii) the precession (the direction of Earth rotational axis) with a period of about 20 kyr (Martinson et al., 1987; Ruddiman, 2006). The interaction between these different timescale cyclic variations are linked to the glacio-eustatic component of the sea level changes and the greatest observed response concerning the ice ages is at the 100 kyr timescales. This rather simplistic picture is however complicated by biological and abiological feedbacks, such as the changes in albedo, the bloom of micro-plankton and the modification of oceanic currents.

The reconstruction of past sea level oscillations is achieved using a variety of techniques, including geomorphology, geology and archeology, through direct sea level reconstruction by investigating geologic and geomorphologic features such as marine erosion features (e.g. Antonioli

et al., 2007), barrier-island-lagoon deposits (e.g. Törnqvist et al., 2004), coral-reef deposits and terraces (e.g. Fairbanks, 1989 and Bard et al., 2010). Another important contribution to the estimate of past eustatic levels is given by isotopic studies carried out on ubiquitous microfossils such as deep-sea foraminifera corroborated by numerical modeling and simulations (Lambeck and Chapel, 2001; Lea et al., 2002). In fact the $\delta^{18}\text{O}$ (the ratio between ^{18}O and ^{16}O) in the ocean provide a time-averaged record of deep-sea temperature and continental ice volume because it increases with the amount of ice on the poles. By combining isotopic sea level records with estimate based on dated coral reefs, which represent natural dipsticks for the eustatic level, several authors reconstructed eustatic oscillation in form of different sea level curves, such as that shown in Fig. 1.2 (Shackleton, 2000; Lea et al., 2002).

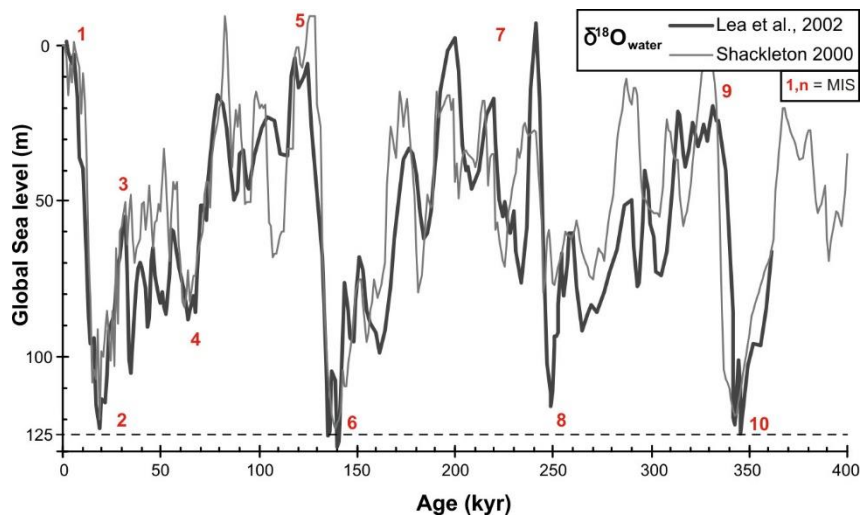


Fig.1.2. Compilation of two different sea level curves for the last 350 kyr modified from Shackleton (2000) and Lea et al., (2002). Red numbers refer to a Marine Isotopic Stage (MIS) from Lisiecki and Raimo (2005).

During the last glacial-interglacial transition, starting from about 19 kyr at the end of the Last Glacial Maximum (LGM, between 26 and 19 kyr cal. BP), the sea level rose from about -120 meters to its modern position (Clark et al., 2009). As highlighted by several authors, the last sea level rise (between ca. 19 and 5.5 kyr BP) was not monotonic, but punctuated by two main steps of enhanced ice melting (Fairbanks, 1989) (Fig. 1.3). The sea level curve shows at least two slope gradients due to intervals of enhanced fresh water discharge, called *Meltwater Pulses* 1A and 1B, starting at 14.2 kyr cal. BP and 11.3 kyr cal. BP, respectively (Fairbanks, 1989).

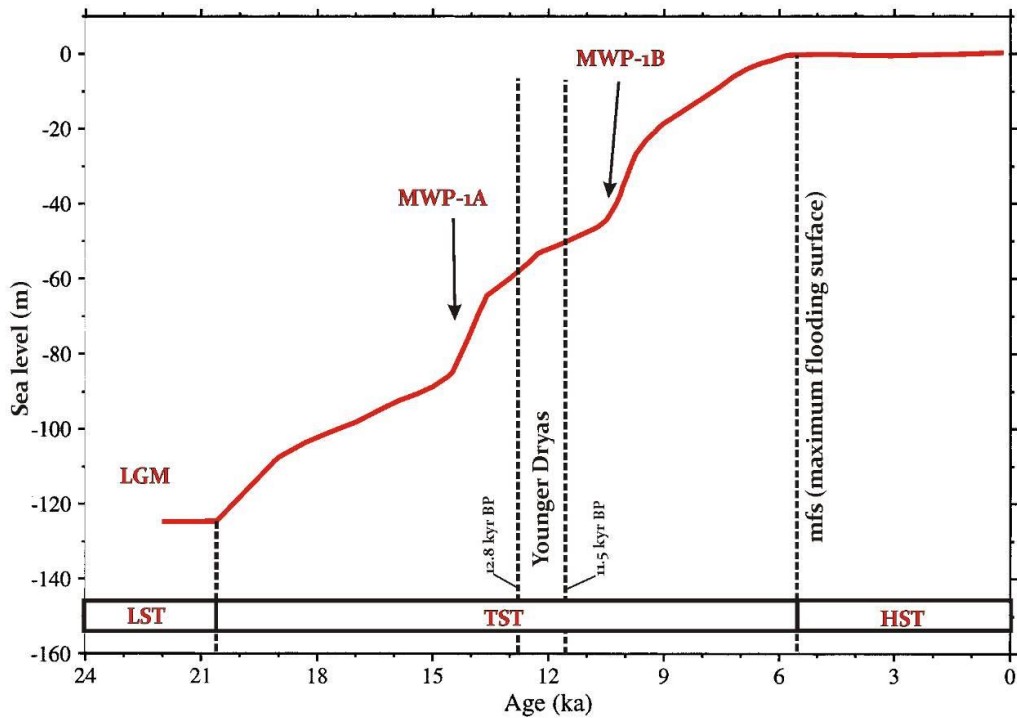


Fig.1.3. Sea level curve for the post – LGM time interval and other information from several authors. Red line is modified from Fleming et al. (1998).

During these phases, the sea level rose about 20 m in less than 500 yr (Bard et al., 1990, 1996; Clark et al., 2002). The meltwater pulses are separated by a short interval of climatic reversal that brought back to colder conditions, known as the *Younger Dryas* event (Allen et al., 1999). During the Late Quaternary, part of the western Adriatic shelves underwent significant subsidence, up to 1.2 mm/kyr (Maselli et al., 2010). This allowed for preservation a relatively expanded record of the last cycle, including the forced-regression deposits (e.g. Ridente and Trincardi, 2002). The uppermost seafloor stratigraphy of north and central Adriatic can be subdivided into two different domains. The shallower portion is characterized by clinofolds formed by sediments delivered to the basin by the Po River and others Apennine rivers after the maximum marine ingressions, and confined landward by marine circulation (Cattaneo et al., 2003; Cattaneo et al., 2007). Conversely, the central portion of the northern Adriatic shelf is characterized by the diffuse presence of low stand alluvial plan deposits, covered by transgressive sandy beds of relict barrier-island systems, formed during to the last sea level rise (Correggiari et al., 1996).

The shallow stratigraphic architecture of the west Adriatic margin is composed of different stratigraphic units related to the Late Quaternary sea level changes (Cattaneo and Trincardi, 1999; Trincardi and Correggiari, 2000):

- the prograding Pleistocene wedges, truncated at their top by a regional erosional surface (ES1) that

recorded a regressive phase encompassing most of the last glacial cycle, from marine oxygen isotope stage 5e to the base of the last glacial maximum (Trincardi and Correggiari, 2000; Ridente and Trincardi, 2002);

- the Transgressive Systems Tract (TST), resting above ES1, that recorded distinctive phases of the last sea level rise and short-term variations of sediment supply and dispersal (Cattaneo and Trincardi, 1999), likely accompanied by changes in the oceanographic regime of the basin (Asioli et al., 2001). Maselli et al. (2011) represents the recent-most summary for this.

- the Highstand Systems Tract (HST), consisting of a shore-parallel prograding mud prism, deposited during the last 5.5 cal kyr BP, which formed above a regional downlap surface (Maximum Flooding Surface, mfs; Correggiari et al., 2001; Cattaneo et al., 2003, 2004 and 2007).

1.3 Physiography of continental margins

Before moving to the next chapter, which describes the geological setting of the study area, it is important to describe how the study of the continental margin physiography could be approached using marine geophysical data.

A continental margin is defined as the outer edge of a major landmass and is generally formed by a sequence of shelf, slope and rise, from the innermost to the outermost physiographic domain, respectively. An alternative to the shelf-slope model is a *ramp*, proposed by Ahr (1973), not considered in this work. The continental shelf is the submerged part of the continents, between the coastline and the *shelf-break*, an abrupt change in the topographic gradient usually located at a depth of 100-160 m. The average topographic gradients on the shelf are some decimal degrees (typically < 1°) and for this reason it undergoes alternated sinking and sub-aerial exposure as a consequence of eustatic oscillations. The continental slope connects the shelf with the abyssal plain, and constitute the by-pass for density currents and hyperpycnal flows. In fact, along the slope we observe relatively high topographic gradients, from 1 to 10°, and typical morphological features associated to high-energy sedimentary processes, including mass wasting and deformation due to gravity driven instability. Continental shelves are generally sites for accumulation of thick stack of sedimentary sequences, characterized by complex structural patterns, and controlled by the combined effects of sediment supply, transport and deposition, as well as the effect of tectonics and erosional processes.

Active continental margins as the MACM, where lithospheric plates converge, coincide with plate boundaries where the upper and lower plates are separated by a subduction zone. These margins have lesser extents and sediment accumulation relative to passive margins, where thermal subsidence

plays a key role in creating accommodation for depositional sequences. One of the major factors controlling development of the continental shelves along active margins is the availability of sediment and its inputs from adjacent continental areas could contribute to the growth of the *accretionary prism*, the wedge of deformed sediments stacking in front of subduction planes. When folded coastal mountain chains develop, as part of a convergent margin, the drainage system may be limited and active continental margins are often characterized by small mountainous rivers carrying relatively large sediment loads to the narrow shelves (Milliman and Syvitski, 1992). Tectonic deformations can lead to the formation of mid-shelf synclinal basins, which can control sediment transport at different time-scales. For example, synclinal basins formed due to tectonic deformations on the shelf are the primary repositories of the Waipaoa and Waiapu River deposits in New Zealand, and the Eel River in California (Clarke, 1987; Foster and Carter, 1997; Lewis et al., 2004). Alternatively, with a more limited accommodation in case of over narrower shelves, most of the sediments delivered to collisional margins are transferred to the adjacent slopes and deep-sea basins during high sea level conditions (Milliman and Syvitski, 1992).

The stratigraphic architecture of a continental margin can be analyzed by unraveling the packaging of stratigraphic units from seismic reflection data. Vail et al. (1977) claimed to recognize a hierarchy of cycles of relative sea level change largely based on the depositional limits of onlaps and toplaps within the coastal facies of marine sediments. The primary meso-scale units of stratigraphy are the depositional sequences. They are coherent packets of genetically related strata correlated at a regional scale. Depositional sequences are recognized in the subsurface using seismic stratigraphic methods, because they are marked by bounding unconformities or laterally correlable conformities (Mitchum et al. 1977). Within each depositional sequence, individual strata can exhibit a variety of geometrical relationship to the depositional boundary. Onlaps, downlaps and toplaps indicate non-depositional hiatuses, whereas truncation indicates an erosional hiatus or the result of structural deformation (Vail et al, 1977). The depositional sequence boundary is useful on seismic reflection profiles because it can be easily recognized by a downward shift in the positions of coastal onlaps. A simplified sketch showing a general stacking pattern of depositional sequence on a typical continental passive margin is shown in Fig. 1.4.

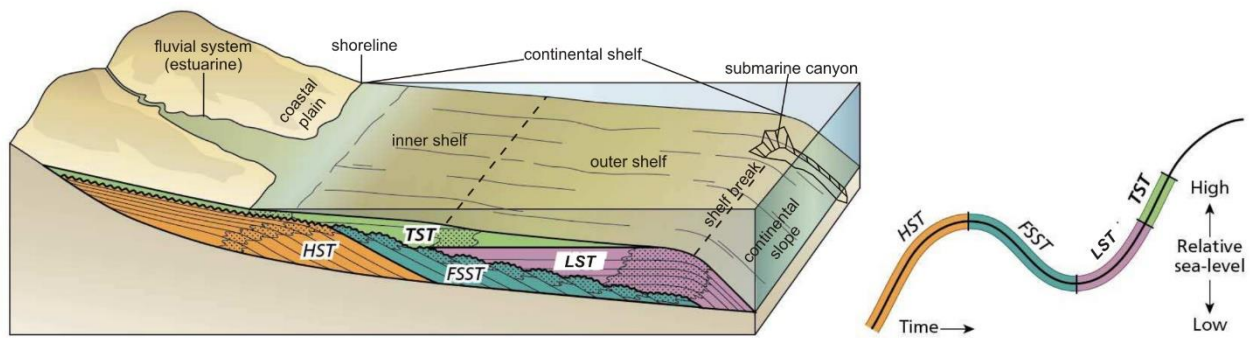


Fig.1.4. Example of general morphologies of continental margin at the late TST phase and the ideal system tract model. Modified from Coe et al. (2003).

The sedimentary sequences in a tectonically active margin may be more complex relative to passive margins due to the tectonic effects. For this reason, analysis of the depositional patterns in margins such as the MACM, requires to separate the effect of vertical movements of the substratum, caused by tectonic deformation, and sea level changes caused by eustasy.

The following chapter provide a geological background of the studied area by the information available in literature, before passing to the analysis of the new data.

References

- Ahr, W.M., 1973. The carbonate ramp-an alternative to the shelf model. *Trans., Gulf Coast Assoc. Geol. Soc.*, 23: 221-225.
- Aliaj S., Adams J, Halchuk S., Sulstarova E., Peci V. and Muco B. 2004. - Probabilistic seismic hazard maps for Albania. - 13th World Conference on Earthquake Engineering, Vancouver, B.C., Canada, August 1-6, 2004, Paper No. 2469.
- Aliaj S. 2008 - The Albanian Orogen: convergence Zone between Eurasia and the Adria microplate. - In: N.Pinter, G.Gyula, S.Stein and D.Medak (eds.), *The Adria Microplate: GPS Geodesy, Tectonics and Hazards*, NATO Science Series, IY, Earth and Environmental Sc., Vol.61, Springer.
- Anderson H. & Jackson J. 1987 – Active tectonics of the Adriatic region. *Geophys. J. R. astr. Soc.*, 91,937-983
- ANSS (Advanced National Seismic System) – Northern California Earthquake Data Center – www.ncedc.org/anss
- Antonioli F., Anzidei M., Lambeck K., Auriemma R., Gaddi D., Furlani S., Orrù P., Solinas E., Gaspari A., Karinja S., Kovacic V., Surace L., 2007 Sea-level changes during the Holocene in Sardinia and in the northeastern Adriatic (central Mediterranean Sea) from archaeological and geomorphological data. *Quaternary Science Review* 26, 2463-2486.
- Argnani A., Bonazzi C., Evangelisti D., Favali P., Frugoni F., Gasperini M., Ligi M., Marani M. and Mele G. 1996. - Tettonica dell'Adriatico meridionale - *Mem. Soc. Geol. It.*, 51, 227-237.
- Asioli, A., Trincardi, F., Lowe, J. J., Ariztegui, D., Langone, L., & Old, F. (2001). Sub-millennial scale climatic oscillations in the central Adriatic during the Late glacial: palaeoceanographic implications, 20.
- Bard, E., Hamelin, B., Fairbanks, R.G., 1990. U–Th ages obtained by mass spectrometry in corals from Barbados: sea level during the past 130,000 years. *Nature* 346, 456–458.
- Bard, E., Hamelin, B., Arnold, M., Montaggioni, L., Cabioch, G., Faure, G., Rougerie, F., 1996. Deglacial sea-level record from Tahiti corals and the timing of global Meltwater discharge. *Nature* 382, 241–244.
- Bard, E., Hamelin, B., & Delanghe-Sabatier, D. (2010). Deglacial meltwater pulse 1B and Younger Dryas sea levels revisited with boreholes at Tahiti. *Science (New York, N.Y.)*, 327(5970), 1235–7. doi:10.1126/science.1180557
- Benetatos C. and Kiratzi A., 2006. – Finite-fault slip models for the 15 April 1979 (Mw 7.1) Montenegro earthquake and its strongest aftershock of 24 May 1979 (Mw 6.2). - *Tectonophysics* 421, 129-143.
- Berne, S., Lericolais, G., Marsset, T., Bourillet, J.F., De Batist, M., 1998. Erosional onshore sand ridges and lowstand shore- faces: examples from tide- and wave-dominated environments of France. *J. Sediment. Res.* 68, 540^555.
- Cattaneo A., Trincardi, F., 1999. The late-Quaternary transgressive record in the Adriatic epicontinental sea: basin widening and facies partitioning. In: Bergman, K.M., Snedden, J.W. (Eds.), *Isolated Shallow Marine Sand Bodies: Sequence Stratigraphic Analysis and Sedimentologic Interpretation*, Spec. Publ. SEPM, 64, 127–146.
- Cattaneo A., Correggiari A., Langone L., Trincardi F. 2003. The Late-Holocene Gargano subaqueous delta, Adriatic shelf: sediment pathways and supply fluctuations. *Marine Geology*, 193: 61-91.

- Cattaneo, A., Correggiari, A., Marsset, T., Thomas, Y., Marsset, B., & Trincardi, F. (2004). Seafloor undulation pattern on the Adriatic shelf and comparison to deep-water sediment waves. *Marine Geology*, 213(1-4), 121–148. doi:10.1016/j.margeo.2004.10.004
- Cattaneo A., Trincardi F., Asioli A., Correggiari A. 2007. Cliniform formation in the Adriatic Sea: energy-limited bottomset. In Milligan T.G., Cattaneo A., (Eds.), Special issue, Sediment dynamics in the western Adriatic. *Continental Shelf Research*, 27: 506-525.
- Chiocci, F.L., Ercilla, G., Torres, J., 1997. Stratal architecture of Western Mediterranean Margins as the result of the stacking of Quaternary lowstand deposits below glacio-eustatic fluctuation base-level. *Sediment. Geol.* 112, 195–217.
- Coe, Angela L.; Bosence, Dam W.J.; Church, Kevin D.; Flint, Stephen S.; Howell, John A. and Wilson, R. Chris L. (2003). *The Sedimentary record of sea-level change*. Cambridge, UK: Cambridge University Press and the Open University.
- Correggiari, A., Field, M., Trincardi, F., 1996. Late Quaternary large dunes on the sediment-starved Adriatic shelf. In: De Batist, M., Jacob, P. (Eds.), *Geology of Siliciclastic Shelf Seas*, vol. 117. Geological Society Special Publication, pp. 155–169
- Correggiari A., Trincardi F., Langone L., Roveri M., 2001 - Styles Of Failure In Late Holocene Highstand Prodelta Wedges On The Adriatic Shelf. *JOURNAL OF SEDIMENTARY RESEARCH*, vol. 71; p. 218-236.
- Clark, P.U., Mitrovica, J.X., Milne, G.A., Turon, J.L., Siani, G., 2002. Sea level fingerprint as a direct test for the source of global Meltwater Pulse 1A. *Science* 295, 2438–2441.
- Clark, P.U., Dyke, A.S., Shakun, J.D., Carlson, A.E., Clark, J., Wohlfarth, B., Mitrovica, J.X., Hostetler, S.W., McCabe, A.M., 2009. The last Glacial Maximum. *Science* 325, 710–714.
- Clarke, S.H., Jr., 1987. Geology of the California continental margin north of Cape Mendocino. In: Scholl, D.W., Grantz, A., Vedder, J.G. (Eds.), *Geology and Resource Potential of the Continental Margin of Western North America and Adjacent Ocean Basins — Beaufort Sea to Baja California*. Circum-Pacific Council for Energy and Mineral Resources, Earth Science Series, 6, pp. 337–351.
- Del Bianco F., Gasperini L., Bortoluzzi G., Giglio F., D’Oriano F., Polonia A., Ravaioli M., Kljajic Z. and Bulatovic A. 2010 – The Montenegro-Northern Albanian continental margin: morphotectonic features in a seismically active region. - *Rapp. Comm. Int. Mer Medit.* Vol.39 p.20
- Dragasevic, T. 1974. Recent structure of Earth's Crust and Upper Mantle in Yugoslavia. – *Zbornik: Metalogenija i koncepcije geotektonskog razvoja Jugoslavije* (Collection: Metallogeny and Concepts of Geotectonic History of Yugoslavia). Faculty of Mining and Geology, Belgrade, 59-72 (in Serbian).
- Dragasevic T. 1983 – Oil geologic exploration in the Montenegro offshore in Yugoslavia. – *NAFTA*, 34: 397-404
- Fairbanks, R.G., 1989. A 17,000-yr glacio-eustatic sea level record: influence of glacial melting rates on the Younger Dryas event and deep-ocean circulation. *Nature* 342, 637–642.
- Foster, G., Carter, L., 1997. Mud sedimentation on the continental shelf at an accretionary margin—Poverty Bay, New Zealand. *N.Z. J. Geol. Geophys.* 40, 157–173.
- Gensous, B., Tesson, M., 1996. Sequence stratigraphy, seismic profiles, and cores of Pleistocene deposits on the Rhone continental shelf. *Sediment. Geol.* 105, 183–190.
- Hunstad, I., Selvaggi, G., D’agostino, N., England, P., Clarke, P. and Pierozzi, M. 2003: Geodetic strain in peninsular Italy between 1875 and 2001. *Geophys. Res. Lett.*, 30: 1181. doi:10.1029/2002GL016447.

- Lambeck, K., & Chappell, J. (2001). Sea level change through the last glacial cycle. *Science (New York, N.Y.)*, 292(5517), 679–86. doi:10.1126/science.1059549
- Lea, D. W., Martin, P. A., Pak, D. K., & Spero, H. J. (2002). Reconstructing a 350 ky history of sea level using planktonic Mg / Ca and oxygen isotope records from a Cocos Ridge core, 21, 283–293.
- Lewis, K.B., Lallemand, S.E., Carter, L., 2004. Collapse in a Quaternary shelf basin off East Cape, New Zealand: evidence for passage of a subducted seamount inboard of the Ruatoria giant avalanche. *New Zealand Journal of Geology and Geophysics* 47, 415–429.
- Lisiecki, L.E., Raymo, M.E., 2005. A Pliocene–Pleistocene stack of 57 globally distributed benthic $\delta^{18}\text{O}$ records. *Paleoceanography* 20, PA1003. doi:10.1029/2004PA001071.
- Martinson, D.G., Pisias, N.G., Hays, J.D., Imbrie, J., Moore Jr., T.C., Shackleton, N.J., 1987. Age dating and the orbital theory of the ice ages: development of a high-resolution 0 to 300,000-year chronostratigraphy. *Quaternary Research* 27, 1–29
- Maselli, V., Trincardi, F., Cattaneo, a., Ridente, D., & Asioli, A., 2010. Subsidence pattern in the central Adriatic and its influence on sediment architecture during the last 400 kyr. *Journal of Geophysical Research*, 115(B12), B12106. doi:10.1029/2010JB007687
- Maselli, V., Hutton, E. W., Kettner, A. J., Syvitski, J. P. M., & Trincardi, F., 2011. High-frequency sea level and sediment supply fluctuations during Termination I: An integrated sequence-stratigraphy and modeling approach from the Adriatic Sea (Central Mediterranean). *Marine Geology*, 287(1-4), 54–70. doi:10.1016/j.margeo.2011.06.012
- Milliman, J., Syvitski, J.P.M., 1992. Geomorphic/tectonic control of sediment discharge to the ocean: the importance of small mountaneous rivers. - *The Journal of Geology* 100, 525-544
- Mitchum, R.M., Vail, P.R., Sangree, J.B., 1977. Seismic stratigraphy and global changes of sea level, part 6: stratigraphic interpretation of seismic reflection patterns in depositional sequences. In: Payton, C.E. (Ed.), *Seismic Stratigraphy — Application to Hydrocarbon Exploration*. AAPG, vol. 26, pp. 117–133. Tulsa, Oklahoma.
- Oluic M., Cvijanovic D., and Prelogovic E. 1982. - Some new data on the tectonic activity in the Montenegro coastal region (Yugoslavia) based on the landsat imagery. - *Acta Astronautica* v 9, No.1, 27-33.
- Pondrelli, S., A. Morelli, G. Ekström, S. Mazza, E. Boschi, and A. M. Dziewonski, 2002. European-Mediterranean regional centroid-moment tensors: 1997-2000, *Phys. Earth Planet. Int.*, 130, 71-101
- Pondrelli S., Salimbeni S., Ekstrom G., Morelli A., Gasperini P. and Vannucci G. 2006. - The Italian CMT dataset from 1977 to the present. - *Phys. Earth Planet. Int.*, doi:10.1016 / j.pepi. 2006.07.008, 159/3-4, pp. 286-303.
- Piper, D.J.W., Aksu, A.E., 1992. Architecture of stacked Quaternary deltas correlated with global oxygen isotopic curve. *Geology* 20, 415–418.
- Ridente, D., & Trincardi, F. (2002). Eustatic and tectonic control on deposition and lateral variability of Quaternary regressive sequences in the Adriatic basin (Italy). *Marine Geology*, 184(3-4), 273–293. doi:10.1016/S0025-3227(01)00296-1
- Ridente, D., Trincardi, F., 2006. Propagation of shallow folds and faults in late Pleistocene and Holocene shelf-slope deposits, central and South Adriatic Margin (Italy). *Bas. Res.* 18, 171–188
- Ruddiman, W.F. (2006), Orbital changes and climate, *Quaternary Science Reviews*, 25, 3092-3112.
- Shackleton, N.J., 2000. The 100,000-year Ice-Age cycle found to lag temperature, carbon dioxide, and orbital eccentricity. *Science* 289, 1897–1902

- Skene, K., Piper, D., Aksu, A., Syvitski, J.P.M., 1998. Evaluation of the global oxygen isotope curve as a proxy for quaternary sea-level by modeling of delta progradation. *J. Sediment. Res.* 68, 1077-1092.
- Tesson, M., Gensous, B., Allen, G.P., Ravenne, C., 1990. Late Quaternary deltaic lowstand wedges on the Rhone continental shelf, France. *Mar. Geol.* 91, 325-332.
- Trincardi, F., Field, M.E., 1991. Geometry, lateral variability, and preservation of downlapped regressive shelf deposits: Eastern Tyrrhenian margin, Italy. *J. Sediment. Petrol.* 61, 75-90.
- Trincardi, F., Correggiari, A., 2000. Muddy forced-regression deposits in the Adriatic basin and the composite nature of Quaternary sea level changes. In: Hunt, D., Gawthorpe, R.L. (Eds.), *Sedimentary Responses to Forced Regressions*, Geol. Soc. London Spec. Publ. 172. 247-271
- Vail, P.R., Mitchum, R.M. and Thompson, S. III, 1977. Seismic stratigraphy and global changes of sea level, Part 3: relative changes of sea level from coastal onlap. In: C.W. Payton (Ed.), *Seismic Stratigraphic Applications to Hydro-carbon Exploration*. American Association of Petroleum Geologists Memories, 26, 63- 97.
- Törnqvist, T.E., Bick, S.J., González, J.L., van der Borg, K., de Jong, A.F.M., 2004. Tracking the sea-level signature of the 8.2 ka cooling event: new constraints from the Mississippi Delta. *Geophysical Research Letters* 31. doi:10.1029/2004GL021429.

CHAPTER 2

THE STUDY AREA

2.1 Morphology and oceanographic setting of the Adriatic Sea

The Adriatic Sea is an epicontinental basin elongated in the NW-SE direction for more than 800 km. Based on its morphology, the western side of the Adriatic margin can be subdivided into three sectors, the Northern, the Central and the Southern basins, separated by the Mid Adriatic Deep (MAD) and the Gargano promontory (Fig. 2.1). The Northern Adriatic Sea, extending for over 350 km from the Gulf of Venice towards southeast, is characterized by very low bathymetric gradient (0.02°) and shallow depths (the area north of the Po Delta is shallower than 35 m). The Central Adriatic includes the MAD, formed by two slope basins, more than 250 meters deep, extending in the NE-SW direction, and delimited eastward by a 50 km wide shelf (ca 0.2° dip) and southward by the Gallignani-Pelagosa Ridge (Ridente and Trincardi, 2006). The Southern Adriatic extends approximately from the Pelagosa Sill (about 160 m deep) to the Otranto Strait where the sill depth is about 800 m (Artegiani et al., 1997). It is formed by a deeper basin called South Adriatic Pit (SAP) (Fig. 2.1) reaching the depth of 1200 m, characterized by complex shelf and slope morphologies (Ridente et al., 2007).



Fig.2.1. Morphobathymetric map of the Adriatic Sea. Data from Gebco 2008.

The presence of sills and structural highs played a major role in the paleoceanographic evolution of

the Adriatic Sea during the past sea level oscillations, sometimes preventing Mediterranean deep water masses to reach and ventilate the Adriatic sea floor (Piva, 2007; Verdicchio et al., 2007).

The entire Adriatic basin is characterised by a microtidal regime, and dominated by a cyclonic circulation (Fig 2.2) driven by thermohaline currents (Poulain, 2001). The Northern Adriatic receives the highest river runoff of the entire Mediterranean, and is sensitive to variations of the sediment inputs as well as to atmospheric conditions due to its shallow depths. Among all the river systems, the Po River, with an average annual discharge of $1500 \text{ m}^3\text{s}^{-1}$, accounts for about 50% of the total Northern Adriatic river runoff (Syvitski and Kettner, 2007). From this river plume, a cyclonic circulation gyre is enhanced and results in trapping fresh waters along the western side of the basin. These river inflows affects marine circulation through the supply a buoyant input, which is one of the major driving forces of the Western Adriatic Coastal Current (WACC; Orlic et al., 1992), and impacts the entire basin by introducing high loads of sediment and related organic matter, nutrients and pollutants (Miserocchi et al., 2007).

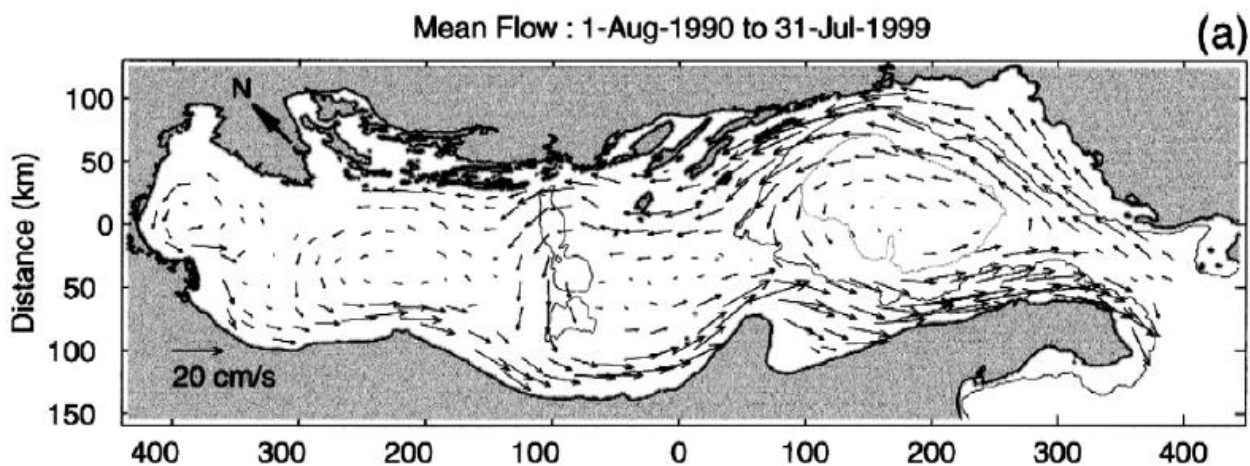


Fig. 2.2. Surface water circulation in the Adriatic Sea. From Poulain (2001).

Otherwise, from the south the Modified Atlantic Waters and Levantine Intermediate Waters (respectively MAW and LIW) reach the Adriatic basin through the Otranto Strait (Orlic et al., 1992). The Southern Adriatic consequently represents the site of convergence of two distinct water masses, the North Adriatic Dense Water and the LIW, and is a site of production of dense waters (Civitaresse et al., 2005). In fact, winter convection and dense water formation take place in the centre of the SAP, at 1200 m water depth, as a result of outbreaks of cold continental air from the Balkan Peninsula, which takes heat from the sea surface layer through cooling and evaporation, and causes movement

through the water column in the centre of a gyre that rotates counter-clockwise (Poulain 2001).

The Montenegro-Albanian shelf and slope is a peculiar sector of the Adriatic Sea circulation, and can be identified as a ROFI (Region of Freshwater Influence) mainly because of the presence of several rivers and abundant precipitations enhanced by the presence of high mountain ranges (Bellafiore et al. 2011). This area is mainly supplied by the Buna-Bojana River (Fig. 1.1) and by several minor streams including the Drini, Mati, Ishimi, Erzeni, Shkumbini, Semani and Vjosa Rivers. The Buna-Bojana River in the SE Adriatic represents the counterpart of the Po River and has the largest single discharge (about $700 \text{ m}^3 \text{ s}^{-1}$); the combined discharge of the Albanian rivers amount to about $1250 \text{ m}^3 \text{ s}^{-1}$ (UNEP 1996; Table 1). Several of the coastal plumes from the Albanian and Montenegro rivers can be readily identified by chlorophyll images, but the largest chlorophyll feature is off the Buna/Bojana delta (Marini et al. 2010). The northward turning of the river plume is consistent with the Coriolis effect (Kourafalou, 1999) and it is also in the direction of prevailing southeastern Adriatic currents (Artegiani et al., 1997). According to Manca et al. (2002), the cyclonic circulation transports relatively fresh water along the western boundary through the southward density-driven WACC. The South Eastern Adriatic current (SEAd; Marini et al. 2010) transports Ionian Surface Water (ISW) along the eastern boundary northward into the Adriatic Sea. The Buna-Bojana plume is deflected northward by the Coriolis apparent force, independently from the dominant local southward wind forcing that should result in southward currents and localized upwelling (Marini et al. 2010). Marini et al. (2010) describe what they call the *South Eastern Shelf Coastal Current* (SESC), which characterizes the oceanographic regime of this region (Fig. 2.3). According to this work, the SESC detaches from the coast in correspondence with the Buna/Bojana outflow and forms coastal eddies that expand the offshore extent of the river plumes. This results in a local complexity in the water circulation.

2.2 Geodynamic and structural setting of the MACM

The Adriatic region includes the relatively stable Adriatic Basin (Po Valley, Adriatic Sea and Apulian foreland), surrounded on the eastern, northern and western margins by the Albanides/Dinarides, the Alps, and the Apennines, respectively (Fig. 1.1). Geodynamic reconstructions of the Adriatic Basin document its evolution from a Mesozoic passive margin to the Cenozoic foreland of the Apenninic and Dinaric thrust belts (D'Argenio and Horvath, 1984; Royden, Patacca and Scandone, 1987) dominated by collisional processes between the African and Eurasian plates (Geiss, 1987).

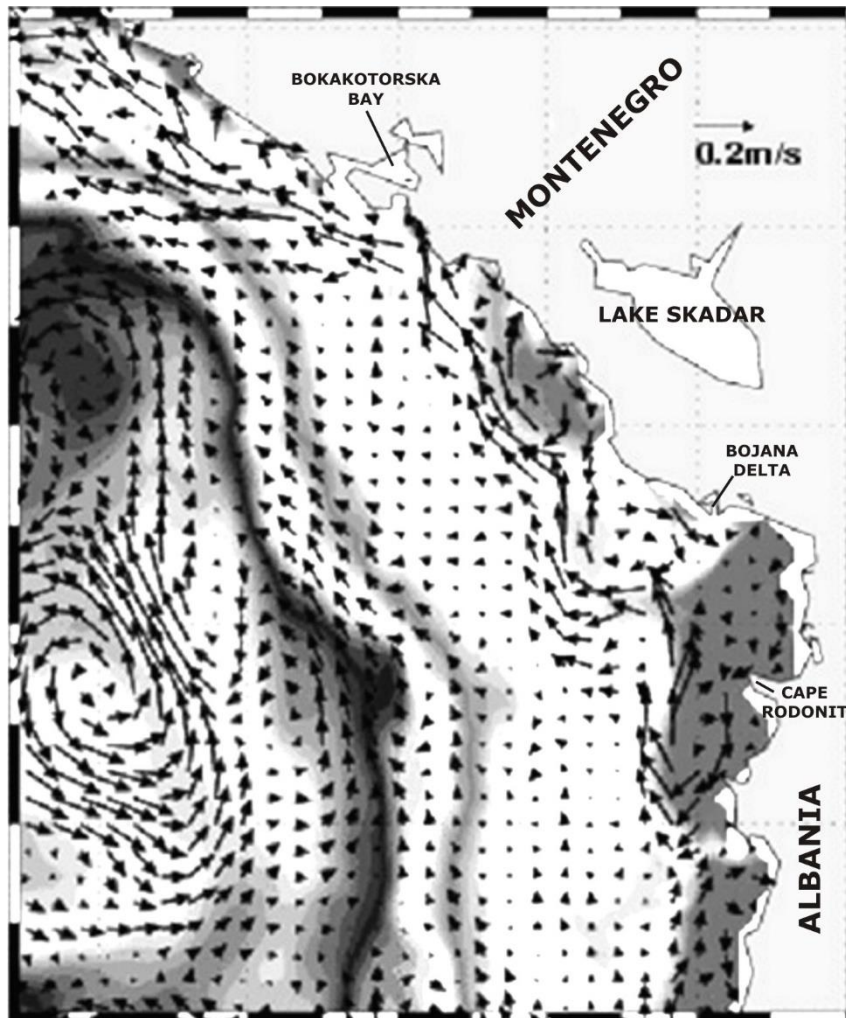


Fig.2.3. Mean horizontal surface distribution of modeled currents at 2m, showing the SESC in the MACM.
 Modified from Marini et al. (2010).

The growth of structural highs east of the Gargano Promontory (i.e., the NW-SE oriented Gallignani and Pelagosa ridges, and the SW-NE oriented Tremiti structural high) started in the Late Pliocene and resulted in the segmentation of the foredeep into two separate basins: the Adriatic foredeep basin, north of the Gargano promontory, and the Bradanic foredeep to the south (Casnedi, 1988; Capuano et al., 1996). In this complex geodynamic setting, the presence of the *Adria Microplate* has been proposed since the earliest studies of this area (Finetti, 1984). Focal mechanisms and epicenter alignments of historical and recent earthquakes, as well as geodetic observations, show NE-SW extension along normal faults crossing the Apennines, N-S convergence across the Alps, as well as strike-slip and thrust fault deformation resulting in NE-SW shortening along the eastern coast of the Adriatic Sea, i.e., the Dinaric and Albanian chains (Anderson and Jackson, 1987; Pondrelli et al., 2002; Hunstad et al., 2003).

Starting from geodetic data studied by McClusky et al. (2000, 2003), Fernandes et al. (2003),

Nocquet and Calais (2003), showing that the Adriatic microplate moves NE at a rate of 4-5 mm/yr relative to Eurasia, Battaglia et al (2004) observed that the existence of Adria offers a better fit to GPS velocity models. The southeastern boundary of Adria is located along the Dinarides/Albanides mountain chains (Fig. 2.4), a SW verging fold-and-thrusts belt formed starting from the Eocene (Rosenbaum and Lister, 2005), that represent the extension towards SE of the Alps.

The Dinarides/Albanides chain shows two different tectonic domains and associated strain regimes: an outer compressional belt, which encompasses the continental shelf and slope; and an inner domain located onshore. The latter is characterized by extensional deformation (Aliaj, 1997) and by alternating ridges and troughs, that form due to incipient extensional deformation along a Plio-Quaternary normal fault system, oriented NW-SE. Conversely, the outer domain, that constitutes the present-day collisional front, shows a compressional regime affecting the entire sedimentary sequence (Aliaj, 1997); this sector of the margin corresponds the MACM, our working area.

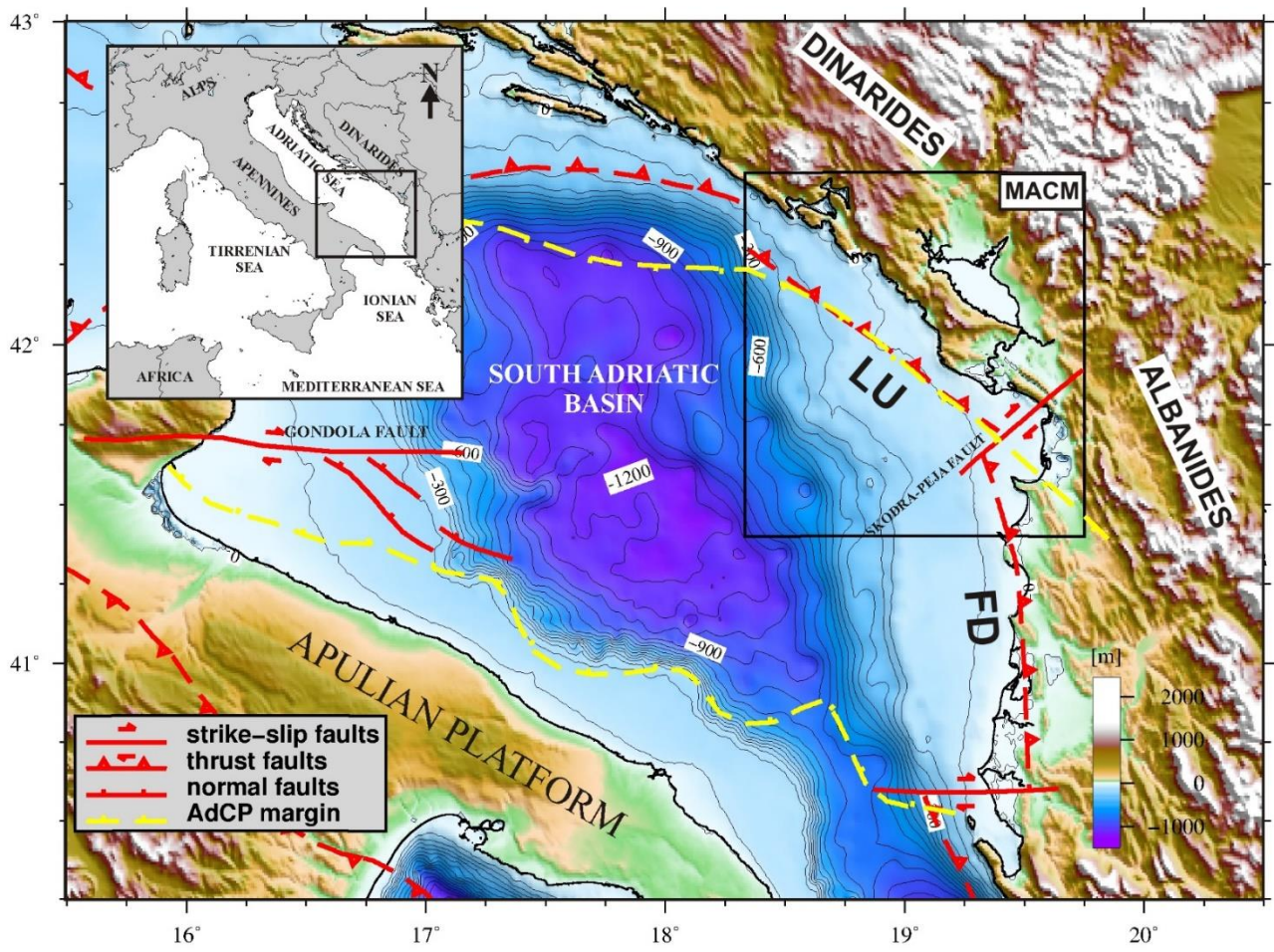


Fig.2.4. Geographical framework of the southeastern Adria Microplate and of the MACM. Segmentation of the SE boundary of Adria Microplate are formed by the LU is Lezha-Ulqini segment and FD is Frakulla-Durrresi segment, these are taken from Aliaj 2000. Topography and bathymetry is from GEBCO.

Dogliani et al. (1999) show that the Adriatic continental lithosphere is subducting below the Dinarides-Hellenides along a shallow NE-dipping plane, representing an eastward subduction of continental lithosphere as the final stage of an oceanic subduction followed by incipient continental collision; this process produced a double-verging Alpine-type orogenic prisms characterized by high structural and topographic relief (Fig. 2.5).

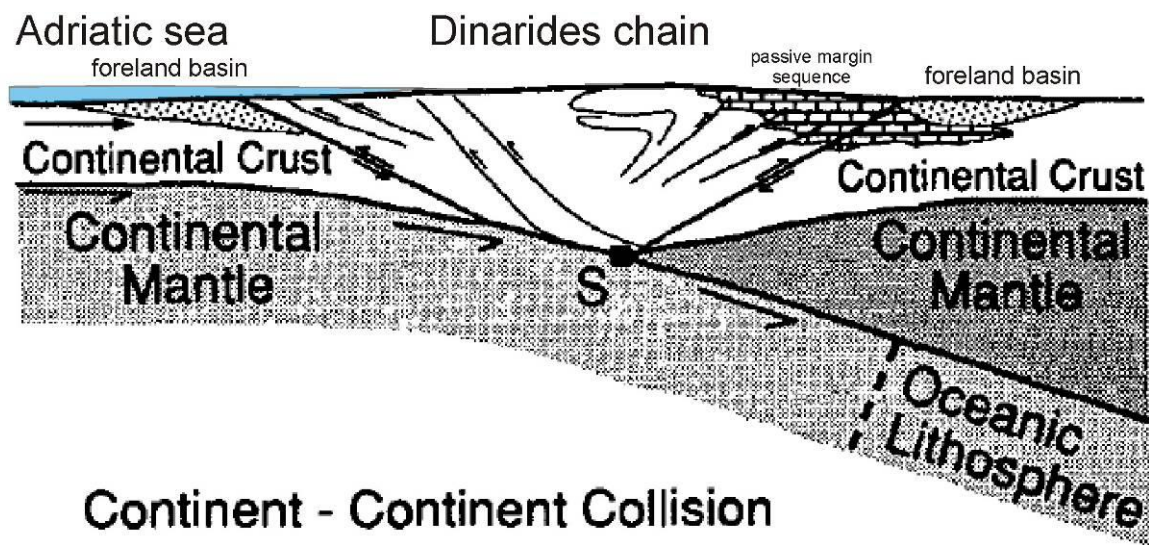


Fig.2.5. Schematic model for continent-continent collision. Modified from Willett et al., 1993

The tectonic features of this convergent system, over which the Dinaride thrusts develop was analysed through the study of a closely spaced grid of multichannel seismic lines, collected during the '80 and the '90 by oil companies. However, these data are still mostly unpublished, if we exclude few line-drawings interpretations in Dragasevic (1974, 1983) and Aliaj (1998, 2000). Using these data, Aliaj (1998, 2000) noted that the accretionary front is displaced by a series of right-lateral transfer faults (Fig. 2.6). The most prominent of these fault systems are, from S to N: the Sazani Island (or Vlora-Tepelena), and the Gjiri Drinit-Lezha (or Shkodra-Peja, or Scutari-Pec, Fig. 2.4). These strike-slip faults separate the MACM in distinct segments, with a diachronous evolution (Aliaj 1998, 2000).

1. The LEZHA-ULQINI segment (Fig. 2.4), located N of the Gjiri i Drinit-Lezha strike-slip

fault shows a WNW orientation and an extent of over 200 kms, from Lezhatown (Albania) to the Montenegro margin along the Adriatic coast. This segment has been described as part of the Kruja zone (Aliaj, 1998; Dragasevic, 1983). In this area, the thrust front is buried below a thick sedimentary sequence, affected by compressive faulting up to the lower Pliocene which appear overprinted by more recent E-NE strike-slip deformations.

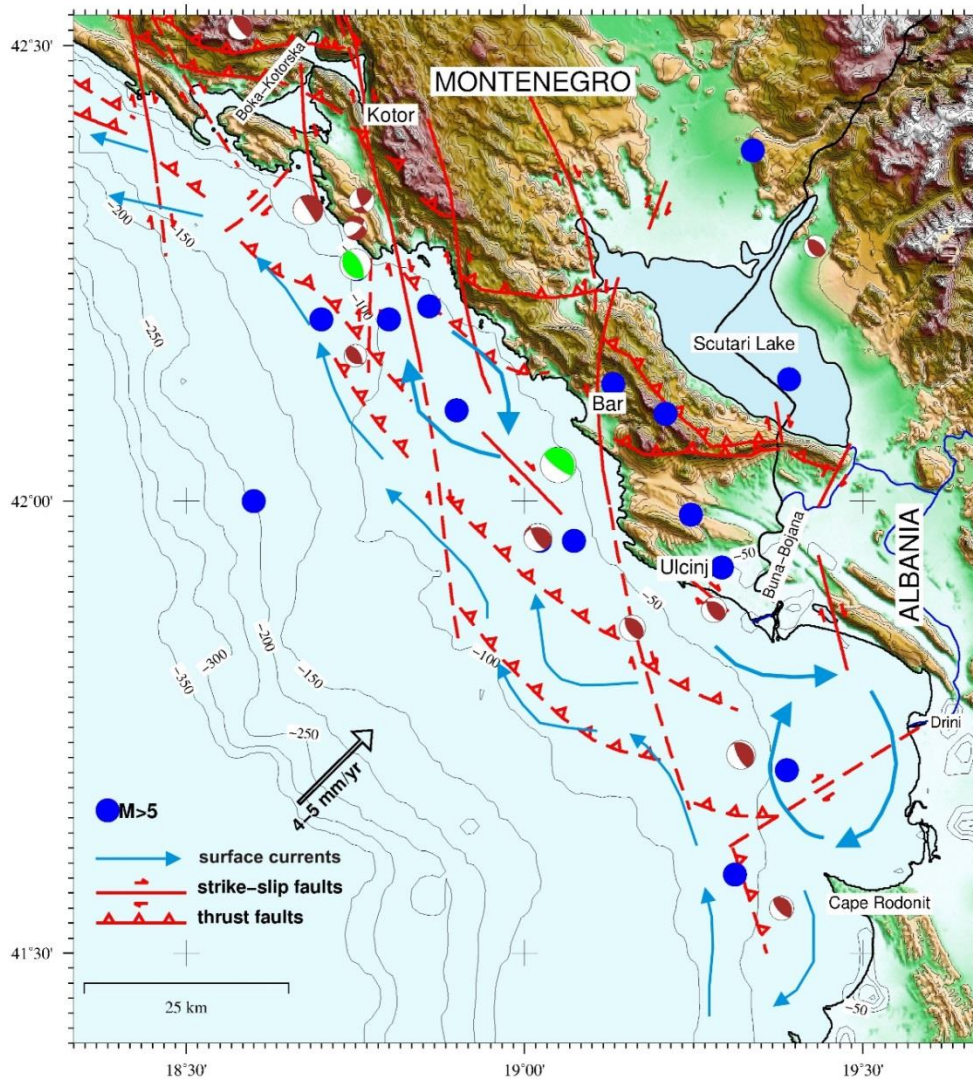


Fig. 2.6. Simplified structural map of the Montenegro/Albanian margin. Location of main structural features is from Oluic et al., (1982), Aliaj et al. (2004) and Aliaj (2008). Epicenters of M>5 earthquakes (blue circles) are indicated (ANSS 1963-2009 <http://www.quake.geo.berkeley.edu/anss/catalog-search.html>), as well as focal mechanism of major recent events (Pondrelli et al., 2006). Surface currents pattern (SESC) is from Marini et al. 2010. Adriatic plate NE convergence vector (fixed Eurasia) is from Grenczy et al. (2005).

2. The FRAKULLA-DURRESI segment (Fig. 2.4) is about 130 km long and shows a N-NNW orientation. It is located in the peri-Adriatic depression propagating from Lezhato Vloratowns and constitutes the outermost lineament of post-Pliocene oblique compressive faults, cut by strike-slip E-NE oriented segments.

On a more local scale, Oluic et al., (1982), based on Dragasevic (1974), shows that the overall setting of the 200 km-long MACM is controlled by two first-order tectonic systems: a thrust-belt chain verging towards ENE; a wrench tectonic system displacing the front into several blocks, consisting of right-lateral strike slip faults whose orientation rotates from N-S in the northern part, to NE-SW towards south (Fig. 2.6).

Being part of the seismically active Dinarides/Albanides fold-and-thrust belt (Aliaj, 1999; 2000), the MACM is characterized by an intense seismic activity, as highlighted by the distribution of $M > 5$ epicenters recorded during the last 50 years (Fig. 2.6). In fact, it is one of the Central Mediterranean coastal areas more prone to seismic hazards, and has been site of large historical earthquakes in the near past, such as, the $M=7$, Dubrovnik event of April 6 1667, the $M=6.5$, June 13, 1593, event, with epicenter close to Kotor, and the destructive June 1, 1905 event, close to Skadar. The recentmost large magnitude (M_w 7.1) earthquake occurred by April 15, 1979 offshore Montenegro, between Bar and Ulcinj (Fig. 2.6); the main shock of this event occurred along a shallow (7 km deep), low angle (14°) thrust fault, parallel to the coastline and dipping toward NE (Benetatos et al., 2006).

References

- Aliaj, S. 1997 - Alpine geological evolution of Albania. *Albanian Journal of Natural & Technical Sciences*, No 3, 69-81
- Aliaj, S. 1998 - Neotectonic structure of Albania. *Albanian Journal of Natural & Technical Sciences*, No 4, 79-97.
- Aliaj, S. 1999 - Transverse faults in Albanian orogen front. *Albanian Journal of Natural & Technical Sciences*, No 6, 121-132.
- Aliaj, S. 2000 - Thrust front along Adriatic collision and seismic potential of its seismogenic nearby zone. *Proc. International Symposium on Earthquake Engineering (ISEE), Montenegro*, 85-93
- Anderson H. & Jackson J. 1987 – Active tectonics of the Adriatic region. *Geophys. J. R. astr. Soc.*, 91,937-983
- ANSS (Advanced National Seismic System) – Northern California Earthquake Data Center – www.ncedc.org/anss
- Artegiani, A., Bregant, D., Paschini, E., Pinardi, N., Raicich, F., Russo, A., 1997. The Adriatic Sea general circulation. Part I. Air-sea interactions and water mass structure. *Journal of Physical Oceanography* 27, 1492-1514.
- Battaglia, M., Murray, M.H., Serpelloni, E., and Bürgmann, R., 2004, The Adriatic region: An independent microplate within the Africa-Eurasia collision zone: *Geophysical Research Letters*, v. 31 doi: 10.1029/2004GL019723.
- Bellafiore, D., Guarnieri, A., Grilli, F., Penna, P., Bortoluzzi, G., Giglio, F., & Pinardi, N. (2011). Study of the hydrodynamical processes in the Boka Kotorska Bay with a finite element model. *Dynamics of Atmospheres and Oceans*, 52(1-2), 298–321. doi:10.1016/j.dynatmoce.2011.03.005
- Benetatos C. and Kiratzi A., 2006. – Finite-fault slip models for the 15 April 1979 (Mw 7.1) Montenegro earthquake and its strongest aftershock of 24 May 1979 (Mw 6.2). - *Tectonophysics* 421, 129-143.
- Capuano 1996
- Casnedi R. 1988. La fossa Bradanica: origine, sedimentazione e migrazione. *Mem. Soc. Geol. It.*, 41,439-448
- Civitares G., Gacic M., Cardin V., Ibello V., 2005 - Winter convection continues in the warming Southern Adriatic. *Eos*, 86: 445-451.
- D'Argenio B., and Horvath F. 1984 - Some remarks on the deformation history of Adria, from the Mesozoic to the Tertiary. *Annales Geophysicae* 1984; 2: 143-146
- Doglioni, C., Harabaglia, P., Merlini, S., Mongelli, F., Peccerillo, a, & Piromallo, C. (1999). Orogens and slabs vs. their direction of subduction. *Earth-Science Reviews*, 45(3-4), 167–208. doi:10.1016/S0012-8252(98)00045-2
- Dragasevic, T. 1974. Recent structure of Earth's Crust an Upper Mantle in Yugoslavia. – *Zbornik: Metalogenija i koncepcije geotektonskog razvoja Jugoslavije (Collection: Metallogeny and Concepts of Geotectonic History of Yugoslavia)*. Faculty of Mining and Geology, Belgrade, 59-72 (in Serbian).
- Dragasevic T. 1983 – Oil geologic exploration in the Montenegro offshore in Yugoslavia. – *NAFTA*, 34: 397-404

- Fernandes, R. M. S., B. A. C. Ambrosius, R. Noomen, L. Bastos, M. J. R. Wortel, W. Spakman, and R. Govers (2003), The relative motion between Africa and Eurasia as derived from ITRF2000 and GPS data, *Geophys. Res. Lett.*, 30(16), 1828, doi:10.1029/2003GL017089
- Finetti, I., 1984. Struttura ed evoluzione della Microplacca Adriatica. *Bollettino di Oceanologia Teorica ed Applicata*, II, 115-123.
- Grenczy, G., Sella, G., Stein, S., Kenyeres, A., 2005. Tectonic implications of the GPS velocity field in the northern Adriatic region. *Geophysical Research Letters*, v. 32.
- Geiss, E. 1987 - A New Compilation of Crustal Thickness in the Mediterranean Area, *Ann. Geophys.* 5B(6), 623–630.
- Hunstad, I., Selvaggi, G., D'agostino, N., England, P., Clarke, P. and Pierozzi, M. 2003: Geodetic strain in peninsular Italy between 1875 and 2001. *Geophys. Res. Lett.*, 30: 1181. doi:10.1029/2002GL016447.
- Kourafalou, V.H., 1999. Process studies on the Po River plume, north Adriatic sea. *Journal of Geophysical Research* 104 (C12), 29963 - 29985.
- Marini, M., Grilli, F., Guarnieri, A., Jones, B. H., Klajic, Z., Pinardi, N., & Sanxhaku, M. (2010). Is the southeastern Adriatic Sea coastal strip an eutrophic area? *Estuarine, Coastal and Shelf Science*, 88(3), 395–406. doi:10.1016/j.ecss.2010.04.020
- Manca, B.B., V. Kovacevic, M. Gacic and D. Viezzoli (2002), Dense water formation in the Southern Adriatic Sea and interaction with the Ionian Sea in the period 1997–1999, *Journal of Mar. Syst.*, 33-34, 133-154.
- Miserocchi, S., Langone, L., Tesi, T., 2007. Content and isotopic composition of organic carbon within a flood layer in the Po River prodelta (Adriatic Sea). *Continental Shelf Research* 27, 338–358.
- McClusky 2000-2003
- Nocquet, J. M., and E. Calais 2003 - Crustal velocity field of western Europe from permanent GPS array solutions, 1996–2001, *Geophys. J. Int.*, 154, 72–88
- Oluic M., Cvijanovic D., and Prelogovic E. 1982. - Some new data on the tectonic activity in the Montenegro coastal region (Yugoslavia) based on the landsat imagery. - *Acta Astronautica* v 9, No.1, 27-33.
- Orlic, M., Gacic, M., La Violette, P.E., 1992. The currents and circulation of the Adriatic Sea. *Oceanologica Acta* 15, 109–124.
- Pondrelli, S., A. Morelli, G. Ekström, S. Mazza, E. Boschi, and A. M. Dziewonski, 2002. European-Mediterranean regional centroid-moment tensors: 1997-2000, *Phys. Earth Planet. Int.*, 130, 71-101
- Pondrelli S., Salimbeni S., Ekstrom G., Morelli A., Gasperini P. and Vannucci G. 2006. - The Italian CMT dataset from 1977 to the present. - *Phys. Earth Planet. Int.*, doi:10.1016 / j.pepi. 2006.07.008, 159/3-4, pp. 286-303.
- Poulain P.M. 2001. Adriatic Sea surface circulation as derived from drifter data between 1990 and 1999. *Journal of Marine Systems*, 29: 3-32.
- Piva, A 2007 - *High-resolution stratigraphy of Central and Southern Adriatic Quaternary deposits of sub-Milankovian climate change on Mediterranean circulation* – PhD Thesis – University of Bologna
- Ridente, D., Trincardi, F., 2006. Propagation of shallow folds and faults in late Pleistocene and Holocene shelf-slope deposits, central and South Adriatic Margin (Italy). *Bas. Res.* 18, 171–188
- Ridente, D., F. Fogliini, D. Minisini, F. Trincardi and G. Verdicchio 2007 - Shelf-edge erosion sediment failure and inception of Bari Canyon on the South-Western Adriatic Margin (Central Mediterranean), *Marine Geology*, 246, 193-207.

- Rosenbaum, G., and Lister, G.S., 2005, The western Alps from the Jurassic to Oligocene: Spatio-temporal constraints and evolutionary reconstructions: *Earth-Science Reviews*, v. 69 pp. 281-306 doi: 10.1016/j.earscirev.2004.10.001.
- Royden L., Patacca E. and Scandone P. 1987. - Segmentation and configuration of subducted lithosphere in Italy: An important control on thrust-belt and foredeep-basin evolution. *Geology*, 15, 714-717
- Syvitski, J.P.M. & Kettner, A.J. (2007): On the flux of water and sediment into the Northern Adriatic. *Continental Shelf Research* (27): 296-308.
- UNEP 1996. Mediterranean Action Plan (MAP), Implications of Climate Change for the Albanian Coast, Technical Reports series No.98.
- Verdicchio G, Trincardi F, Asioli A (2007) Mediterranean bottom- current deposits: an example from the Southwestern Adriatic Margin. *Geol Soc Lond Spec Publ* 276:199–224
- Willett, S., Beaumont, C., and Fullsack, P., (1993), Mechanical model for the tectonics of doubly vergent compressional orogens: *Geology*, v. 21, p. 371–374

CHAPTER 3

Morphology, present-day sediment dispersal system, and Late Quaternary depositional sequences along the Montenegro/N. Albania Continental Margin

3.1 Introduction to scientific papers

We used high-resolution morphobathymetric and seismic reflection data to describe morphology and the Late Quaternary stratigraphy of the MACM. Furthermore, intensive sampling of the seafloor sediments, and gravity cores collected in key sectors of the margin enabled us to ground-truth geophysical data and to estimate ages of deposits using AMS ^{14}C and ^{137}Cs and ^{210}Pb chronology.

In paragraph 3.2, high-resolution multibeam morpho-bathymetric maps and a dense-spaced grid of seismic reflection profiles show relict geomorphological features along the Montenegro/Northern Albanian Continental Margin. These morphologies appear controlled by sedimentary processes such as progradation at river outflows, erosion, and reworking of sediments by longshore currents, as well as by gravity-driven process caused by sediment loading and earthquake shaking. Physiographic domains along this shelf-slope margin include an inner and an outer shelf, separated by two major topographic highs, the Kotor and the Bar ridges; a drowned lobate delta formed during the last phase of sea level fall, likely fed by the Buna/Bojana drainage basin and a continental slope affected by gravity-driven faulting and mass-wasting processes. Seafloor reflectivity maps, ground-truthed by grain-size analysis of bottom sediments, reveal that fine-grained deposits accumulate in the inner shelf, while other sectors appear starved. The effects of the last sea level rise is testified by the presence of seabed forms diagnostic of erosion or depositional processes, such as large dunes, sediment ridges and sediment waves, were also studied to infer the effect of bottom currents under the present-day oceanographic regime and in the recent past.

In paragraph 3.3, the analysis of high-resolution seismic reflection profiles and core samples shows that the latest post-glacial mud wedge is confined into mid-shelf basins partially bounded toward sea by tectonic highs, while the outer shelf exposes low stand deposits locally covered by a thin veneer of Holocene mud. The oldest deposits encompasses four major seismic sequences marked by forced-regression units deposited during Marine Isotope Stages (MIS) 10,8,6 and 2. Position and age of buried shorelines of the four latest low stand phases indicate that the outer shelf subsidence rate was about 1.2 mm/yr during the last ~350kyr, while a morphological analysis operated on the present depth of the LGM paleoshoreline suggests that this sector was uplifted of several tens of meters during the last ~20 kyr.

Finally, in the last work (paragraph 3.4) the geochemical and sedimentological character of seafloor sediments sampled from two major Holocene depocenters in the continental shelf, suggests that present-day accumulation takes place with rates ranging from 1-2 mm/yr and is mostly supplied by the Buna-Bojana outflow. An important role is played by tectonic deformation, that creates accommodation, and by the longshore current system, whose prevalent direction is from S to N.

We discuss these topics in three scientific papers, two already submitted to international journals, and one in preparation:

- 1) **Seafloor morphology of the Montenegro / N. Albania Continental Margin (Adriatic Sea - Central Mediterranean).** Del Bianco F., Gasperini L., Giglio F., Bortoluzzi G., Kljajic Z. and Ravaioli M. - Submitted to *Geomorphology*
- 2) **The stratigraphic architecture of the Montenegro/N. Albania Continental Margin (Adriatic Sea - Central Mediterranean).** Del Bianco F., Gasperini L., Angeletti L., Giglio F., Bortoluzzi G., Montagna P., Kljajic Z. and Ravaioli M. - Submitted to *Marine Geology*.
- 3) **Present-day sedimentation patterns along the Montenegro/N. Albania Continental Margin from geochemical analysis (Adriatic Sea - Central Mediterranean).** Giglio F., Del Bianco F., Gasperini L., Bortoluzzi G., Albertazzi S., Kljajic Z., Castelli A. and Ravaioli M. - In preparation.

3.2 Seafloor morphology of the Montenegro/N. Albania Continental Margin (Adriatic Sea - Central Mediterranean)

Del Bianco F., Gasperini L., Giglio F., Bortoluzzi G., Kljajic Z. and Ravaioli M.

Abstract

High-resolution multibeam morpho-bathymetric maps and a dense grid of seismic reflection profiles show relict and palimpsest geomorphologic features along the Montenegro/Northern Albanian Continental Margin. This sector of the Eastern Adriatic shelf, at the external front of the Dinarides Chain, is characterized by highly variable seafloor patterns and depositional styles, and shows a peculiar alternation of large-scale troughs and ridges, probably caused by tectonic compressive deformations. These tectonically controlled morphologies are overprinted by sedimentary processes such as progradation at river outflows, erosion, and reworking of sediments by longshore currents, as well as by gravity-driven process caused by sediment loading and earthquake shaking. Physiographic domains along this shelf-slope margin include (i) an inner and an outer shelf, separated by two major topographic highs, the Kotor and the Bar ridges; (ii) a drowned lobate delta formed during the last phase of sea level fall, likely fed by the Buna/Bojana drainage basin and (iii) a continental slope affected by gravity-driven faulting and mass-wasting processes. Seafloor reflectivity maps, ground-truthed by grain-size analysis of bottom sediments, reveal that fine-grained deposits accumulate in the inner shelf, while other sectors appear starved. The effects of the last sea level rise is testified by the presence of seabed forms diagnostic of erosion or depositional processes, such as large dunes, sediment ridges and sediment waves, were also studied to infer the effect of bottom currents under the present-day oceanographic regime and in the recent past.

1. Introduction

Seafloor morphologies are shaped by a number of natural processes such as longshore currents, earthquake shaking, sediment overloading, and tectonic deformation. The first step in the geological study of continental margins is to characterize incipient or active processes that control their physiography. This is generally achieved using high-resolution morpho-bathymetric maps, that could highlight the occurrence of active, relict or palimpsest deposits (Swift, 1972) than can be discriminated based on diagnostic morphologies, and high-resolution seismic reflection profiles, that give information on the internal architecture of sedimentary bodies including reflectivity and facies analysis. These geophysical “indirect” data should be subsequently ground-truthed by direct sampling of the seafloor.

Seabed morphologies along continental shelves closely reflect sedimentary deposits that might record the effects of global scale processes, such as sea level changes. An important role played by Quaternary high-frequency sea level changes over sediment distribution at continental margins is also the case of the Adriatic Sea, where the Montenegro/Albanian Continental Margin (hereafter called MACM) is located. In fact, due to the low topographic gradients, the eustatic changes caused broad horizontal shifts of the coastal zones in such area. These shifts, in turn, are also recorded by morphological features created by bottom-currents, whose distribution reflects changes in sediment input and current-regime caused by sea level variations. Relict or active current-related sedimentary features are widely described in the worldwide shelves, and include sediment wave fields, sediment drift, and moats particularly developed where the seafloor gradient changes occur (e.g. Roberts and Kidd, 1979; Cavaleri and Stefanon, 1980; Kenyon, 1986; Faugeres et al., 1993; Howe et al. 1994; Howe, 1995; Correggiari et al., 1996; Stoker, 1998; Masson et al., 2002; Reeder et al., 2002; Viana, 2002; Verdicchio et al., 2007). In most of these case studies, the presence of diagnostic morphologies at the seafloor allows to infer natural process and reconstruct paleoceanographic evolution, identifying phases of intensification of relaxation of the bottom-hugging contour-parallel currents (Marani et al., 1993; Roveri, 2002; Verdicchio and Trincardi, 2008).

We present the results of a geomorphological study of the MACM (Fig. 1) which is based on recently collected multibeam bathymetric maps and high-resolution seismic reflection profiles and accompanied by a preliminary analysis of sampled seafloor sediments. Although the western Adriatic shelves have been intensively investigated and are now covered by dense marine geological/geophysical data, including swath-bathymetry, sediment samples and sub-bottom profiles, the eastern sector remains, to date, almost unknown. We collected on the MACM a new dataset in the framework of the ADRICOSM-STAR Project with the financial support of the Italian Ministry for

the Environment, Land and Sea and the coordination of CMCC. The aim of this project was to fill this gap by gathering marine geological/oceanographic and biogeochemical data, which were collected during several expeditions organized starting from 2008. Part of these data are presented and discussed here.

2. Geological and oceanographic setting

The MACM is located in the southeastern Adriatic Sea, a semi-enclosed basin elongated in NW-SE direction over a 800x200 km surface and showing a remarkable variability in continental shelf and slope morphologies. The Northern Adriatic is flat and shallow (average depth 70 m) whereas the Southern Adriatic is deeper and morphologically more complex. The deepest reaches down to 1200 m, are in the South Adriatic Depression (SAD) between the Apulian Platform and the Montenegro/Albanian Continental Margin (MACM) (Fig. 1). Along the MACM the prevailing longshore current direction is, according to Poulain (2001), from S to N (Fig. 1). Marini et al. (2010) describe The South Eastern Shelf Coastal Current (SESC) characterizes the oceanographic regime of this region; it detaches from the coast in correspondence of the Buna/Bojana outflow and forms coastal eddies expanding offshore, resulting in a local complexity of the water circulation, both at the surface and close to the seafloor, that may result in adjacent areas of erosion and deposition within short distances (20-30 km). As shown by circulation vectors of Fig. 1, areas where deposition of sediments is favored should coincide with the centers of local eddies, i.e., the Gjiri-Rodonit Bay, and the inner shelf between Budva and Bar.

The MACM encompasses the external front of the Dinarides/Albanides fold-and-thrust belt (Aliaj, 1999; 2000) whose tectonic deformations affect the shelf and continental slope. Tectonic structures forming the external boundary of the NE convergent Adria microplate show a NW-SE orientation, parallel to the coastline, although strike-slip transverse faults are also present (Fig.1). This margin is characterized by intense seismic activity and has been site of large historical earthquakes (Pondrelli et al., 2006).

3. Methods

Marine geophysical data and sediment samples were collected during six oceanographic expeditions onboard R/V Dallaporta, (Star08), R/V Urania, (ADR02_08, 2008; MNG01_09, 2009; MNG03_1, 2010; MNG04_10, 2010) and R/V Mariagrazia (MNG02_09). Technical reports of these

cruises are available online (<http://www.ismar.cnr.it/prodotti/reports-campagne>). Swath bathymetry data were collected using a Reson 8160 multibeam echo sounder in ADR02_08 expedition; a Kongsberg EM-710 onboard of R/V Urania and a Kongsberg EM3002 double head multibeam, onboard of R/V Mariagrazia. High-resolution seismic reflection profiles were collected using a hull mounted 16 transducer Benthos Chirp II sub-bottom profiler (2-7 kHz frequency) and a towed Sparker system, a Geo-Source 200 (200 tip electrode modules) operated with Geo-Spark 1000J solid state pulsed power supply. Positioning was corrected for the offsets between DGPS antenna and transducers using gyro-compass and CMG data and provides an accuracy of 1 m.

Because of the relatively limited ship-time compared to the extent of the area, mostly characterized by shallow waters that do not favor full multibeam data coverage, the swath-bathymetry map does not cover the entire shelf. For this reason, we focused our acquisition on those areas characterized by complex seafloor morphologies as possibly diagnostic of relevant geologic processes. Reflectivity information of the seafloor was obtained by chirp profiles analysis using the open software package SeisPrho (Gasperini and Stanghellini, 2009). This parameter was used in conjunction with a qualitative analysis of acoustic facies, following the approach proposed by Damuth (1980), and “ground-truthed” by grain-size determinations of seafloor samples. Processing and interpretation of seismic reflection profiles, as well as reflector picking and correlation and estimates of sediment thickness, were carried out using SeisPrho. Most maps were created using GMT (Wessel and Smith, 1998), also employed for spatial data gridding.

A 40 cm diameter box-corer was used to collect bottom sediment samples that have been consequently sub-sampled using short liners. Grain size analyses were performed with a pre-treatment with H₂O₂ to remove organic matter, dried at 60°C, a subsequent wet sieving at 63 µm to separate silty-clay fraction from sand. The former was further subdivided in silt and clay fractions by using a Micrometrics RX-5000D sedigraph. Sand fractions were sieved every half phi.

4. Results

We used high-resolution morpho-bathymetric data and seafloor reflectivity maps compiled after analysis of chirp-sonar sub-bottom profiles, to describe the seabed morphology and acoustic patterns of the MACM, which appears quite variable at a variety of spatial scales. The high-resolution morpho-bathymetric seafloor images, do not cover the whole extent of the shelf margin (Fig. 3). Some sectors, only partially covered by multibeam data, were analyzed using high-resolution chirp-sonar profiles, which give only partial information regarding seafloor morphologies. Chirp-sonar profiles

have shown different degrees of penetration in the sub-bottom due to the variable distribution of unconsolidated sediments, and to the presence of outcropping high-reflectivity deposits. We combined analysis of morpho-bathymetric maps and acoustic facies of the uppermost deposits penetrated by seismic reflection profiles, to classify different sectors of the MACM.

4.1 Acoustic seafloor characterization

The high repeatability of the chirp-signal source enabled us to evaluate seafloor reflectivity patterns along the shelf and the upper slope. Reflectivity maps were analyzed in combination with the analysis of acoustic facies observed in chirp-sonar profiles, following the approach proposed by Damuth (1980). Four seafloor types are present (Fig. 2), each corresponding to a characteristic pattern.

- 1. Low reflectivity:* maximum penetration of the signal within the transparent substratum, smooth topography, and well defined internal reflectors with an overall parallel stratification related to the uppermost seismic unit; sediment samples analysis indicate the presence of fine grained sediments at the seafloor (silty clay and clayey silt). In the inner shelf, we found two distinct areas showing these characters, i.e., off Kotor and the Buna/Bojana River outflow (Fig. 2). We observe a similar pattern of reflectivity/acoustic facies along the upper slope, where penetration of the signal progressively increases basinward.
- 2. Medium reflectivity and rough sea floor:* medium to low penetration below the seafloor, highlighting complex internal geometries and angular unconformities of the uppermost seismic unit. This pattern characterizes three sectors of the margin: 1) the offshore of Boka Kotorska Bay; 2) the inner shelf of the Central Area between the coastline and the system of a ridges parallel to the shore; 3) the outer shelf of the Southern Area. While in the Northern Area we observe prevailing complex internal geometries diagnostic of erosion at the seafloor, in the southern areas, characterized by medium reflectivity, the uneven morphology seems related to mass-wasting processes such as submarine sliding, debris flows and possible creeping.
- 3. Medium to high reflectivity:* rough and irregular sea floor morphology, low penetration of the signal in the substratum, constituted by probably dominant over-consolidated sediments. In the Northern Area, we find this type of bottom along the inner scarp, in a narrow sector located landward of the Kotor Ridge, while in the South it characterizes most of the external inner

shelf.

4. *High reflectivity*: very rough and irregular sea floor, with outcrops of rocks or diagenetically altered sediments. Heavy erosional features are common, and we observe minimum or no penetration of the signal in the substratum; for this reason, internal geometries are hardly observable. This pattern is found in correspondence of the structural highs (Kotor and Bar ridges) and in the southeastern sector near the Gulf of Drini.

Over 80 sediment samples collected in different sectors of the MACS were analyzed for grain-size (Table I). Sediment was classified based on different contents of clay, silt and sand, according to the Shepard Classification (Shepard, 1954), and plotted in form of color-coded circles (Fig. 2). This map integrates a number of seafloor observations carried out in different areas along the MACM. Two main sectors characterized by low-reflectivity and associated smooth topography are observed offshore Kotor and the Buna/Bojana outflow, in the northern and southern portions of the study area, respectively (yellow sectors in Fig. 2). A good matching is found between the low-reflectivity areas and the occurrence of silty-clay/clayey silt at the seafloor (red and blue circles) and particularly in the prodelta area located in front of the Bojana River. This prodelta area passes gradually to coarser sediments (sand and silt) closer to the coastline. We observe a similar pattern in the northern area, offshore Kotor, where, however, only one sediment analysis is available to validate geophysical observations.

4.2 Morpho-bathymetry

The shelf is characterized by two major morphological domains: an *inner scarp*, at depths between 100 and 130 m, and an *outer scarp*, between 220 and 230 m of water depth (Figs. 2 and 3). These features separate the shelf into two relatively flat areas, an *inner* and an *outer* shelves, characterized by different patterns of seafloor morphology (Figs. 2 and 3). Seaward of the outer shelf, along the continental slope, topographic gradients increase progressively, and we observe gullies and incisions perpendicular to the margin (heads of canyons) from -420 m, sloping down to the -1200 m of the SAD. Our data image only the uppermost part of the slope, landward of the canyon heads, and we refer to this sector as the *upper slope*.

In the Northern Area (Figs. 2 and 3), the *inner scarp* develops parallel to the coastline and bounds a narrow shelf that reaches here its minimum width (12-17 km). It shows an average slope of about 4.5° and runs parallel to the coast. About 30 km toward the southeast, its morphological expression progressively decreases, until it gradually disappears becoming flat (Figs. 2 and 3).

Moving further toward the SE, the inner scarp starts running N-S, almost perpendicular to the margin, and becomes the N side of a lobate feature that occupies the southern inner shelf and reaches its maximum extent (about 45 km) in correspondence of its maximum width (Figs. 2 and 3). Here, the seafloor is rough, and displays a suite of different morphologies that will be analyzed in more detail below. Seaward of the inner scarp, we note that the *outer scarp* constitutes the shelf-break. In the northern sector the *outer scarp* is rectilinear and continuous, although it is intersected by a series of extensional fractures/faults oriented WNW-ESE (Figs. 2 and 3), while towards S it becomes arc-shaped and runs parallel to the inner scarp lobe, becoming gradually steeper. From about 41°20' toward south, it disappears in a rough seafloor.

The *inner shelf* shows alternating flat and rough morphologies, developing in a generally flat area with low topographic gradients ranging from 0.1° in the N, to 1.3° towards S (Figs. 2, and 3). In the NW sector, the inner shelf appears concave upward, forming a sort of trough. Here we observe a complex morphology made of alternating ridges and troughs oriented N-S and another set of elongated mounds parallel to coast (Fig. 4). Toward the south, we observe sediment-waves fields and erosional scars (Fig. 6).

The *outer shelf*, between the inner and the outer scarps, shows a flat topography gently dipping towards sea, with average slopes between 0.3 and 0.6° and depths ranging from 220 to 230 m. The seafloor is rather flat, except for the southern sectors, where there are evidence of gravity-driven processes (see next section).

The *upper slope* is characterized by a variety of morphological features. As the topographic gradients exceed 1–1.3°, we observe an increasing seafloor complexity due to the presence of a system of extensional faults that run parallel to the outer scarp (Figs. 2 and 3). Starting from the north, we observe two different patterns: 1) extensional faults and trenches parallel to the isobaths; 2) a system of arc-shaped trenches cutting through the outer scarp and displacing the seafloor by several meters. Here, two major steps oriented ENE-WSW offset the seafloor along the continental slope by about 10 m (see section 3.5 for more details). We focused our observations in four sectors of the MACM: two inner shelf areas, offshore Bokakotorska Bay (Fig. 4) and Bar (Fig. 9); a sector of the southern outer shelf/upper slope characterized by “Medium reflectivity sea floor” (Figs. 2 and 3); a wedge-shaped lobate feature, occupying a large portion of the southern study area (Fig. 3, right).

4.3 The Bokakotorska offshore area

The continental shelf offshore *Bokakotorska Bay* (Fig. 4) is an area of about 54 km² showing four

domains with distinctive morphologies. From NE to SW, we note (Fig. 4): (1a) an elongated ridges area on the inner shelf; (1b) a large dune area close to the shelf-break; (1c) an area in the outer shelf with rough seafloor; (1d) a major topographic ridge (the Kotor Ridge).

(1a) This area is characterized by a field of elongated ridges striking from 115 to 124°, in a sector of the inner shelf stretching WNW-ESE over about 47 km² and between 110 and 125 m water depth. These ridges form a sort of chain 16 km-long, with crests spaced 200-300 m apart and with individual height of a few meters. The ridge crests are sub-parallel although they tend to slightly converge proceeding from ESE to WNW. The chirp profile MNG0209_33 (Fig. 5f2) documents a *wavy* upper sedimentary unit which includes two more prominent ridges in the NE sector; these features are asymmetric, with a shorter and gentler upslope flank and a longer and steeper downslope flank. In this section, the internal reflector geometry within the bedforms suggests an upslope migrating pattern changing progressively into a sub-parallel stratified deposit. This wavy unit is bounded at its base by an erosional surface showing erosional truncation (Fig. 5f2) that is marked by an high-amplitude and irregular reflector. The aggradational bed forms follow the pre-existing morphology of the underlying unit. Due to the presence of these transparent deposits at the seafloor this area is included in the *low reflectivity* class, while the grain-size analysis of the seafloor samples indicates silty-clayey sediments (Fig. 2).

(1b) The central sector of the *Bokakotorska* offshore area (bounded with a blue line in Fig. 4) is characterized by the presence of large dunes showing a variable degree of asymmetry as well as orientations. This sector extends on the inner shelf for about 28 km² with a N-S direction, in water depths ranging from 106 to 120 m, and is organized in a variety of distinct elongated bedforms. We observe six N-NNW trending major dunes, sequentially numbered 1 to 6 from West to East (Fig. 4a), showing low-sinuosity crests slightly diverging towards the North, that can be traced continuously over up to 6 km. Spacing between crests is variable and progressively increase towards SE, from 380 m to over 1 km. In cross section (profile ALT_354 in Fig. 5d), the dunes show a clear asymmetry, with steeper flanks (1.5° to 4°) facing westward while gentler slopes characterize the eastern flanks (about 0.6°). Maximum wave heights over 10 m are reached in the more external sector (Fig. 5e), matching the buried anticlines axis (red-white line in Fig. 4b), where the dunes are more pronounced and well developed. Landward, the dunes become progressively smoother, and in the NE sector appear covered by the low-reflectivity *wavy* upper unit described in the previous section. Chirp-sonar profiles MNG0209_033 and KOT_42 collected in the inner part of this sector (Fig. 5, f and c), show that the innermost ridges n. 5 and 6 are covered by acoustically transparent deposits overlapping a lower more reflective feature. This buried feature is well visible on MNG0209_033 (Fig. 5f1, detail) where, in correspondence of dune n. 6, we observe the sharp transition between the buried, more

reflective dune top and the transparent unit made of fine-grained deposits above. This “overlapping zone” between different bottom features is only present at the northern boundary of the large dune domain marked by a light green area in Fig. 4b. The deep base of dune n.6 is marked by an irregular reflector indicating a high contrast of acoustic impedance. However, this surface is not flat (Fig. 5f,f1), and this could indicate that these dunes are superimposed over outcropping seafloor morphologies exhumed by erosional processes. In the same figure, the internal geometry suggests the presence of an overlapping trend of different buried dune-like features. Moreover, we observe that this coincide partially with the “overlapping zone”. The NW-SE trending Chirp-sonar profile ALT_354 (Fig. 5d) crosses perpendicularly the ridges, not penetrating the seafloor because of its relatively high reflectivity. However, in this profile, as for KOT_42 (Fig. 5c), limited zones of enhanced penetration of the signal it is possible to discern a sub-horizontal reflector at the base of ridges 3 and 4. This reflector was picked and correlated over the entire area as shown by the blue dotted line in Fig. 5a,b,c,d,e,f,g1.

(1c) The westernmost sector of the *Bokakotorska offshore* area is characterized by a very *rugged seafloor region* (Fig. 4b) related to the presence of small ridges and aligned bioherms (sampled during MNG02_09 oceanographic cruise). This is a narrow and elongated area extending for about 14 km² in WNW-ESE direction, with water depths ranging from 124 and 140 m. Multibeam bathymetry displays a peculiar rugged seafloor that corresponds, in the chirp-sonar profiles, with an erosional truncation. In Fig. 5a, b, seismic profiles KOT_36 and CAL_10 highlights the presence of such truncated reflectors and of the bioherms, that display hyperbolic scattering of the seismic signal. The alignment of bioherm barriers continues outside this area and is also visible in the *sediment ridges* sector (Fig. 4a).

(1d) The external sector of the *sediment ridges field* and the *rugged seafloor region* are located on a major topographic high, the Kotor Ridge (Fig. 4b). The latter coincides with the *inner shelf* external boundary, immediately landward of the *inner scarp*. It develops parallel to the coastline and its morphologic expression is visible for about 8 km above the seafloor. Its seaward flank corresponds to the inner scarp, with an average slope of 4.5°. The land-facing flank is less steep, with slopes ranging between 0.1-0.2° in the central sector of the inner shelf. On chirp profiles KOT_36 and CAL_10 in Fig. 5a, b we note that the Kotor Ridge is located on top of a layered folded structure. Its internal geometry is best visible in the Sparker profile MNG11_02 (Fig. 5g) where we observe an asymmetric fold with a marked erosional unconformity (drawn by a red dotted line in Fig. 5g) at its top. This is an anticline structure with the seaward facing flank steeper and a flexural bending on the opposite side.

(1f) Finally, there are three well-defined sectors characterized by general NW-SE trending

complex morphological features showing internal sediment layering, in Fig. 4b bounded by white lines, and partially crossed by chirp sonar profile in Fig. 5a,b. These sedimentary bodies grow up over the same reflector (blue dotted line) that characterizes the base of the large dunes field.

4.4 The offshore Bar area

This is an area on the shelf about 80 km² wide (Fig. 6) gently dipping towards west and characterized by two distinct sectors displaying peculiar morphologies: (2a) a field of sediment waves; and (2b) two elongated ridges showing a very rough topography at their top. Most part of this area falls in the “Medium to high” and “High” classes of seafloor reflectivity (Fig. 2).

(2a) the sediment waves field, about 50 km² wide (delimited by a blue line in Fig. 6b), lays in water depths ranging between 80 and 120 m. The field is bounded towards the west by the inner scarp, and is separated by another secondary scarp that forms a terrace with sediment waves located near its seaward edge. The wave crests show a constant sinuosity and an average orientation of 75°(about E-NE). In the southern sector the crests reach the maximum extent and can be traced continuously for about 3-4 km. Wavelengths varies from 142 m to the north, to 115 m to the south, and amplitudes are between 1 and 4 meters. In cross section the northern flank of the waves appear generally steeper. Chirp sonar profile MNG0209b_21-10 as well as MNT_103 and ALT_290 in Fig. 7, cut through the wave fields without imaging internal geometries due to the high reflectivity of the seabed. Only the chirp profile MNG0209b_21-10 (Fig. 7a) crosses the waves with a high angle, highlighting the asymmetry of the waves, with steeper northern flanks. This asymmetry is appreciable also in the multibeam maps. Two sediment sampling stations on top of these waves (A49 and A48 in Table I) collected clayey silt and silty clay, from the crests and the troughs, respectively, indicating that these features are covered by a thin veneer of fine-grained sediment not visible in our seismic images.

(2b) In this sector, a couple of elongated ridges are visible (Fig. 9), covering about 20 and 11 km² each. They are aligned along a 120°N direction. The NW ridge shows an elliptical base, 7x3 km wide, and reaches several meters of elevation relative to the adjacent seafloor. From multibeam data its top appears irregular and patchy. Chirp-sonar profile MNT_095 (Fig. 8) crossing orthogonally this ridge shows a high reflectivity pattern, with poor penetration of the signal, and its flanks are partially covered by an onlapping transparent unit. The ridge corresponds to the “high reflectivity/rocky” seafloor of Fig. 2 map. The SW ridge (Fig. 6) is 7x2.2 km wide and reaches about 20 m above the seafloor. Its top appears dominated by erosional features and shows a very rough and irregular seafloor, as shown also in chirp profile of Fig. 9. Between the two aligned ridges, in a water depth ranging between 105 and 160 m, the seafloor appears irregular and patchy for an area of about 3 km².

The peculiar morphology of the eastern ridge is due to the presence of several aligned reliefs (Fig. 6) forming a sort of double concentric terrace with oblique flanks bounding an intermediate flat zone, as visible also in chirp-sonar profile MNT_114 (Fig. 9). This profile shows a high reflectivity seafloor; its internal geometry is only visible in a small “acoustic windows”. In this way, we observe the opposite dip of the internal reflector between the ridge flanks. This sector is included in the “high reflectivity/rocky” seafloor class of Fig. 2. The deeper stratigraphy of this sector is imaged by sparker profile MNG11_04 (Fig. 10) running between the two ridges. It shows that both ridges form along the same buried anticline similar to that forming the Kotor Ridge. Also this buried anticline, called Bar anticline, shows an heavily eroded top, marked by a high reflectivity seafloor. In Fig.10 sparker profile, a circular mounds is observed, about 220 m in diameter and elevated of 25 m above the seafloor. We note that this prominent feature is centered in the nucleus of the Bar anticline, suggesting a diapiric formation. Both observed ridges in offshore Bar area have similar morphologies and internal structures and are referred to as a single structure we called the Bar Ridge.

4.5 The outer shelf / upper slope area

Along the southern outer shelf we observe rough and patchy seabed morphologies, made of buried mass-wasting and mass-transport deposits (Fig. 2 and 3). This is particularly evident on chirp profiles SL3 (Fig. 11b) crossing orthogonally this sector. This profile show that the outer shelf is characterized by a set of minor morphologic scarps characterizing an irregular seafloor and that this is the top of transparent, well-layered deposits. Below of this deposit several interlayering bodies appear composed of discontinuous to chaotic deposits probably reflecting ancient mass-transport processes (Fig. 11b). Similar features have been described on the western side of the Adriatic Sea (Trincardi et al., 2004) and, more recently, on the Eastern Niger Delta at the front of a delta prograding wedges (e.g. Garziglia et al., 2010). In the SE portion of this area, immediately landward of the inner scarp between inner and outer shelf, a chaotic seafloor pattern (Fig. 3) is indicative of the occurrence of irregular blocks distributed along the scarp face. In profile SL4 (Fig. 11c), the seismic-reflector geometry shows the presence of oblique to tangential clinoforms. This evidence suggests that they were part of a partially dismantled clinoform's topset. In the same profile, the diffuse presence of chaotic deposits in the prograding body (depicted in Fig.11c as “Paleodelta system”) suggests either fossil or incipient gravity-driven instability.

In the northern MACM, seaward of the outer-shelf scarp and along the *upper slope*, we observe increasing topographic gradients ($>1^\circ$), and two distinct areas of deformation (Fig. 2). The first set includes relatively shallow structures that develops parallel to the *outer scarp*, or along directions

striking about NNW-SSE. Seismic profile SL1 (Fig. 11d) shows examples of such features (marked as group 1 deformations), which lead to extensional fracturing of the sedimentary sequence. We assume that these deformations are mainly driven by slope instability, since they develop perpendicular to the direction of maximum gradient. The second group of deformations (Figs. 2 and 11d) affects deeper sediment layers, producing vertical displacements in the order of 20 msec TWT. This deformation area shows an average orientation parallel to the regional tectonic features (Fig. 1), and cut through the entire sedimentary sequence (Fig. 2 and 3), thus pointing to extensional tectonic stress.

4.6 The drowned delta area

South of the Bar Ridge area, multibeam maps (Fig. 2 and 3b) highlight the presence of a wide multiple-lobe morphologic feature that extends southward for about 70 km along the shelf. In plain-view (Fig. 3b) this feature is bounded seaward by the *inner scarp* that becomes less prominent towards the South where mass-wasting deposits are present at the seafloor (Figs. 2 and 3). Seismic profiles SL2, SL3 and SL4 (Fig. 11) image internal architecture of this feature, made of transparent well-layered deposits forming oblique-tangential clinofolds showing offlapping geometries diagnostic of seaward progradation. Toward the outer-shelf, the topset of this prograding body appears heavily eroded. Shape, internal geometries and position relative to the coastline suggest that this feature formed as a river delta, abandoned because of the post-glacial sea level rise. Following the scheme by Galloway (1975) and subsequent modifications, we classify this feature as a lobate delta, typified e.g. by the Nile and Ebro deltas in the Mediterranean and characterized by high fluvial influence and sedimentary discharge.

Above this delta system, in the southern area is present a large sector characterized by the presence of N-S oriented, several meters high, ridges that disappear southward, approaching the inner scarp (Figs. 2 and 3). Observing the chirp profiles SL2 (Fig. 11a), these scarps correspond to outcropping eroded strata, corresponding to the erosional truncation at the top of low-angle-dipping clinofolds forming the paleodelta system. Locally are also visible small overlapping of transparent bodies (detail of Fig. 11a). Landward, patches of erosional remnants, showing a sub-parallel internal reflector pattern (Fig. 11a, c), overlap the top of paleodelta system. This area of the MACM corresponds to the *medium to high* area of seafloor bottom reflectivity and is bounded by sectors of *low-* and *medium-reflectivity* to the west and the south, respectively (Fig. 2).

5 Discussion and conclusions

A composite pattern of relic, palimpsest and active bedforms characterizes the seafloor on the shelf and the upper slope along the MACM. These features originated either through modern sedimentary processes, or from processes that were active during the last sea level lowstand some 20,000 years BP. In particular, a field of *elongated ridges (1a)* is visible in the northern sector, encompassing deposits of a well-defined, transparent seismo-stratigraphic unit. In agreement with its class of *low reflectivity* (Fig. 2) and internal well-stratified and parallel-to-wavy reflectors, this unit is made of fine-grained deposits; we assume it represents the Holocene mud wedge. As to the observed contour-parallel seafloor undulations, they are similar to correlative features in Late Holocene mud wedges observed in the W Adriatic shelf and in relatively shallow-waters by Correggiari et al. (2001) and Cattaneo et al. (2004), as well as in deeper environments such as the Bay of Biscay (Faugères et al., 2002). These authors interpreted these features as caused by the interaction between deposition, bottom-hugging currents and gravity deformation processes, such as localized syn-depositional deformation at different scales. They could be considered a sort of “multi-process” sediment waves, relatively common on the continental margin (Faugères et al., 2002). Considering that the wavy geometry refers to the entire involved unit reaching the seafloor, we considered these features presently active.

The large dunes (1b) area. Although presently available high-resolution seismic data do not allow for accurate 3-D geometry reconstructions and sediment sampling is very limited, an interpretation of the origin of these dunes should consider that their base constitutes a continuous high-amplitude and irregular reflector marking an erosional surface that outcrops on the seafloor along the -120 m isobaths (Fig. 5a,b,c,g1), the minimum eustatic level reached during the LGM (Lea et al., 2002). This lead to the conclusion that the base of the dunes was exposed to sub-aerial erosion until about 20 kyr (Rohling, 1998), and most probably the dunes field was formed soon after the LGM. The overlapping Holocene mud wedge, which represents the recent most deposit in the area provides another time constraint. Consequently, this large field of bedforms formed possibly as a coastal dunes partially reworked by marine processes and buried by transgressive deposits in a time interval from the LGM to the succeeding sea level rise. After the last transgression, these deposits were colonized by bioherms. This reconstruction shows similarities with the formation and drowning of the elongated dunes observed on the North Adriatic shelf in 24 m of water depth, offshore the Venice Lagoon (Correggiari et al., 1996).

The Kotor and Bar ridges (1d) (2b) are relevant morphological units observed along the MACM. From analysis of chirp sub-bottom and sparker profiles (Figs. 5, 8, 9 and 10) they display a deep tectonic control related to the presence of compressional features at the Dinarides front. Although the axis of these fold is not visible due to erosion at the seafloor, overall geometry and the

opposite dip internal reflectors suggests it could be a fault-propagation fold (Suppe, 1985). Consequently, we can assume that the Kotor and the Bar Ridges constitutes the surficial expression of a buried, deep-seated compressive tectonic feature. Moreover, these features are aligned, and show similar morphologies relative to the system of alternating ridges and troughs that marks the chain front onshore (Fig. 2). For this reason, the Kotor and Bar Ridges could be considered the offshore counterparts of these onland tectonic structures, which show evidence of ongoing compressive deformations.

Another important morphologic element constituting the shelf along the MACM is a *drowned paleodelta system*, identified in the southeastern sector. The shelf-break in this sector corresponds to the delta front. In seismic profiles (Figs. 11 and 12), it is marked by the clinoform breakpoint, located between 110 and 130 m of water depth. Being the -120 m isobath the level reached during the latest lowstand, about 18-15 kyr (Fleming et al, 1998) we might assume that the paleodelta formed during the Marine Isotopic Stage (MIS) 2 and that the clinoform breakpoint can be approximated, for this purpose, to the paleoshoreline during the Last Glacial Maximum (LGM), as described in the simplified sketch of Fig. 14. In this figure, the coastal physiography during the LGM is simplified, and we observe a shoreline about 45 km seaward relative to the present-day. The delta plain reached the present-day inner scarp, and the shelf break was located in correspondence with the modern outer scarp (section 3.2). Following classification described in Porebski and Steel 2003 and 2006, this represents a mid-shelf delta formed during the falling stage and the lowstand, where the lithosome did not reach the shelf break (Fig. 11b).

We may conclude that most of the MACM shelf and upper slope include depositional and morphological units that formed during the LGM or during intervals of the subsequent sea level rise and highstand, and are presently not in equilibrium with the modern sedimentary processes acting at the depths where they occur. The only exception is constituted by the area of elongated ridges (1b) where transgressive/high-stand deposits are reworked by bottom-hugging currents. These morphologies are exposed at the seafloor for the combined action of a relatively limited sediment supply, and the action of relatively efficient longshore currents, that enable only a thin veneer of high-stand Holocene mud to presently reach the outer shelf and upper slope.

Acknowledgements

We are indebted to officers, crew, and colleagues for their skilful cooperation during Cruises on board R/V *Urania*, *Mariagrazia* and *Dallaporta*. Partial funding was provided by ADRICOSM-STAR Project (ADRIatic sea integrated COaStal and river basin management system: Montenegro coaStal ARea and Bojana River catchment) with the financial support of the Italian Ministry for the Environment, Land and Sea and the coordination of *Centro Euro-Mediterraneo sui Cambiamenti Climatici* (CMCC). We thank M. Taviani for two sediment samples provided for this study, collected during ALTRO 2013 oceanographic cruise. We are grateful to A. Polonia for helpful discussion in the tectonic interpretation and to A. Correggiari for fruitful discussions about the large-scale bedforms. This is ISMAR-CNR scientific contribution no. XXXX.

Figures with caption

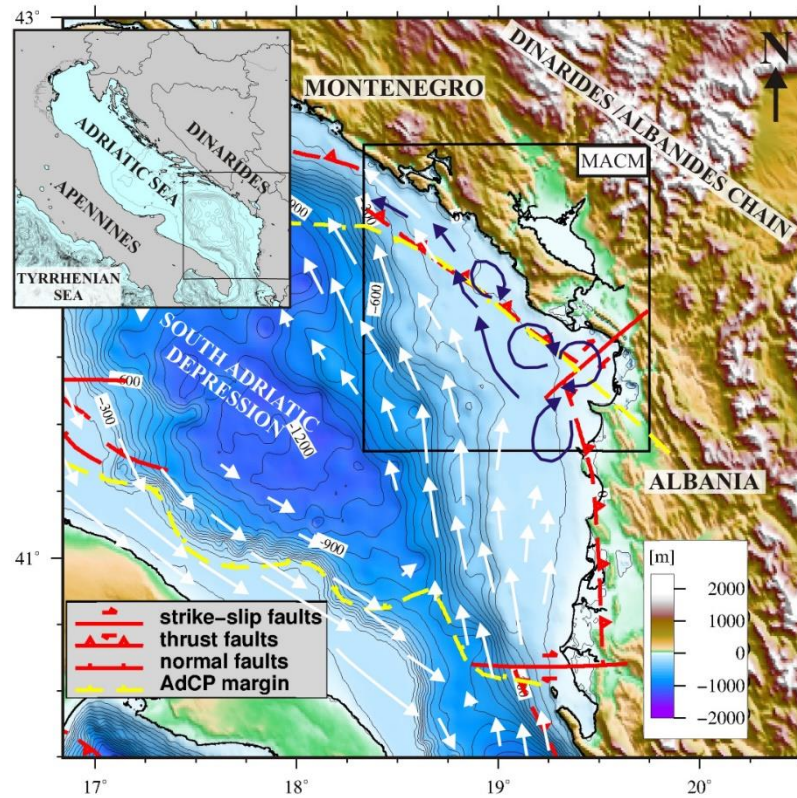


Figure 1. Geological and oceanographic setting of the South Adriatic Sea, with location of external thrust as limits of the Adria microplate (From Billi et al., 2007; G.M.O.T.M.; Dragičević and Velić, 2002; Vlahovic et al., 2005). Blue and white vectors indicate direction and intensity of regional and local currents, from Marini et al. (2010) and Poulain (2001), respectively. Black box indicates the Montenegro/N. Albanian Continental Margin (MACM).

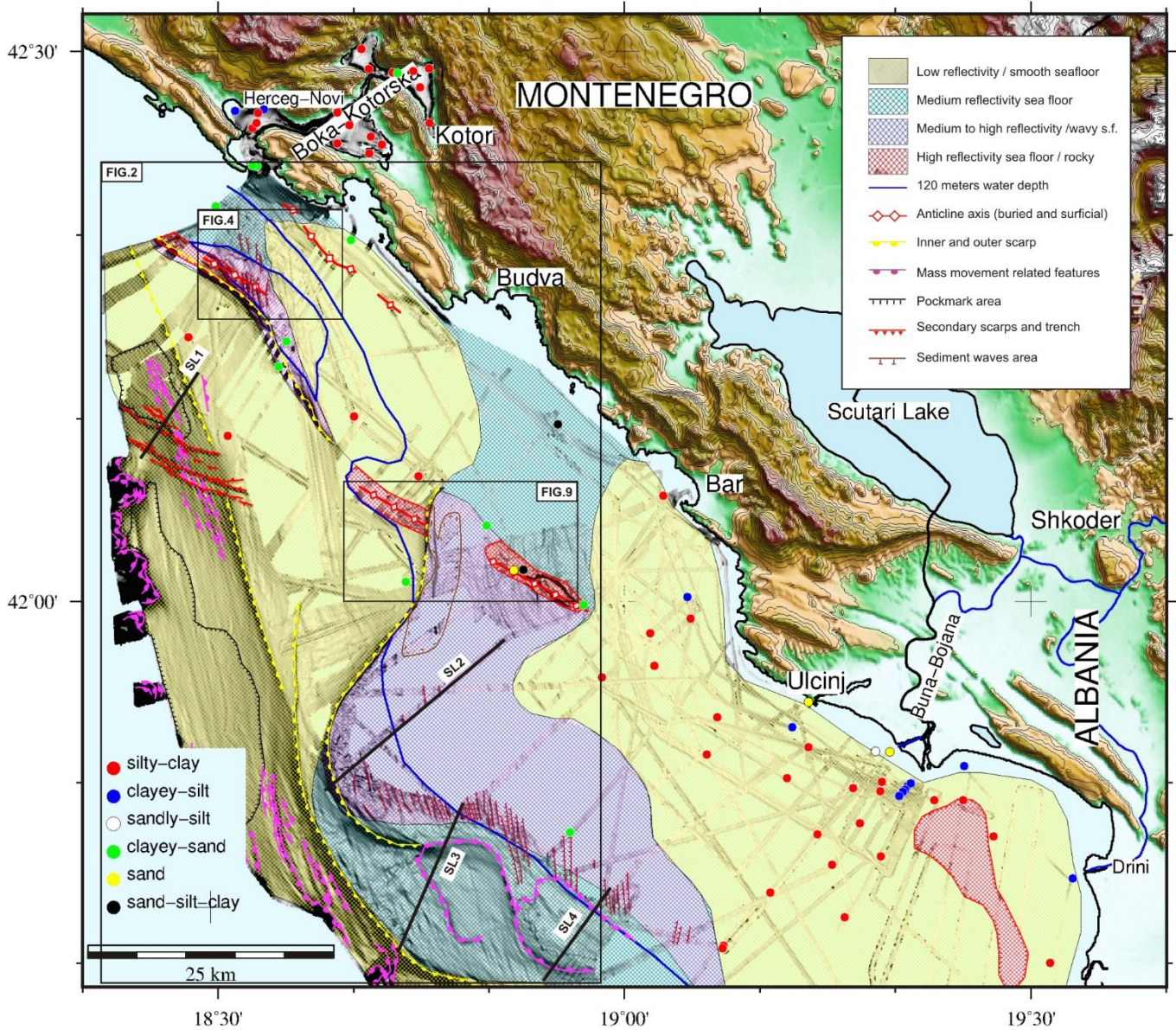


Figure 2. Seafloor characterization of the MACM superimposed over multibeam morphobathymetric map. Classes of color-coded seafloor type are based on integrated interpretation of reflectivity and sediment grain analysis of bottom samples (color-coded circles). Morphological features are indicated in the legend. Topography is from GEBCO 08 database.

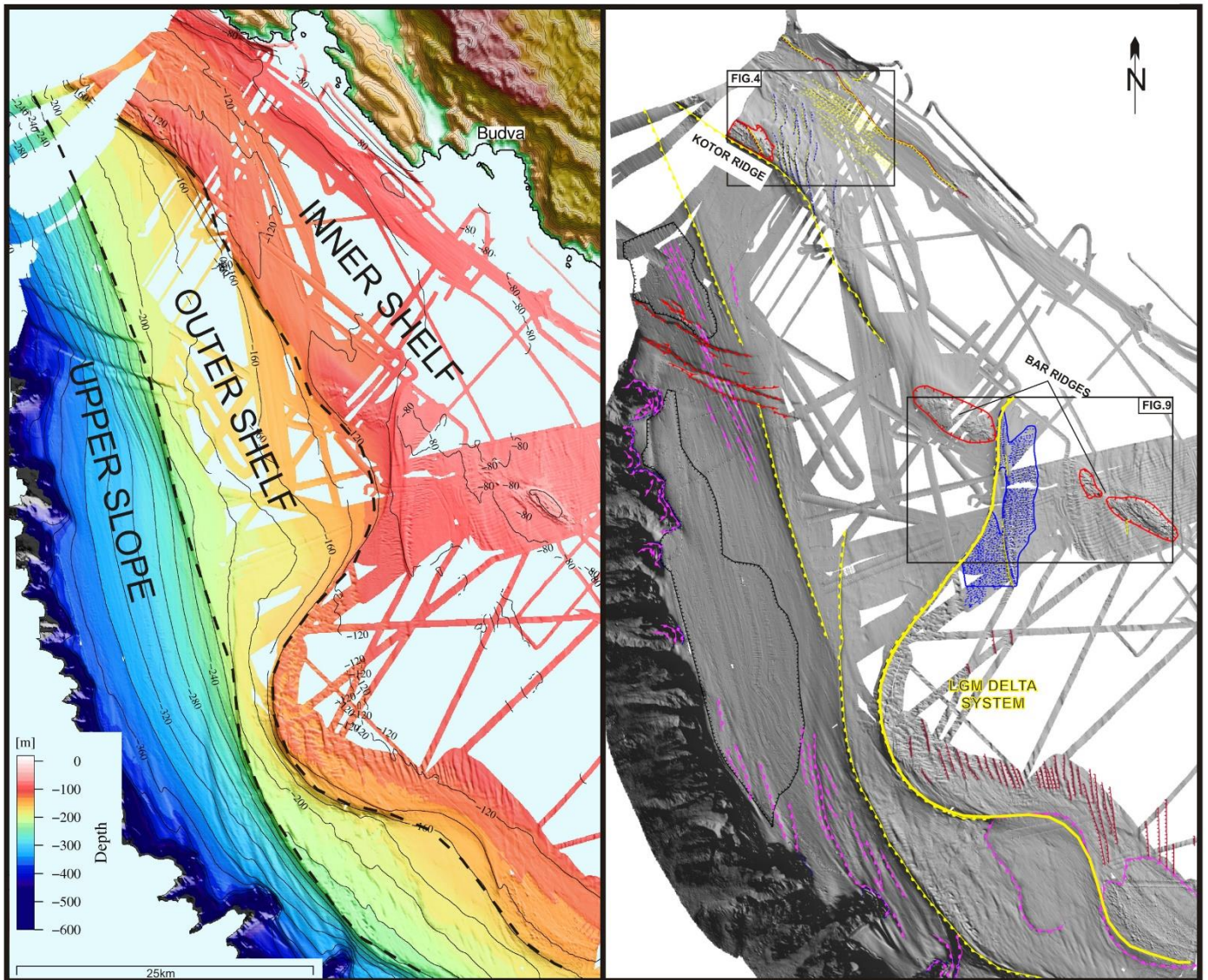


Figure 3. Left: shaded-relief, morphobathymetric map of the Montenegro continental shelf and upper slope. Depth contours every 20 m. Main physiographic elements are indicated. Right: slope map of the same region with major morphologic unit indicated for a better understanding, using the same symbology of Fig.2.

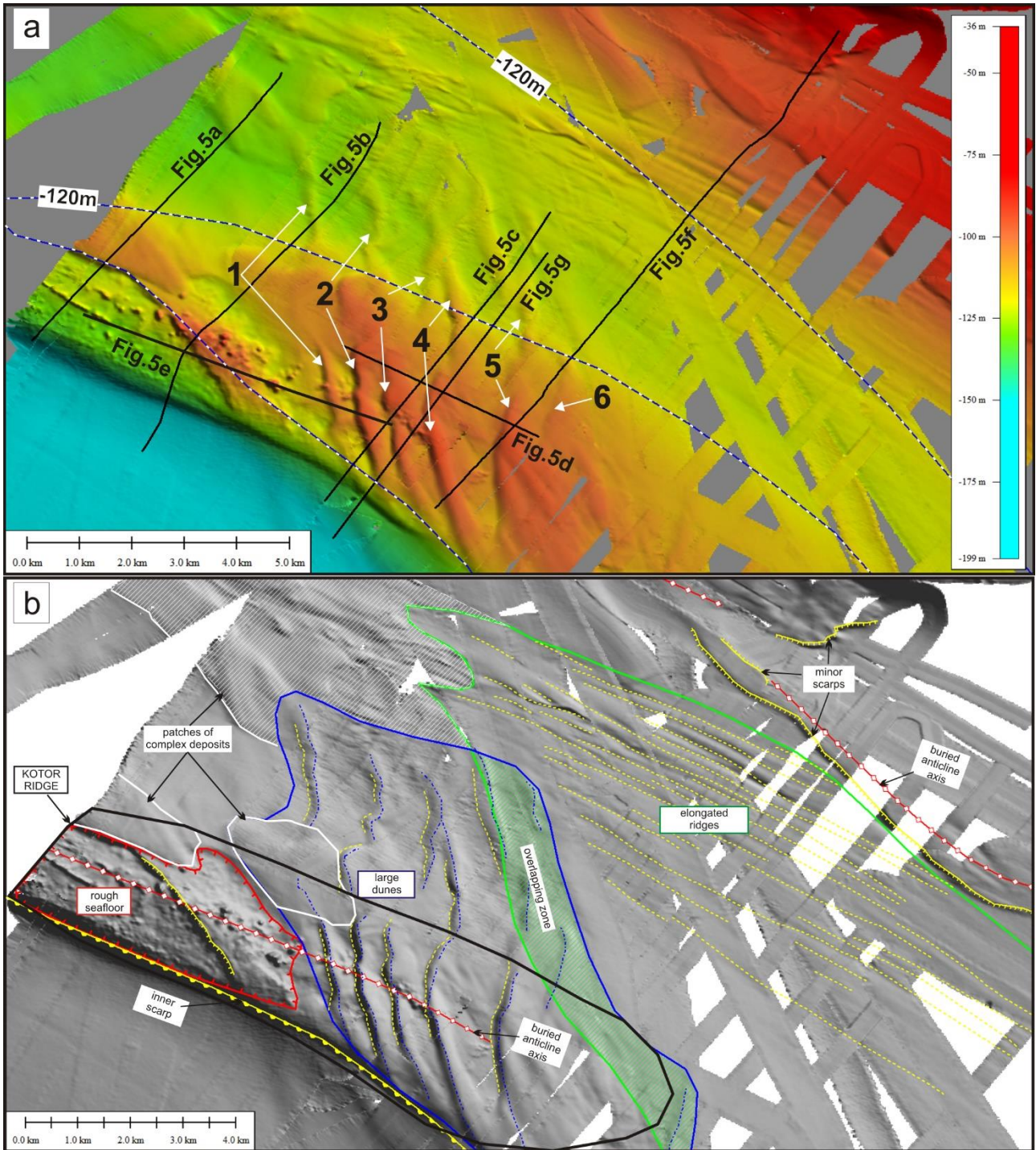
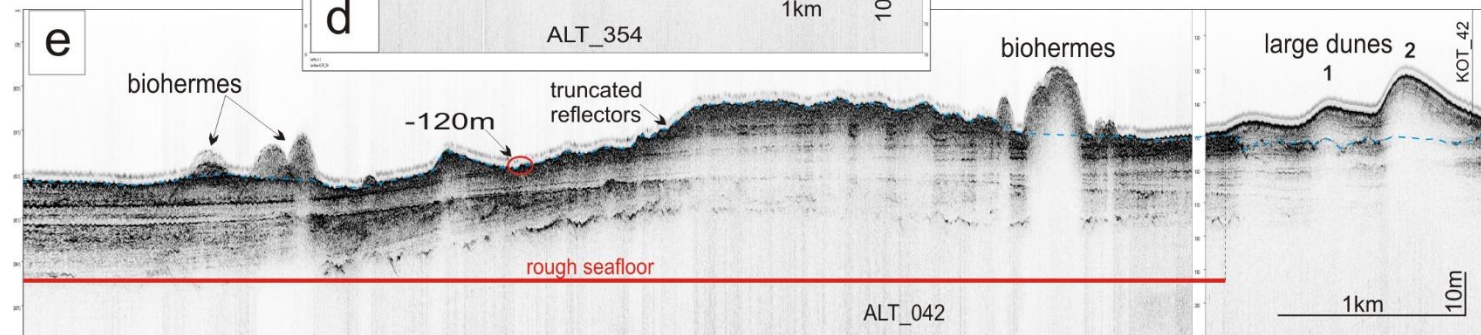
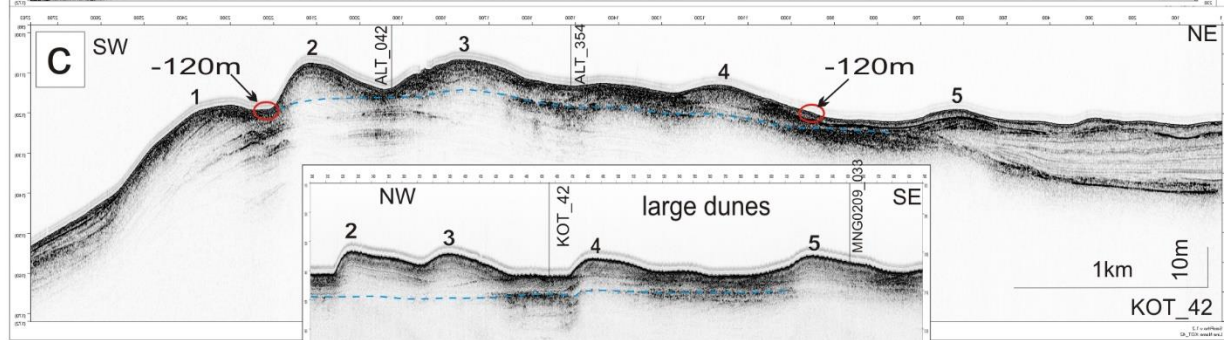
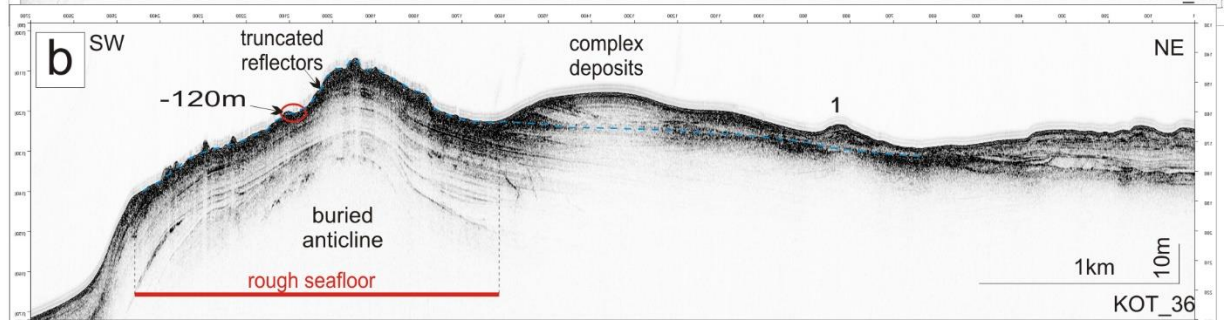
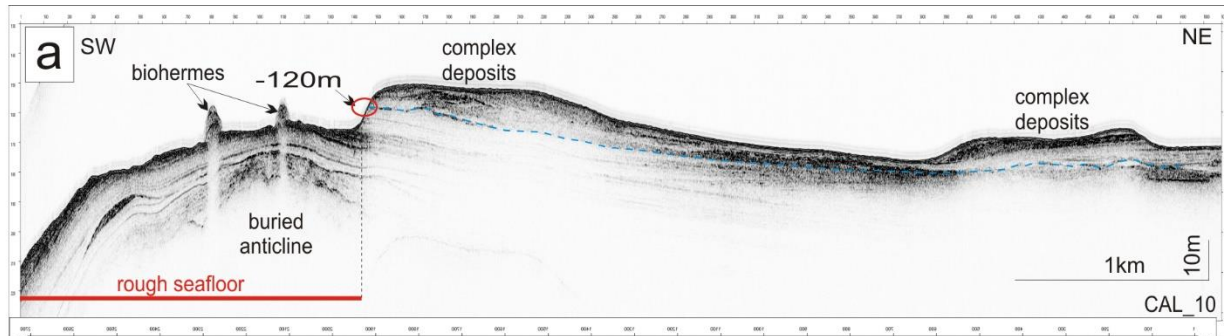


Figure 4. Detailed multibeam morphobathymetry of the Bokakotorska offshore area. a: multibeam shaded-relief map with location of sub-bottom profiles displayed in Fig.5. Six major ridge numbered from 1 to 6 are indicated. b: slope map of the same area, displaying four different morphological domains described in the text.



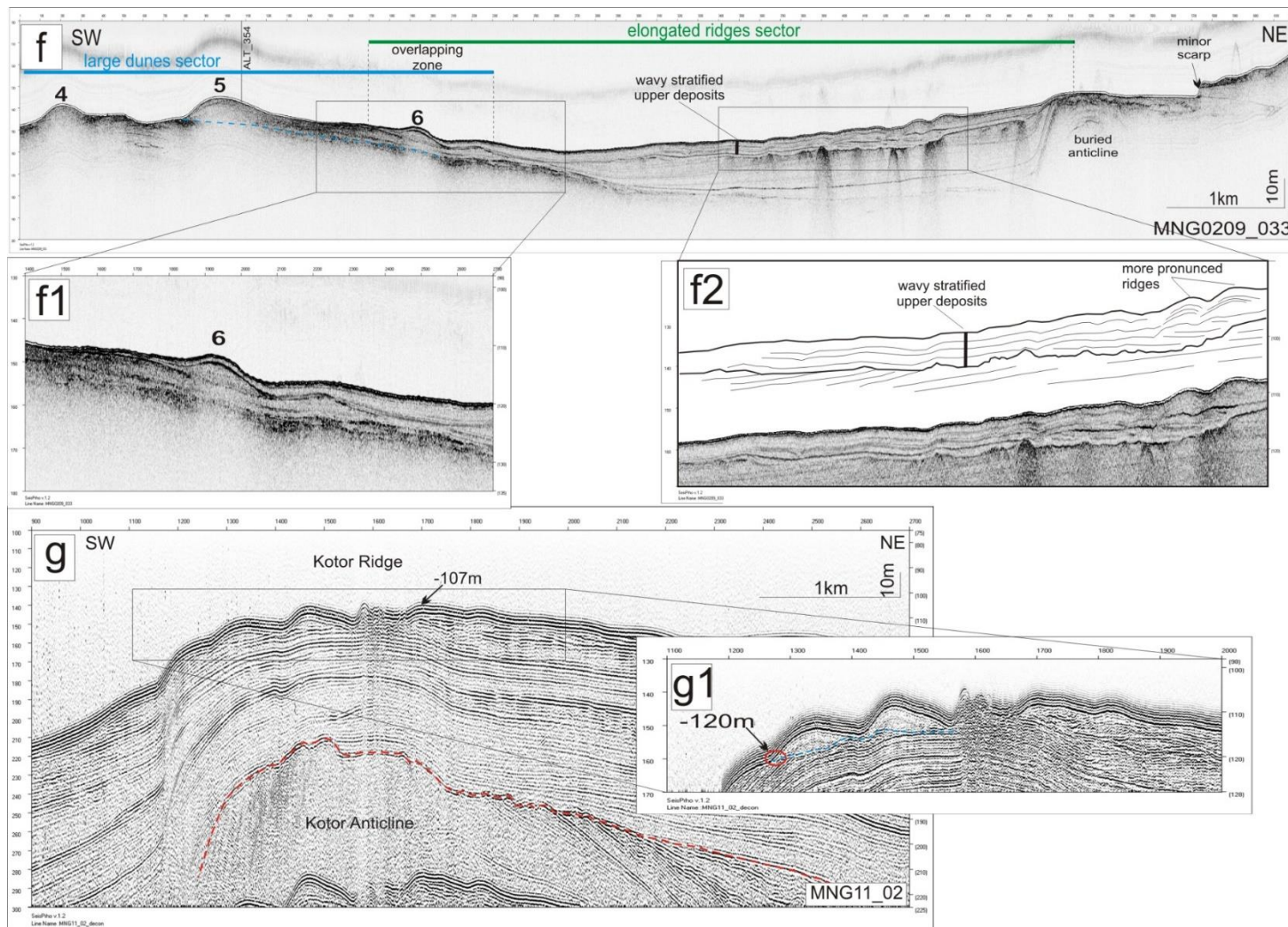


Figure 5: Seismic reflection profiles (location in Fig.4) from the northern Bokakotorska offshore area. A,B,C,D,E and F are close-up of chirp-sonar profiles; G, is from a sparker profile.

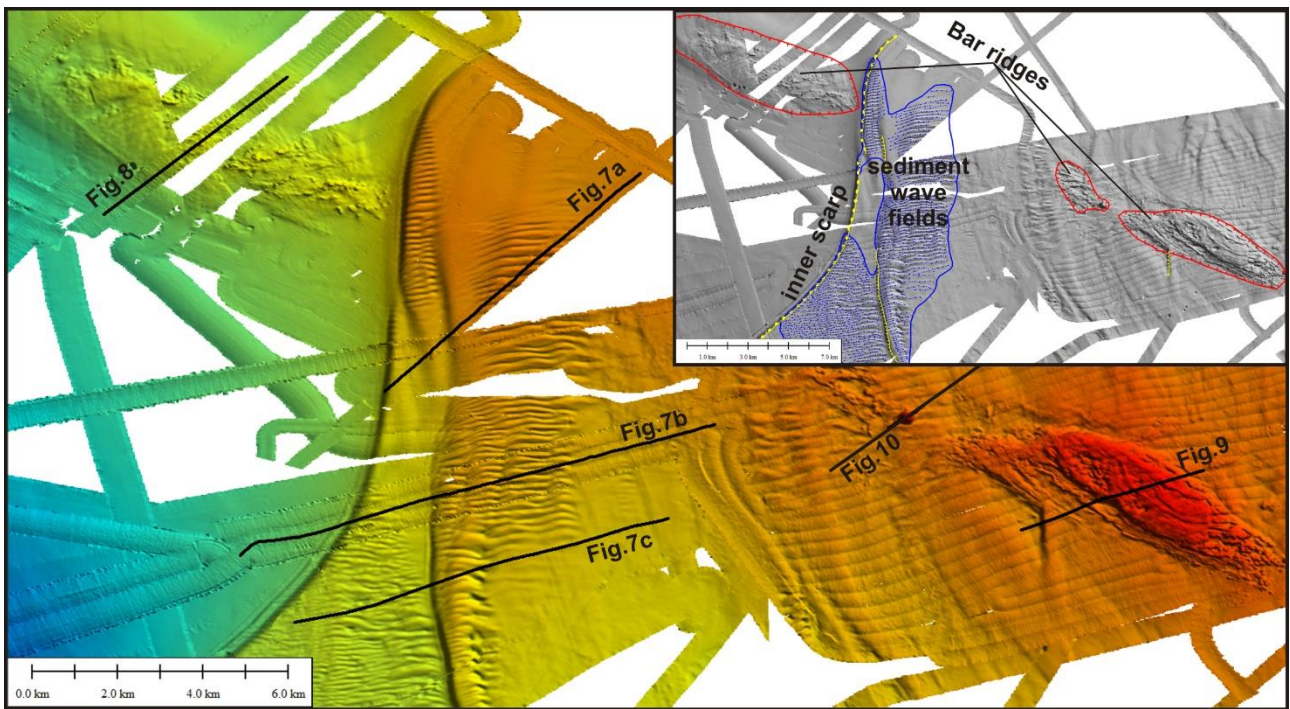


Figure 6. Detailed multibeam shaded-relief morphobathymetric map of Area 2. Location of chirp sonar profile described in the text are indicated (see reference to each figure). Main morphologic units discussed in the text are also indicated (see inset).

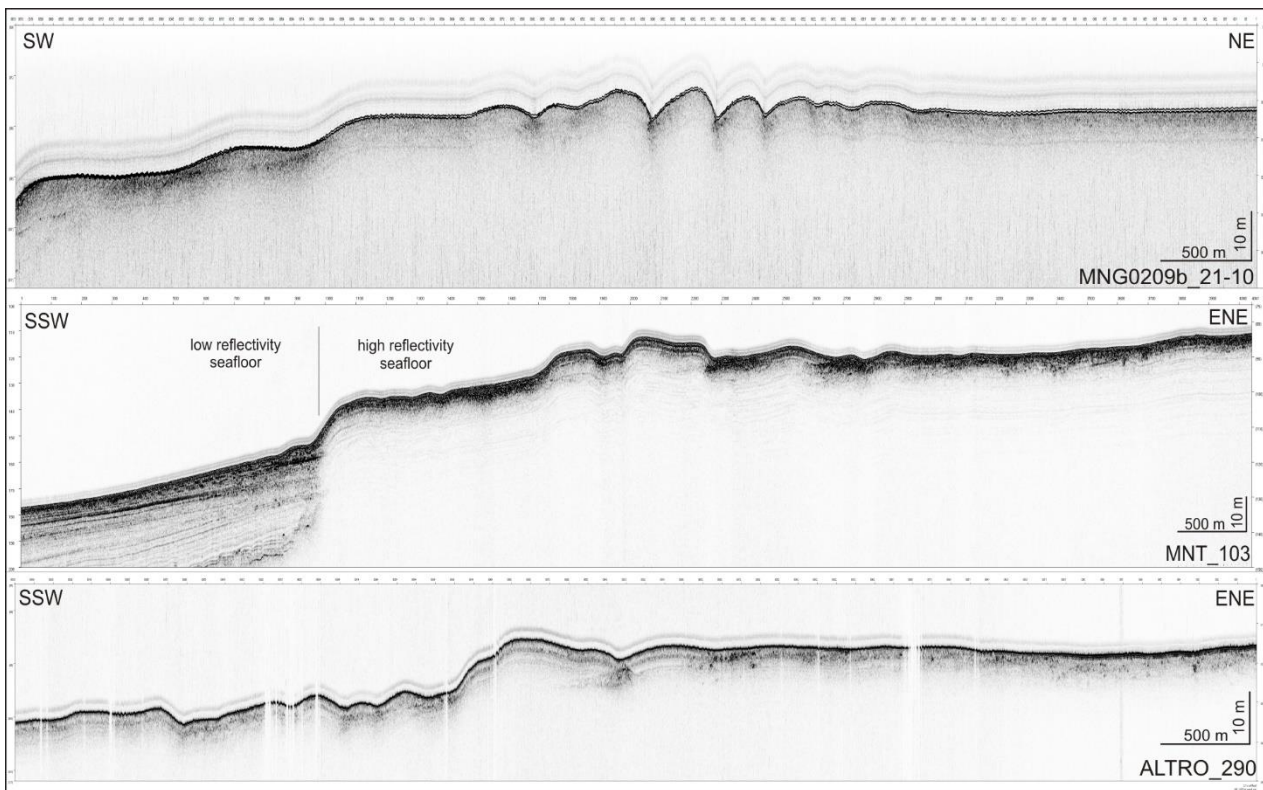


Figure 7. Chirp sonar profile MNG_135, MNG0209b_21_10, MNT_103, ALTRO_290 (location in Fig.6).

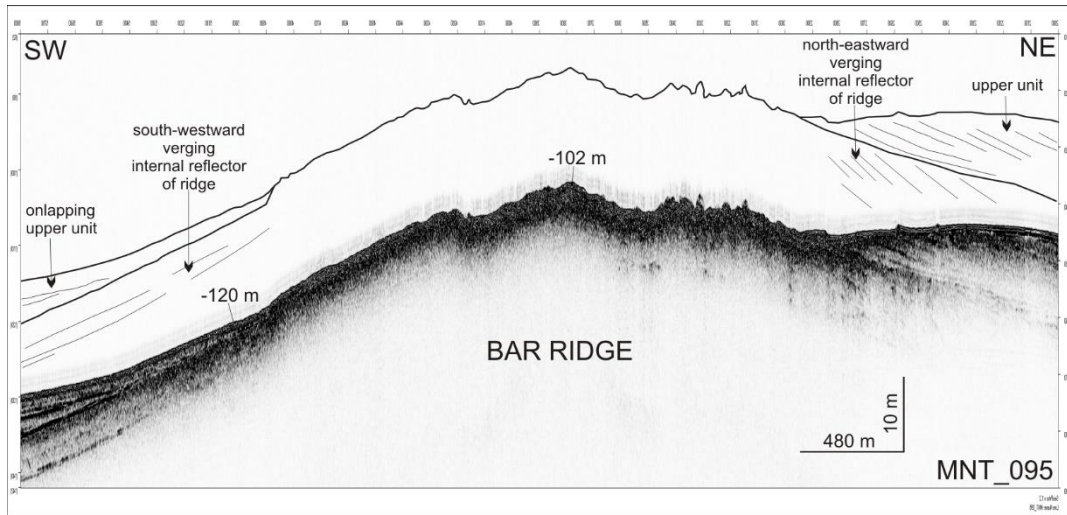


Figure 8. Chirp sonar profile MNT_095 (location in Fig.6)

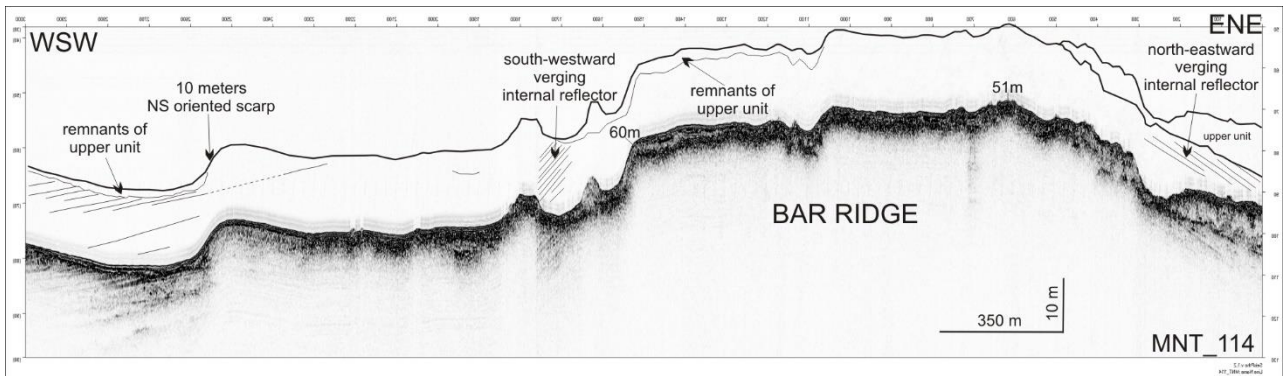


Figure 9. Chirp sonar profile MNT_114 (location in Fig.6)

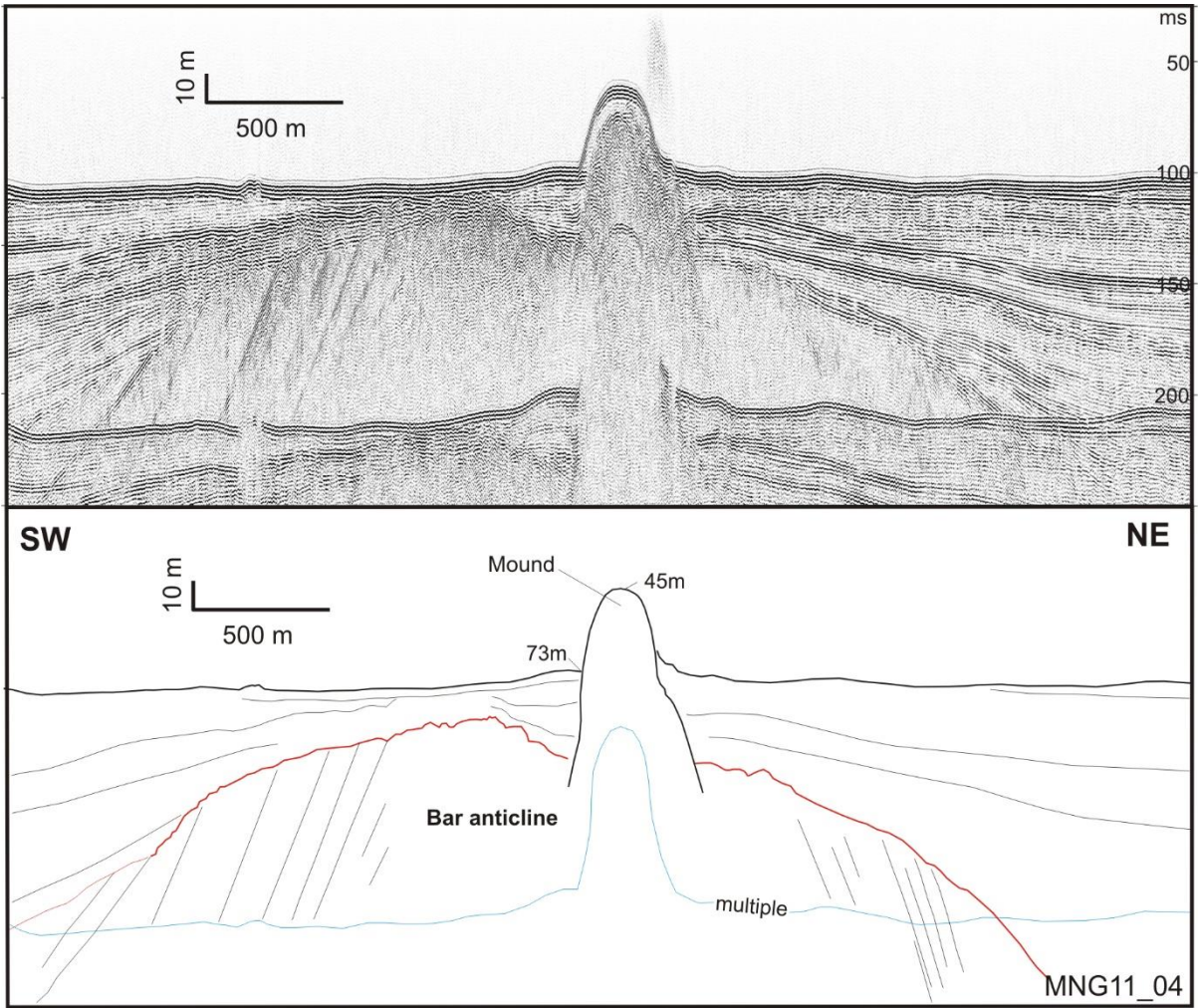


Figure 10. Sparker profile MNG11_04 crossing the Bar Ridge (location in Fig.6)

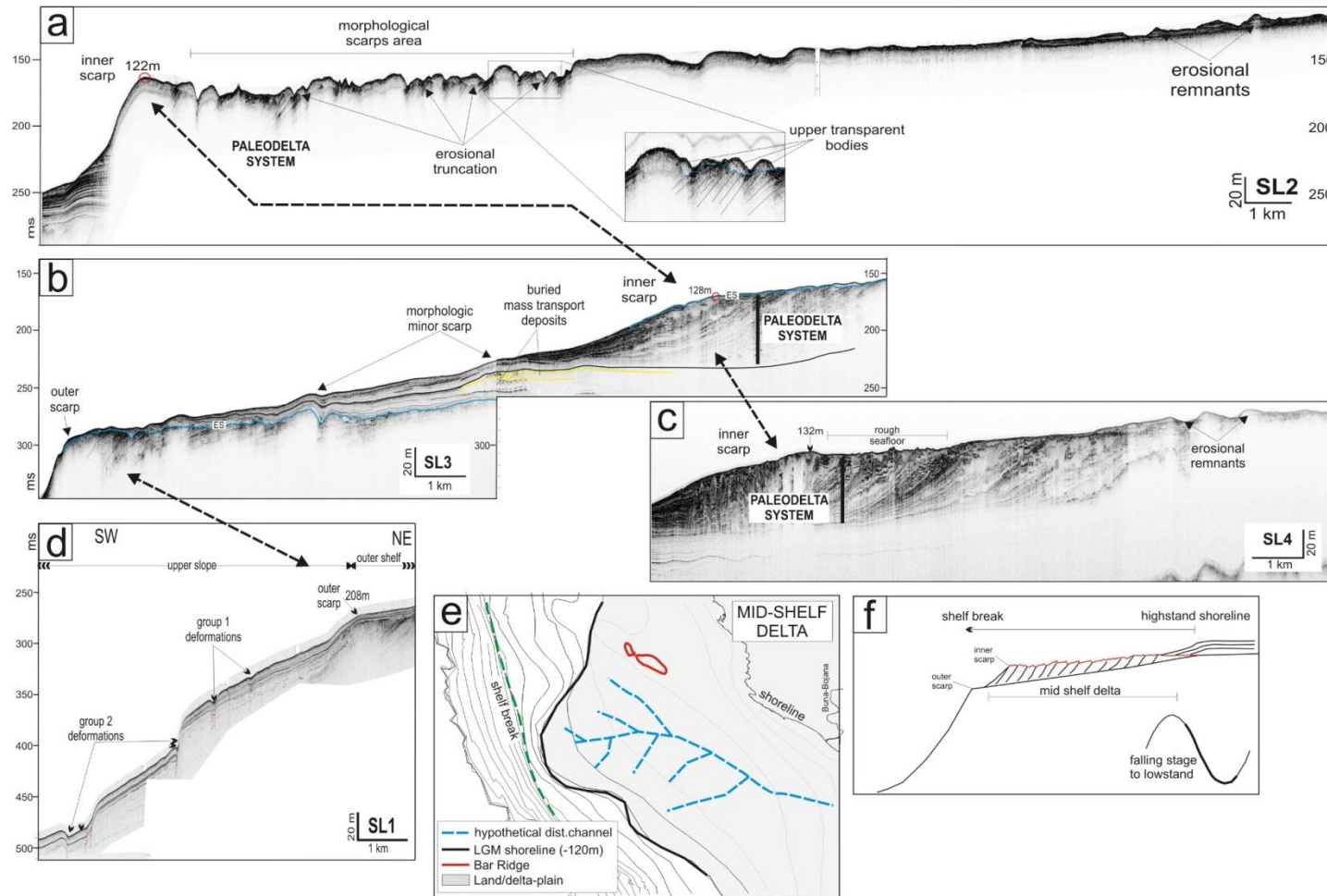


Figure 11. a,b,c,d: chirp sonar profiles across located MACM shelf and upper slope (locations in Fig.2). e: simplified sketch map of the mid-shelf delta during the LGM. Inset f: conceptual dip section showing the accommodation-driven mid-shelf delta (based on Porebsky and Steel 2003)

Table I. Location and grain-size analysis of seafloor sediment samples collected along the MACM.

Sample Name	Longitude	Latitude	Sand (%)	Silt (%)	Clay (%)	Cruise
Gr1	19.3087933	418605050	28.03	52.74	19.22	Adr02-08
Gr2	19.2267167	419053333	92.28	6.25	147	Adr02-08
Gr3	19.401667	419661333	47.09	36.86	16.05	Adr02-08
Gr4	19.0480067	42.0944550	190	48.18	49.74	Adr02-08
Gr5	19.5479983	42.3953500	54.83	20.97	24.20	Adr02-08
Gr6	18.7603817	42.4346517	10.20	33.59	56.21	Adr02-08
Gr7	18.7211767	42.4799217	60.30	10.81	28.89	Adr02-08
Gr8	18.6465083	42.4442417	11.58	33.40	55.02	Adr02-08
Gr9	19.4169200	418155117	2.11	45.16	52.73	Adr02-08
Gr10	19.3269883	415462583	5.04	49.00	45.96	Adr02-08
Gr11	19.3270267	415455283	47.26	21.95	30.79	Adr02-08
Bj1	19.3812833	418152999	5.74	42.92	51.61	Star08
Bj2	19.3177000	418323666	2.28	48.66	49.06	Star08
Bj3	19.2002667	418358832	9.66	24.03	66.31	Star08
Bj4	19.1144500	418914832	1.00	28.31	70.68	Star08
Bj5	19.0366833	419389499	4.01	24.38	71.61	Star08
Bj6	18.9498500	419945499	64.15	8.75	27.10	Star08
Bj7	18.8308500	42.0673166	58.79	11.25	29.96	Star08
Bj8	18.6676833	42.1671332	6.54	19.35	74.12	Star08
Bj9	19.3156333	417640999	0.40	27.79	71.82	Star08
Bj10	19.4544000	417821999	0.6	26.44	72.96	Star08
Bj11	19.5236000	416656832	2.21	34.13	63.66	Star08
Bc01	19.2554833	417562500	0.44	33.22	66.34	MNG01-09
Bc02	19.2898667	417943667	0.36	37.14	62.50	MNG01-09
Bc03	19.3145667	418236000	0.85	49.43	49.73	MNG01-09
Bc04	18.9721500	419283500	4.17	29.30	66.53	MNG01-09
Bc05	19.0317000	419686667	0.52	35.59	63.89	MNG01-09
Bc06	19.0772667	42.0021500	0.33	50.59	49.08	MNG01-09
Bc07	18.8638667	42.0266167	84.07	5.36	10.57	MNG01-09
Bc08	18.8755667	42.0268000	27.93	22.77	49.13	MNG01-09
Bc09	18.7487567	42.4674083	3.72	25.51	70.77	MNG02_09
Bc10	18.7595917	42.4842683	5.90	28.08	66.02	MNG02_09
Bc11	18.7150050	42.4807283	6.09	24.42	69.49	MNG02_09
Bc12	18.6765267	42.5021667	7.12	36.46	56.42	MNG02_09
Bc13	18.6852400	42.4840500	3.42	25.53	71.04	MNG02_09
Bc14	18.6614550	42.4325950	16.47	27.18	56.35	MNG02_09
Bc15	18.6883167	42.4221750	1.54	33.71	64.75	MNG02_09
Bc16	18.7019017	42.4150100	3.29	38.29	58.42	MNG02_09
Bc17	18.6858450	42.4066883	3.98	32.85	63.17	MNG02_09
Bc18	18.5212533	42.4458400	1.23	69.84	28.93	MNG02_09
Bc19	18.5475850	42.4348783	2.02	40.40	57.58	MNG02_09
Bc20	18.5567683	42.4471017	6.53	47.79	45.68	MNG02_09
Bc21	18.5423917	42.4301100	1.14	41.32	57.55	MNG02_09
Bc25	18.6470350	42.4160400	9.13	34.58	56.29	MNG02_09
Bc28	18.6636883	42.3283617	39.20	24.95	35.85	MNG02_09
Bc29	18.5840817	42.2357483	70.78	8.20	21.02	MNG02_09
Bc30	18.5121717	42.1493867	17.08	26.55	56.37	MNG02_09
Bc31	18.5747933	42.2129367	70.87	8.36	20.77	MNG02_09
Bc32	18.9182533	42.1600417	31.18	23.96	44.85	MNG02_09
Bc33	18.7313450	42.0160050	51.01	14.89	34.10	MNG02_09
Bc38	19.112367	418576050	0.43	32.62	66.95	MNG02_09
Bc39	19.2263983	418640817	0.15	45.83	54.02	MNG02_09
Bc42	19.2709533	417080183	0.22	34.60	65.17	MNG02_09
Bc43	19.3452567	418252117	1.66	56.91	41.43	MNG02_09
Bc45	19.3523450	418309667	3.07	61.86	35.07	MNG02_09
Bc46	19.3484567	418284217	3.73	66.19	30.09	MNG02_09
Bc47	19.3423067	418231967	0.93	51.67	47.39	MNG02_09
Bc48	19.3378667	418196017	0.89	51.02	48.09	MNG02_09
Bc01	18.5204167	42.3437000	36.55	23.03	40.42	MNG04_11
Bc02	18.4640000	42.2394167	22.95	25.19	51.86	MNG04_11
Bc03	19.3220500	418590000	50.60	34.73	14.67	MNG04_11
Bc04	19.2816167	418264667	0.30	34.30	65.40	MNG04_11
Bc05	19.2372000	417840000	4.14	38.35	57.52	MNG04_11
Bc06	19.1793167	417307500	0.46	31.24	68.30	MNG04_11
Bc07	19.1207667	416792500	4.92	32.04	63.04	MNG04_11
Bc09	19.2064333	418827333	0.11	51.45	48.44	MNG04_11
Bc11	19.0815000	419821667	0.20	47.89	51.91	MNG04_11
A48				17.8	63.6	ALTRO
A49B				67.7	19.7	ALTRO
A49T				38.7	44.6	ALTRO
5.4	19.5516333	417438500	4.2	53.44	42.36	MARIN2012
HN	18.5491500	42.4437833	0.12	47.48	52.4	MARIN2012
4.5	19.121333	416818500	1.28	42.68	56.04	MARIN2012
6.5	19.211167	416296500	0.00	39.52	60.24	MARIN2012
KO	18.7403000	42.4818833	2.68	28.28	68.64	MARIN2012
2.4	18.7469000	42.1260000	20.64	30.04	49.32	MARIN2012
3.5	18.9328333	417861500	47.88	18.4	33.72	MARIN2012
11	18.5420333	42.3960833	58.64	14.00	27.36	MARIN2012
12	18.4974667	42.3587500	43.16	20.36	36.48	MARIN2012
7.3	19.2752833	414507333	0.92	52.42	46.56	MARIN2012
7.1	19.4089833	414510000	1.32	61.76	36.92	MARIN2012
5.1	19.412667	418469000	17.64	53.32	29.04	MARIN2012
6.1	19.5300000	416289833	1.64	25.52	45.84	MARIN2012
4.1	19.3262167	418597333	73.32	12.28	14.40	MARIN2012

References

- Aliaj, S., 1999. Transverse faults in Albanian orogen front. *Albanian Journal of Natural & Technical Sciences* 6, 121-132.
- Aliaj, S., 2000. Thrust front along Adriatic collision and seismic potential of its seismogenic nearby zone. *Proc. International Symposium on Earthquake Engineering (ISEE), Montenegro*. 85-93.
- Cavaleri, L., & Stefanon, A., 1980. Bottom features due to extreme meteorological events in the North Adriatic Sea. *Marine Geology*, 79, 159-170.
- Cattaneo, A., Correggiari, A., Marsset, T., Thomas, Y., Marsset, B., Trincardi, F., 2004. Seafloor undulation pattern on the Adriatic shelf and comparison to deep-water sediment waves. *Mar. Geol.* 213 (1-4), 121-148.
- Correggiari, A., Trincardi, F., Langone, L., Roveri, M., 2001. Styles of failure in late Holocene highstand prodelta wedges on the Adriatic shelf. *J. Sediment. Res. Part B* 71, 218-236.
- Correggiari, A., Field, M.E., Trincardi, F., 1996. Late Quaternary transgressive large dunes on the sediment-starved Adriatic shelf. *Geology of Siliciclastic Shelf Seas*, Geological Society Publication No. 117, pp. 155-169.
- Damuth, J.E., 1980. Use of high frequency 3.5-12 kHz echograms in the study of near bottom sedimentation processes in the deep sea: a review. *Marine Geology* 38, 51-75.
- Del Bianco, F., Gasperini, L., Bortoluzzi, G., Giglio, F., D'Orlando, F., Polonia, A., Ravaioli, M., Kljajic, Z. and Bulatovic, A., 2010. The Montenegro-Northern Albanian continental margin: morphotectonic features in a seismically active region. *Rapp. Comm. Int. Mer Medit.* Vol. 39 p. 20.
- Flaming K., Johnston, P., Zwart, D., Yokoyama, Y., Lambeck, K., & Chappell, J. 1998 - Refining the eustatic sea-level curve since the Last Glacial Maximum using far- and intermediate-field sites, *163*, 327-342.
- Faugères, J.C., Stow, D.A.W., 1993. Bottom-current controlled sedimentation: a synthesis of the concourite problem. *Sedimentary Geology*, 82(1-4), 287-297.
- Faugères, J.C., Gonthier, E., Mulder, T., Kenyon, N., Cirac, P., Gribouard R., Berné, S., Lesuavé, R., 2002. Multi-process generated sediment waves on the Landes Plateau (Bay of Biscay, North Atlantic). *Marine Geology* 182, 279-302.
- Galloway, W. E., 1975. Process framework for describing the morphologic and stratigraphic evolution of deltaic depositional systems. In Broussard, M. L. (Ed.), *Houston Geological Society, Deltas*, pp.87-98.
- Garziglia, S., Sultan, N., Cattaneo, A., Ker, S., Marsset, B., Riboulot, V., Voisset, M., Adamy, J., Unterseh, S., 2010. Identification of shear zones and their causal mechanisms using a combination of cone penetration tests and seismic data in the Eastern Niger Delta. In: Mosher, D., et al. (Ed.), *Submarine Mass Movements and Their Consequences*, 28. *Advances in Natural and Technological Hazards Research*, Springer, pp. 55-65.

- Gasperini, L., Stanghellini, G., 2009. SEISPRHO: An interactive computer program for processing and interpretation of high-resolution seismic reflection profiles. *Computers and Geosciences*, 35(7), 1497–1507. doi:10.1016/j.cageo.2008.04.014
- Howe, J.A., Stoker, M.S., Stow, D.A.V., 1994. Late Cenozoic sediment drift complex, northeast Rockall Trough, North Atlantic. *Paleoceanography* 9, 989-999.
- Howe, J.A., Humphrey, J.D., 1995. Photographic evidence for slope-current activity, Hebrides Slope, NE Atlantic Ocean. *Scot. J. Geol.* 30, 107-115.
- Kenyon, N.H., 1986. Evidence from bedforms for a strong poleward current along the upper continental slope of Northwest Europe. *Mar. Geol.* 72, 187-198.
- Lea, D. W., Martin, P. A., Pak, D. K., & Spero, H. J., 2002. Reconstructing a 350 ky history of sea level using planktonic Mg / Ca and oxygen isotope records from a Cocos Ridge core. *Quaternary Science Reviews* 21, 283–293.
- Marani, M., Argnani, A., Roveri, M., Trincardi, F., 1993. Sediment drifts and erosional surfaces in the central Mediterranean: seismic evidence of bottom-current activity. *Sedimentary Geology*, 82, 207-220.
- Marini, M., Grilli, F., Guarnieri, A., Jones, B. H., Klajic, Z., Pinardi, N., Sanxhaku, M., 2010. Is the southeastern Adriatic Sea coastal strip an eutrophic area? *Estuarine, Coastal and Shelf Science*, 88(3), 395–406. doi:10.1016/j.ecss.2010.04.020
- Masson, D. G., Howe, J. A., Stoker, M. S., 2002. Bottom-current sediment waves, sediment drifts and contourites in the northern Rockall Trough. *Marine Geology*, 192, 215-237.
- Mix, A.C., and Ruddiman, W.F., 1985. Structure and timing of the last deglaciation: oxygen isotope evidence. *Quaternary Science Reviews* 4, 59-108.
- Pondrelli, S., Salimbeni, S., Ekstrom, G., Morelli, A., Gasperini, P. and Vannucci, G., 2006. The Italian CMT dataset from 1977 to the present. *Phys. Earth Planet. Int.* 159/3-4, pp. 286-303. doi:10.1016 / j.pepi. 2006.07.008
- Porębski, S. J., Steel, R. J., 2003. Shelf-margin deltas: their stratigraphic significance and relation to deepwater sands. *Earth-Science Reviews*, 62(3-4), 283–326. doi:10.1016/S0012-8252(02)00161-7
- Porebski, S. J., Steel, R. J., 2006. Deltas and Sea-Level Change. *Journal of Sedimentary Research*, 76(3), 390–403. doi:10.2110/jsr.2006.034
- Poulain, P.M., 2001. Adriatic Sea surface circulation as derived from drifter data between 1990 and 1999. *Journal of Marine Systems*, 29, 3-32.
- Reeder, M.S., Rothwell, G., Stow, D.A.V., 2002. The Sicilian gateway: anatomy of deep- water connection between East and west Mediter- ranean basins. In: Stow, D.A.V., Pudsey, C.J., Howe, J.A., Faugères, J.C., Viana, A.R. (eds) *Deep-Water Contourite Systems: Modern Drift and Ancient Series, Seismic and Sedimentary Characteristics*. Geological Society, London, *Memoirs*, 22, 171-189.
- Roberts, D.G., Kidd, R.B., 1979. Abyssal sediment wave fields on Feni Ridge, Rockall Trough: long-range sonar studies. *Mar. Geol.* 33, 175-191.

- Rosenbaum, G., and Lister, G.S., 2005. The western Alps from the Jurassic to Oligocene: Spatio-temporal constraints and evolutionary reconstructions: *Earth-Science Reviews*, v. 69, 281-306. doi: 10.1016/j.earscirev.2004.10.001.
- Roveri, M., 2002. Sediment drifts of the Corsica Channel, northern Tyrrhenian Sea. In: Stow DAV, Pudsey CJ, Howe JH, Faugères JC, Viana AR (eds) *Deep-water contourite systems: modern drifts and ancient series, seismic and sedimentary characteristics*. *Geol Soc Lond Mem* 22, 191–208.
- Rohling, E.J., Fenton, M., Jorissen, F.J., Bertrand, P., Ganssen, G., Caulet, J.P., 1998. Magnitudes of sea-level lowstands of the past 500,000 years. *Nature* 394, 162–165.
- Shepard, F.P., 1954. Nomenclature based on sand-silt-clay ratios: *J. Sediment Petrol.*, v.24, p.151.
- Sydow, J., Roberts, H.H., 1994. Stratigraphic framework of late Pleistocene shelf-edge delta, Northeast Gulf of Mexico. *AAPG Bull.* 78 (8), 1276–1312.
- Swift, D.J.P., Kofoed, J.W., Saulsbury, F.B., Sears, P.C., 1972. Holocene evolution of the shelf surface, central and southern Atlantic shelf of North America. In: Swift, D.J.P., Duane, D.B., Pilkey, O.H. (Eds.), *Shelf Sediment Transport: Process and Pattern*, Stroudsburg, Pennsylvania. Dowden Hutchinson & Ross, Stroudsburg, PA, 499–574.
- Stoker, M. S., 1998. Sediment drift development on the Rockall continental margin, off NW Britain. In: Stoker, M.S., Evans, D., Cramp, A. (eds) *Geological Processes on Continental Margins: Sedimentation, Mass-Wasting and Stability*. Geological Society, London, Special Publications, 129, 229-254.
- Suppe, J. 1985. *Principles of Structural Geology*. Prentice-Hall, Englewood Cliffs, NJ.
- Verdicchio, G., Trincardi, F., Asioli, A., 2007. Mediterranean bottom- current deposits: an example from the Southwestern Adriatic Margin. *Geol Soc Lond Spec Publ* 276, 199–224.
- Verdicchio, G., Trincardi, F., 2008. Mediterranean shelf-edge muddy contourites: example from Gela and South Adriatic Basins, *Geo-Mar. Lett.*, 28, 137–151. doi:10.1007/s00367-007- 0096-9.
- Viana, A., 2002. Seismic expression of shallow- to deep-water contourites along the south-eastern Brazilian margin. *Marine Geophysical Researches*, 22, 509-521.
- Vlahović, I., Tišljarić, J., Velić, I., & Matičec, D., 2005. Evolution of the Adriatic Carbonate Platform: Palaeogeography, main events and depositional dynamics. *Palaeogeography, Palaeoclimatology, Palaeoecology*, 220(3-4), 333–360. doi:10.1016/j.palaeo.2005.01.011
- Wessel, P., Smith, W.H.F., 1998. New, Improved Version of Generic Mapping Tools Released, *EOS Trans.*, AGU, 79 (47), p. 579.

3.3 Stratigraphic architecture of the Montenegro/N. Albania Continental Margin (Adriatic Sea - Central Mediterranean)

Del Bianco F., Gasperini L., Angeletti L., Giglio F., Bortoluzzi G., Montagna P., Kljajic Z. and Ravaioli M.

Abstract

The Montenegro/Northern Albanian Continental Margin (MACM) of the Eastern Adriatic Sea is a convergent margin at the Dinarides Chain front supplied by major fluvial systems, such as the Buna/Bojana and Drini rivers. Analysis of high-resolution seismic reflection profiles and core samples, which included paleobiologic legacy of macrofossil assemblages and radiometric dating shows that the latest post-glacial mud wedge is confined into mid-shelf basins partially bounded toward sea by tectonic highs, such as the Kotor and Bar ridges, while the outer shelf exposes lowstand deposits locally covered by a thin veneer of Holocene mud. The oldest deposits encompasses four major seismic sequences marked by forced-regression units deposited during Marine Isotope Stages (MIS) 10, 8, 6 and 2. This is mostly observed in correspondence of the shelf-break, at water depths of 200-220 m, where we described a stack of sedimentary sequences recording sea level changes at the scale of 100 kyr. Position and assumed ages of buried shorelines of the four latest lowstand phases indicate that the outer shelf subsidence rate was about 1.2 mm/yr during the last ~350 kyr, while a morphological analysis operated on the present depth of the LGM paleoshoreline, across the Bar ridge, suggests that this sector was uplifted by several tens of meters during the last 20 kyr.

1. Introduction

The stacking of stratigraphic sequences of continental margins reflects interactions between several natural processes, such as sea level changes, tectonic deformation (subsidence or uplift), sediment supply and reworking by bottom currents. This is also the case of the Adriatic Sea, a Mediterranean epicontinental basin located between three orogenic belts, the Apennines to the west, the Dinarides to the east and the Alps to the north (Fig. 1). The stratigraphy of the Adriatic margin is mainly controlled by the Quaternary high-frequency glacio-eustatic changes, which caused extended horizontal shifts of the coastal zone due to the low topographic gradients. During the last eustatic cycles this effect, combined with long-term subsidence, allowed the preservation of a relatively expanded sequence. This includes sedimentary deposits during all different stages of sea level fluctuations, such as the High-stand (HST), the Falling-stage (FSST), the Lowstand (LST) and the Transgressive (TST) systems tracts, differently preserved and widely recovered and studied in the Adriatic Sea and other Mediterranean margins (e.g. Tesson et al., 1990; Trincardi and Field, 1991; Piper and Aksu, 1992; Gensous and Tesson, 1996; Chiocci et al., 1997; Somoza et al., 1998; Bernè et al., 1998; Skene et al., 1998; Ridente and Trincardi, 2002; Maselli et al., 2011).

The eastern and western Adriatic shelves, are characterized by similar geodynamic settings and a common history of Late Quaternary paleogeographic changes, culminated ~21 kyr in the last episode of glacio-eustatic lowstand (-120 m below the present-day datum; Clark et al., 2009). In its northern part, the western Adriatic shelf is characterized by high accommodation due to the constant and high subsidence rate at the front of the Apennine Chain that led to deposition of a thick sedimentary sequence. South of the Mid Adriatic Depression (Fig. 1), compressive deformations reach the uppermost part of the stratigraphic sequence (Ridente and Trincardi, 2006). In such zones, accommodation is limited, and highly variable along the margin reflecting the growth of gentle synclines and anticlines.

Recently, Maselli et al. (2010) presented a compilation of subsidence-rate estimates in different sectors of the western Adriatic margin, from several authors; these rates range from 1.2 mm/yr in the Northern Adriatic shelves to 0.3 mm/yr in the Central part of the Adriatic. Conversely, the Southern Adriatic shelf surrounding the Apulia swell is uplifting at rates in the order of 0.2-0.3 mm/yr. In contrast with the Italian side, the eastern Adriatic continental shelf at the Dinarides front is still poorly covered by marine geological and geophysical data. In particular, seismo-stratigraphic studies are lacking along the Montenegro- N. Albanian Continental Margin (hereafter called MACM), with the exception of seismic reflection datasets collected by oil companies and yet mostly unpublished (Dragasevic 1974; Oluic 1982). Therefore, a description of the Late Quaternary

stratigraphic architecture is still lacking.

The MACM is a convergent margin supplied by major fluvial systems, such as the Buna/Bojana and the Drini rivers that carry the sediment loads to the narrow shelf. Source areas for these sediments are the Dinaric Alps, and the watershed of fluvial systems that drain mainly clastic deposits of lower to middle Triassic and Jurassic/Cretaceous carbonate rocks.

In the framework of ADRICOSM-STAR, we carried out six oceanographic cruises along the MACM, on board of the research vessels of the Italian National Research Council (CNR). Although the main-focus of the project was to study the present-day oceanographic regime and the environmental status of the coastal areas, during these expeditions a variety of ancillary geophysical data, including high-resolution seismic reflection profiles and multibeam swath bathymetry were acquired, along with the sampling of several gravity and box cores.

Here we present a first analysis of such data, that enabled us to investigate the depositional patterns of the Late Quaternary sedimentary sequences, i.e., the uppermost tens to hundreds of meters of the sedimentary record, and to unravel relationships between tectonic and sea level changes. Our work includes stratigraphic analysis and thickness maps of the latest post-glacial mud wedge, as well as the MIS6 sediment dispersal system. We finally attempt an estimate of the subsidence rate along the MACM during the last ~350 kyr, based on identification of paleoshorelines associated to three buried forced-regression sediment wedges in analogy with the most recent and dated one.

2. Geologic setting

The MACM is a convergent margin located in the southeastern sector of the Adriatic Sea, bounded to the northeast by the Dinarides/Albanides chain. The associated sedimentary basin constitutes the foredeep of the Dinaride-Albanide fold-and-thrust belt (De Alteriis, 1995; Argnani et al., 1996; Bertotti et al., 2001), that started forming in the Eocene along the southeastern branch of the Alpine chain (Rosenbaum and Lister, 2005). According to Argnani et al. (1996) the MACM morphology is partly inherited from the Mesozoic paleogeography, because the southern Adriatic developed over a Mesozoic epicontinental basin between the Dalmatian and Apulian shallow-water carbonate platforms, to the N and the S, respectively.

The outer domain of the Dinarides/Albanides chain, which includes the coastal area and the continental shelf, constitutes the present-day collisional front and is marked by compressive deformation along deep-seated thrust faults that cut through the entire sedimentary sequence (Aliaj, 1997). The fold-and-thrust belt developing offshore was imaged at crustal depths by closely spaced

grids of multichannel seismic lines collected during the '80 and the '90 for exploration purpose. However, these data are still largely unpublished, if we exclude a few lines or line-drawings interpretations in Aliaj (1998, 2004) and Oluic et al. (1982) based on published seismic sections in the Montenegro offshore (north of Gulf of Drin). Such seismic lines show evidence of post-Messinian, or even Upper Pliocene to Quaternary, deformation Dragasevic (1983). Focal mechanisms of recent earthquakes, as well as geodetic observations, suggest compressive deformations along the eastern Adria lithospheric block (Anderson and Jackson, 1987; Pondrelli et al., 2002; Hunstad et al., 2003), which appears displaced by a series of N-S oriented strike-slip faults. This faulting resulted in a NE-SW shortening along the Dinarides and Albanian chains, at estimated rates of 4-4.5 mm/yr (Grenerczy et al., 2005).

2.1 The Adriatic Sea

The Adriatic Sea (Fig. 1) is a semi-enclosed basin elongated in NW-SE direction with a length of about 800 km and a width of 200 km that shows a remarkable latitudinal variability in the shelves and slopes morphology. While the Northern Adriatic is flat and shallow (average depth 70 m), the Southern Adriatic, between the Apulian platform to the W, and the MACM to the E, is relatively deep (up to 1200 m) in the South Adriatic Depression (Fig. 1). The MACM displays a double system of morphological scarps that bound the continental shelf. The first scarp, between 100 and 130 m water depth, delimits the inner shelf that reaches its minimum width of 12-17 km in the northern sector and widens in the southern part of the MACM reaching over 45 km in correspondence of a submerged lowstand delta (Del Bianco et al., in prep). The outer scarp system, between 220 and 230 m of water depth, marks the beginning of the continental slope that connects with the -1200 m deep of the South Adriatic Depression.

Along the MACM, sediments are mainly supplied by the river called Buna in Albania and Bojana in Montenegro, which constitutes the political boundary between the two countries. It is the Adriatic second main river in terms of sediment supply after the Po River, and the primary freshwater inflow in the southeastern Adriatic Sea, with a mean annual discharge of about $700 \text{ m}^3\text{s}^{-1}$ (UNEP, 1996; Table 1). Prevalent longshore current directions are from S to N (white arrows in Fig. 1). The northward bending of the river plume is consistent with the combined effects of Coriolis (Kourafalou, 1999) and prevailing longshore currents in the region (Artegiani et al., 1997a). The South Eastern Shelf Coastal Current (SESC) characterizes the oceanographic regime of this region Marini et al. (2010). The SESC detaches from the coast near the Buna/Bojana outflow and forms coastal eddies that stretch offshore the extent of the river plumes inducing variations in the water circulation pattern,

both at the surface and close to the seafloor, which could favor alternating areas of erosion and deposition within short distances (20-30 km). As shown by local field circulation pattern (Fig. 1), areas where deposition of sediments is favored should coincide with the centers of local eddies, i.e., the Gjiri-Rodonit Bay, and the inner shelf between Budva and Bar.

3. Methods

Marine geophysical data and sediment samples were collected during seven oceanographic cruises, one on board the R/V Dallaporta, (Star08), R/V Urania, (ADR02_08, 2008; MNG01_09, 2009; MNG03_1, 2010; MNG04_10, 2010; ALTRO, 2012) and R/V Mariagrazia (MNG02_09). The technical report for each cruise is available online (<http://www.ismar.cnr.it/prodotti/reports-campagne>).

High-resolution seismic reflection profiles were collected using a hull-mounted 16 transducer Benthos Chirp II sub-bottom profiler (2-7 kHz frequency) and a towed Sparker system. Sparker profiles were acquired using a Geo-Source 200 system (200 tip electrode modules) operated with Geo-Spark 1000J solid-state pulsed power supply. Chirp and Sparker data positioning was corrected for the offsets between DGPS antenna and transducers using gyrocompass and CMG data; associated error is 1 m.

Geophysical data in this work include several thousand kms of chirp sonar profile used to describe the sediment architecture and the distribution of deposits in the margin and compile sediment thickness maps. The more penetrative sparker seismic reflection profiles were used to study the stratigraphy at depth. Processing and interpretation of seismic profiles, as well as reflector picking and correlation, were carried out using the open software package SeisPrho (Gasperini and Stanghellini, 2009). Most of the displayed maps were created with GMT (Wessel and Smith, 1998), also used for spatial data gridding.

Core samples were collected using a 1.2 tons gravity corer mounting a 6-meter long barrel, with penetration reaching the full length in mud or silt/sand alternations. After collection of whole-core magnetic susceptibility logs using a Bartington MS2 meter coupled with a MS2C core logging sensor, the cores were split, described and sampled. Bottom samples used to analyze the ^{210}Pb were collected using a box corer.

Radiocarbon ages were obtained by AMS from mollusc shells and selected foraminifera (Table 1) at Poznan Radiocarbon Laboratory (PRL) and were calibrated using CALIB v.7 (Stuiver et al, 2013).

$^{210}\text{Pb}/^{210}\text{Po}$ analyses were performed at ISMAR-CNR Bologna. ^{210}Pb was determined using alpha spectrometry through its ^{210}Po daughter, and measured with a silicon barrier detector coupled with a multichannel analyzer, according to Frignani and Langone (1991) and Frignani et al. (1993). Supported ^{210}Pb activities were obtained from the constant values at depth in the cores. Excess ^{210}Pb ($^{210}\text{Pbex}$) activities were obtained by subtracting supported ^{210}Pb from total activities. If the flux of ^{210}Pb to the site has been constant with time, a CF-CS model (Constant Flux-Constant Sedimentation; Robbins, 1978) is applied to the $^{210}\text{Pbex}$ and the assessment of accumulation rates and chronologies from $^{210}\text{Pbex}$ -depth profiles is based on a model calculation discussed by Frignani et al. (2005). Since the simplified conditions of the conceptual models are not always met in the working area, the assumptions are affected by a degree of uncertainty. When the $^{210}\text{Pbex}$ profiles were too different from theoretical cases, a crude estimate of sediment accumulation rates (SAR) was obtained. The value of supported ^{210}Pb activity was assumed constant along-core and estimated from the values of the deepest sediment samples, where ^{210}Pb was assumed to be in radioactive equilibrium with its parent ^{226}Ra , i.e. by dividing the depth where supported background value of ^{210}Pb was reached by 100 years. All concentrations and activities were calculated on a dry weight basis.

Absolute ages were obtained by U-series dating from fossil samples of the deep-water coral *Caryophyllia smithii* retrieved from one sediment core. The thecal wall of two specimens was carefully cleaned using a fine diamond saw to remove any visible contamination and leached with 0.1N HCl. About 100mg of cleaned material was dissolved in 3 ml double distilled HCl (10%) and mixed with an internal triple spike (“TT5”) with known concentrations of ^{229}Th , ^{233}U , ^{236}U , calibrated against a Harwell Uranite solution assumed to be at secular equilibrium. The solutions were evaporated to dryness at 70°C, redissolved in 0.8ml 3N HNO₃ and then loaded into a 500µl columns packed with UTEVA resin (Eichrom Technologies, USA) in order to remove the carbonate matrix and isolate uranium and thorium from the other major and trace elements. U and Th isotopes were then measured using a Multi-Collector Inductively Coupled Plasma Mass Spectrometer (ThermoScientific NeptunePlus) at the *Laboratoire des Sciences du Climat et de l'Environnement* at Gif-sur-Yvette (France) following the analytical protocol reported in Fontugne et al. (2013).

4. Results

4.1 Seismic stratigraphy

Figure 2 shows the seismic reflection profiles described in this chapter. Chirp sonar profiles CP1 and CP2 (Fig. 3 top) cut orthogonally the MACM from -176 m to -90 m and from -374 m to -80

m water depths, respectively, across the shelf and the upper slope. In the inner shelf, we note the presence of an uppermost transparent unit, called U1 (Fig. 3 top). Although its internal geometry is highly variable, acoustic facies of U1 appears rather consistent over the entire Northern Area, being characterized by a fine layered and transparent texture that might indicate prevalent fine-grained, relatively homogeneous sediment. Internal geometries of this unit show a wavy internal pattern and a progressive thinning northward, where it becomes very patchy and localized in a series of troughs running parallel to the inner scarp (CP2 profile, Fig. 3). U1 is bounded at its base by a high-amplitude reflector that marks an erosional unconformity (ES, Fig. 3 top) correlated over the Northern inner shelf. Locally, ES is overlain by high reflectivity bodies (tens of meters in width) that correspond to buried morphological highs probably made of coarse grained deposits (Fig. 3 top).

Below ES, unit U2 (Fig. 3 top) is bounded at its base by an erosional unconformity. U2 is characterized by fine-grained deposits and shows a gently seaward-dipping stratification and offlapping internal geometries. The landward basal termination of U2 deposits appears tilted, as visible in seismic profile CP1 (Fig. 3) suggesting that this unit might record syn-depositional deformation. No further information about U2 is available but the seismic facies and the internal geometry of this unit are similar to those of a forced regression deposit recorded in a local thick depocenter offshore the Gargano Promontory (Ridente and Trincardi, 2002). Seaward, U1 and U2 onlap a topographic high, the Kotor Ridge (Fig. 3), whose top appears very rough due to the presence of mounds and troughs that reach a minimum depth of 107 m, and constitutes the morphological boundary between the inner and the outer shelves (Del Bianco et al, in prep) . The presence of these features at the seafloor suggests non-deposition or submarine erosion. On chirp sonar profiles, the Kotor Ridge appears acoustically blind and asymmetrical, with its seaward flank being steeper. Internal reflectors, visible within confined acoustic windows, suggest that the ridges are made of sediment beds composed of relatively lithified material, such as coarse-grained or diagenetically altered sediments (Fig. 3). Internal geometries of discontinuous reflectors indicate the presence of incipient folding, particularly clear in sparker profile images (e.g., line SP1, Fig. 3 bottom). Seaward of the Kotor ridge, in the outer shelf domain, an uppermost transparent unit, called U3, is visible (Figs. 3, 4 and 5). It is formed by transparent, fine layered sediments, alternating with coarser beds. Internal reflectors show a parallel stratification conformable with the seafloor and continuous over the entire outer shelf. In Fig. 3 (top), the U3 deposits towards the base of the Kotor Ridge show a sort of scouring probably caused by the erosional activity of bottom currents (e.g., Verdicchio, 2008). Unit U3 is bounded at its base by an erosional unconformity (ES2, Fig. 3), progressively more marked towards distal domains, where it shows higher acoustic-impedance contrasts, indicating the presence of an underlying coarser-grained unit. The character of ES2 changes in correspondence of the outer

shelf break, where it becomes conformable with the underlying deposits (MIS6 roll-over point in Fig. 3). Layers below ES2 show seaward dipping oblique-tangential clinoforms, with breakpoints aligned in correspondence of outer scarp. Being bounded at its base by ES2, unit U3 becomes conformable with underlying deposits in the upper slope, and is formed by a thick stack of transparent fine-layered sediments with parallel stratification. In this area, we observe a good penetration of the chirp sonar signal, up to 50 msec two-way traveltime (TWT). The dip of the upper slope exceeds $1-1.3^\circ$ and appears to reflect the effects of gravity-driven processes affecting the entire upper sequence. This leads to the formation of complex seafloor morphologies, with chaotic beds and blocks displaced by normal collapse faults (Fig. 3).

CP4 and CP5 profiles (Fig. 4), crossing the central area of the MACM, show the same stratigraphic architecture of CP1 and CP2. Comparing CP4 and CP5, the width of the non-deposition/erosional area, characterized by rough morphology and high reflectivity, changes significantly along the margin. In CP5, the topographic high that separates the inner and the outer shelf corresponds to the Bar Ridge (Fig.2), and displays the same acoustic pattern observed below the Kotor Ridge in the Northern Area.

Seismic reflection sparker profile SP1 (Fig. 3 bottom) crosses the northern MACM from the inner shelf to the slope, imaging the upper hundreds of meters of the sedimentary sequence. In this section the high-angle normal faults, clearly depicted also by chirp sonar profiles (CP2, Fig. 3 top), cut deeply into the sedimentary sequence. In this sector, at a depth of about 580 msec TWT, there is a feature that resembles an anticlinal deformation (dotted red line in Fig. 3 bottom). Line SP1 crosses orthogonally the Kotor Ridge showing that it coincides with an asymmetric fold. Along this line, at a depth of 230 msec TWT, we observe an anticline with a steeper seaward flank and a flexural bending on the opposite side (Fig. 3, bottom). This feature is marked on its top by an erosional unconformity and is interpreted as a compressive tectonic feature, the Kotor Anticline (Del Bianco et al., in prep) (Fig. 3 bottom).

CP3 and SP2 profiles (Fig. 5) cross orthogonally the Southern Area, from the upper slope to the outer shelf, showing two stacked sedimentary wedges, WA and WB, bounded at their top by erosional unconformities, ES1 and ES2, respectively. In the outer shelf, these wedges are separated by discontinuous to chaotic deposits probably due to gravity-driven failures (Fig. 5). Similar features have been recently observed in the Eastern Niger Delta at the front of a delta prograding wedges (e.g. Garziglia et al., 2010) and in the western side of the Adriatic (Trincardi et al, 2004).

Sparker profile SP1 (Fig. 3, bottom) penetrates through the three stacked sedimentary wedges that built the outer shelf, WB, WC and WD, from top to bottom (insets A, B and C in Fig. 3). If we exclude WD, all these bodies are characterized by internal oblique-tangential clinoforms, and display

seaward migration of the offlap breaks (progradation) with a foreset steepness of about 1.8, 1.5 and 1 degree, respectively (this value is progressively more uncertain because of increasing compaction with depth). The distal part of WB shows an internal wavy facies similar to undulations observed in other continental margins interpreted as sediment waves (Migeon et al., 2001; Lee et al., 2002) or deformation structures evolving into depositional bed-forms (Cattaneo et al., 2004). WD (Fig. 3C) is not well resolved in seismic images, but displays internal steepest foreset and the basal bottom set, which become parallel towards basin. Furthermore, a high-amplitude reflector at its top indicates progradational offlapping geometries.

4.2 Stratigraphic correlations

In order to tie the observed seismo-stratigraphic units to a chrono-stratigraphic reference framework, several sediment samples were collected in different sectors of the MACM using gravity and box corers. (Fig. 3). The 280 cm long sediment core C37 (Fig. 3 for location) was collected in 79 m water depth along the inner shelf of the Southern Area, about 5 km offshore *Ulcinj*. Correlation with chirp sonar profiles suggests that C37 penetrates U1 entirely and reaches the top of the more reflective shingled unit below (Fig. 8). Core Bj08 is about 160 cm long and sampled U1 in the Northern Area, as displayed in its CP5 projection (Fig. 4 bottom). The 150 cm long Co05, in the Northern Area (Fig. 4D), encompasses U1 and the top of U2. Core A85 (270 cm long) was collected in the outer shelf of the Northern Area at about 220 m of water depth (Fig.3), while core A17 (145 cm long) was collected in the Southern shelf-edge at 240 m of water depth. Both cores, A85 and 17 sampled U3 and reached the underlying more reflective unit WB (Fig. 3 inset A and Fig. 5 bottom).

Stratigraphic logs, facies analysis, radiometric dating and correlations illustrated in Fig.6 enabled us to assign each stratigraphic unit to a phase of the global sea level curve (Fig. 7), following a sequence-stratigraphic approach (Posamentier et al., 1988).

4.2.1 Unit 1

Unit 1 (U1) is made of silt and clay deposits interbedded by centimetric layers of clayey silt (Figs. 3, 4 and 6). In C037, Bj08 and CO05 cores, the thickness of U1 is less than 2 m. Based on macrofaunal content, U1 is divided into 2 subunits: lower U1a and upper U1b. U1a contains mollusks typical of brackish euryhaline environment, as well as the bivalve *Gastrana fragilis*. The top of this sub-unit shows an increasing sand content, and mixed/reworked shell fragments, which include *Nuculana pella*, *Abra* spp., *Spisula subtruncata*, *Pododesmus* sp., *Nassarius prismaticus*, *Corbula*

gibba. This assemblage, if fed by multiple sources, resembles a condensed deposit over the ravinement surface (RS). U1b is made of shelf muds, with a distributed macrofaunal content that includes *Turritella communis*, *Pteria hirundo*, *Nucula* spp., *Acanthocardia paucicostata*, etc., all typical of muddy environments, compatible with present water depths. One shell of *A. paucicostata* was dated by ^{14}C -AMS, giving an age of 1974 ± 278 yr cal BP (Table1).

Isochronopach map of U1 (Fig.2) was obtained using all available chirp sonar profiles along the MACM. Depositional styles along the margin show a high degree of variability, which reflects the distribution of the U1 deposits (Fig. 3) into two separate depocenters located in the inner shelf, parallel to the coastline (Fig. 3). Maximum thickness of these deposits exceeds 35 m in the northern depocenter, while in the southern area it is limited to about 30 m, assuming in both cases a 1500 m/s P-waves velocity.

To characterize the present-day sediment deposition, $^{210}\text{Pb}/^{210}\text{Po}$ analysis of core samples were performed (Fig 10). The ^{210}Pb activities show maximum values at the surface, up to 120 and 200 Bq kg^{-1} at station Bj08 and Bj04, respectively (Fig. 11). Conversely, at station Bj01 southeastward the Buna-Bojana outflow, values are lower, probably due to higher river inputs that weaken the ^{210}Pb signal. In fact, the SAR in this station is the highest with a value of 1.5 mm/yr, which suggests the vicinity of sediment input. The shape of the ^{210}Pb profile (activity vs depth) reflects the sediment accumulation pattern and provides additional information on the processes affecting sediment deposition. Where sediment accumulates at a relatively constant rate, a characteristic ^{210}Pb profile consists of an upper region of logarithmically downward decreasing activities. The exponential trend of our profiles suggests that primary stratification of the sediment is preserved and consequently no physical or biological mixing is present on the seafloor. ^{210}Pb profiles suggest a continuous sedimentation over the last ~150 years, with SAR ranging between 0.8 to 1.5 mm/yr. This confirms that in both depocenters of U1, offshore Kotor and the Buna/Bojana outflow, there was a continuous sediment accumulation during considered time span.

Geometry and acoustic facies of U1, as well as the age constrains supported by ^{210}Pb analysis and macrofossil assemblages suggest that this unit was deposited in the Late Pleistocene-Holocene above a ravinement surface (RS) and constitutes the late TST and the HST. The underlying more reflective unit visible in southern depocenter, below U1 (shingled unit in Fig. 8) was sampled only at its top by core C037. In seismic images, this unit shows a shingled internal geometry and probably encompasses the early TST deposits, whose complexity is similar to that observed for correlative deposits on western margin of the Adriatic Sea (Cattaneo and Trincardi, 1999; Maselli et al., 2011). Most likely, its basal unconformity is a regional erosion surface attributed to ES1, although further

stratigraphic constraints are lacking.

4.2.2 Unit 2

Unit 2 (U2) shows a well distinguishable seismic unit on seismic reflection profiles that enables a correlation along most part of the study-area. A chrono-stratigraphic correlation for this unit, which is intermediate between U1 and U3, is lacking since sediment samples were not collected.

4.2.3 Unit 3

Unit 3 (U3) is acoustically transparent and shows downlap reflector terminations over a major unconformity. It correlates over the entire area, although it is observed only in the outer shelf domains (Figs. 3, 4 and 5). While its base and internal geometries change when crossing different domains of the margin, from the upper slope to the shelf, acoustic facies of U3 appears rather uniform, as well as the internal geometries, characterized by low angle sub-parallel clinofolds. U3 is made of homogeneous, gray silty-mud, and shows thicknesses <10 m (Figs. 4 and 6). Associated macrofaunal content includes abundant pectinids of glacial Pleistocene age (*Pseudamussim peslutrae*), and subordinate *Ditrupa arietina* serpulids. Two *P. peslutrae* valves were dated by ¹⁴C-AMS (Tab. 1) giving ages of 15865±622 yr cal BP (A85: Figs. 3 and 6) and 21350±504 yr cal BP (A17: Figs. 3 and 6). Macrofaunal assemblages and radiometric ages suggest that U3 deposits constitute the LST of the MIS2 glacio-eustatic cycle and formed in a mud-dominated prodelta environment.

4.2.4 Older stratigraphic units

To define the chrono-stratigraphic position of WA, we consider that U1 encompasses the latest TST and HST, and that the TST deposits (shingled unit in Fig. 8) overlap ES1, the subaerial erosion formed during the LGM. ES1 represents the erosional top of WA, and its seaward termination represents the roll-over point on its top, that marks the limit of the subaerial erosion. Consequently, we can assume that the roll-over point represents (or it is very close to) the shoreline on the MIS2.2 (Fig. 5) and is found presently in this sector at a water depth of 128 m.

The top of WB was reached by cores A17 and A85 (Figs. 3 and 6) and is represented by the sandy basal sub-unit of these cores. These deposits are formed by medium to fine sands, characterized by numerous specimens of the solitary scleractinian coral *Caryophyllia smithii* typically inhabiting the middle-outer shelf. The results of the ²³⁰Th/U dating are reported in Table 2. The uranium

concentration (~4.2 ppm) is comparable to mean values measured on other live-collected deep-water corals (Cheng et al., 2000a; Montagna et al., 2005). Based on the measured atomic ratios the U-series ages were calculated using the half-life of Cheng et al. (2000b) and Jaffey et al. (1971) ($\lambda_{238} = 1.551 \times 10^{-10}/\text{yr}$, $\lambda_{234} = 2.8263 \times 10^{-6}/\text{yr}$ and $\lambda_{230} = 9.1577 \times 10^{-6}/\text{yr}$).

Due to the high values for $^{230}\text{Th}/^{232}\text{Th}$ ratio (> 18000) no correction was applied for the non-radiogenic ^{230}Th fraction. In fact, a correction for initial ^{230}Th would be minor where the activity ratio of $^{230}\text{Th}/^{232}\text{Th}$ exceeds 20 (e.g. McCulloch et al., 2010). The initial $\delta^{234}\text{U}$ [$\delta^{234}\text{U}_{(0)} = (^{234}\text{U}/^{238}\text{U})_{\text{sample}} / (^{234}\text{U}/^{238}\text{U})_{\text{standard}} - 1) \times 1000$] for both coral fragments is higher than that of modern seawater ($146.8 \pm 0.1\%$, Andersen et al., 2010), indicating that they might have experienced open-system U-series behavior. This is likely caused by alpha recoil mobilization of ^{234}Th and ^{230}Th with a potential simultaneous increase in the initial $\delta^{234}\text{U}$ value and $^{230}\text{Th}/^{238}\text{U}$ ratio and hence over-estimation of the age relative to a closed system (Thompson et al., 2003, Frank et al. 2006).

We tentatively calculated open-system U-series ages using the open-system age equations of Thompson et al. (2003) (Table 2), even though the fact that we have only two measurements does not enable us to confirm the expected mixing slopes predicted by the Thomson model. Therefore, at the moment there are not enough data to approve or reject the calculated model-dependent ages. However, considering the lower value of $\delta^{234}\text{U}_{(0)}$ for sample ALTRO 17 (137cm), which is closer to the modern seawater value, the open-system age of 132.2 kyr is considered more reliable.

Therefore, we consider the deposit containing the coral specimens chronologically related to the end of MIS6. Correlation with the mud/sand transition in correspondence to unconformity ES2, which marks the erosional top of WB in the entire area, suggest that this is a regional unconformity formed during MIS6. Seismo-stratigraphic analysis (section 3.1) and the chrono-stratigraphic constraints of units WA and WB suggest that these wedges represent preserved deposits formed during sea level fall and lowstand stages, known in literature as forced-regression deposits (Trincardi and Field, 1991; Plint, 1991; Posamentier et al., 1992). Sparker profile SP1 (Fig. 3) shows that, below WB, the outer shelf is formed by a stack of sedimentary sequences, locally interbedded by two distinct buried sedimentary wedges at different depth, WC and WD, bounded on their top by high-amplitude reflectors (ES3, ES4 in Fig. 3).

Although no direct sampling of these surfaces is available, we think that they correspond to stacked sequence boundaries controlled by global sea level changes, considering that the alternating recentmost phases of rising and falling of sea level show comparable magnitudes and environmental conditions (Fig. 7). A similar proceeding is described in other continental margin where more stratigraphic constraints are available (e.g. Berné et al., 2002; Ridente et al., 2008; Riboulot et al., 2012). Accordingly, we tentatively assume that each of these regional unconformities formed during

the most recent glacial-interglacial phases at the 100 kyr scale. In this case, sedimentary wedges A, B, C and D are made of stacked forced-regression deposits. Lacking any further stratigraphic constraints, this hypothesis will be tested using a simple subsidence model for the MACM outer shelf (see next section).

4.3 Subsidence rate estimate

Based on the seismic profiles CP1 and SP1 (Fig. 3) it is possible to determine the roll-over point between topset and foreset beds in clinoforms for the uppermost wedges A, B and C; from top to bottom these are found at 300, 380 and 520 msec TWT. Following the top of WB, it is possible to observe the basinward limit of the lowstand subaerial erosion, marked in Fig. 3 (inset A) as MIS6 roll-over point. WC and WD show less steep foreset beds, and the roll-over point is assumed to be at the inflection (or flexural) point along the upper high-amplitude reflector, where it changes its dip. Taking the wedges as indicators of paleo-depth, we attempted to reconstruct the subsidence curve in the interval MIS10-MIS2 along the Northern Area of the MACM. This was done by measuring the net subsidence of each sequence boundary at corresponding domains, such as the transition between preserved progradational geometries and subaerial erosion, which should mark (or is close to) the position of the paleoshorelines. A similar approach has been previously applied in other continental margins, including the Gulf of Lions and the western Adriatic (Rabineau et al., 2006; Maselli et al., 2010). Subsidence rate estimates were carried out along seismic profile SP1 (Fig. 3); the reference point to identify the drowned shoreline relative to each cycle is the basinward limit of the lowstand subaerial erosion observed for WA and the roll-over point between topset and foreset beds in clinoforms for WB and WC. However, these features are also observed in 20-30 m water depth (Vail et al., 1977; Steckler, 1999; Cattaneo et al., 2003, 2007), adding uncertainties in our estimate of the subsidence. MIS2 shoreline position was fixed at 125m below present-day sea level based on the presence of LGM shoreface deposits at the top of the Kotor Ridge (Del Bianco et al., in prep). The depths of the roll-over points (Fig. 7) were calculated using an average sound velocity of 1600 m/s, with depths of 240, 308 and 417 m below sea level corresponding to MIS6, MIS8 and MIS10, respectively. The three points (depth vs. age), together with the MIS2 depth, plot along a line (Fig. 7), suggesting that the margin has been affected by constant subsidence at a rate of 1.2 mm/yr over the last ~350 kyr.

Based on the analysis of seismic reflection and morphobathymetric data, we assume that the MIS2 shoreline corresponds to a paleo-depth range of a drowned lowstand delta front (Del Bianco et al., in preparation). Jouet et al. (2006), reviewed the MIS2 lowstand sea level position proposed by

several authors using different isotope sea level curves. According to Jouet et al. (2006), we assume a MIS2 sea level between 110 and 120 m below present datum. However, we should consider that the vertical movements were not homogeneous along the margin. In fact, comparing the modern shoreline position with the -120 m isobaths, and plotting these differences *vs* the latitudinal position of reference points (Fig. 8) we note different trends in the Northern and Southern areas. Despite the subsidence estimates of submerged paleoshorelines are affected by relatively large error-bars (about 30 m, as pointed out in the previous section) we observe uplift in the Northern Area, in correspondence of the Bar ridge, and subsidence in excess of tens of meters relative to the neutral -120 m level in the Southern Area (Fig. 9). These opposite behaviors reflect probably different deformation patterns along the margin.

4.4 Modern prodelta mud wedge

A sketch of the mud-wedge dispersal system in correspondence of the modern Buna/Bojana delta during the LGM is shown in Fig. 10. Vectors are only indicative, and show the direction of sediment dispersal taking into account: a) the modern inputs from the Buna/Bojana outflow and how it is affected by prevalent longshore currents and local eddies (Fig.3); and b) the presence of a drowned delta system active during the LGM and its relative paleo shelf-break.

Fig. 10A shows that the late-Pleistocene/Holocene depocenters (U1) of the prodelta mud wedge supplied by the Buna/Bojana are located in the inner shelf and divided by a wide area of erosion/non-deposition, also visible in seismic profiles (Figs. 3 and 5). Conversely, during MIS2, the coastline was coincident with the drowned delta front (-120 m isobath) and the prodelta deposits were distributed along the outer shelf (Fig. 10B). The increasing thickness of U3 towards N, observed in core logs and seismic profiles, suggests that also during the LGM the prevailing transport direction was from S to N, although the presence of canyons at the shelf margin indicates an efficient sediment delivery towards deep basins. The LGM shelf-break (green line in Fig. 10B) is located at a depth of -220 m, in correspondence of the present-day outer slope and stratigraphically coincident with the clinoform break point of WB. During the TST deposition, the Kotor and Bar ridges (red lines in Fig. 10) were transitional barrier-island systems parallel to the coast. The back-barrier plain, in correspondence of the southern U1 depocenter, was probably a site of coastal lagoons and/or estuarine environment, as indicated by the brackish euryhaline macrofossil facies identified in the basal sub-unit of C37. In fact, this sediment core is characterized by “transitional” facies that correlate with the shingled unit underlying U1 (Fig.7). Such deposits were also observed in the North Adriatic, where the late-Quaternary TST is typically a few meters thick and consists of a variety of back-barrier

deposits and marine components (Trincardi et al., 1994).

5.0 Discussion

During the modern phase of sea level highstand, sediment accumulation along the MACM is limited to narrow inner-shelf basins parallel to the coastline. Maximum thicknesses of these depocenters are < 35 m, corresponding to a deposition rate of 3-4 mm/yr during the Late Pleistocene-Holocene (e.g. U1 related deposits). This rather low and confined sediment accumulation could be the result of the combined effect of a limited sediment supply and relatively strong longshore currents that cause efficient dispersal. Moreover, the role played by the peculiar physiography of the margin is evident. In fact, we observe tectonic deformations with folding in correspondence of the inner shelf edge, along the Kotor and Bar anticlines, and flexure towards land. This latter effect creates subsidence and accommodation in localized mid-shelf basins (e.g. thrust-top, piggyback or wedge-top basins) where sediments supplied by Buna-Bojana and Drini rivers are deposited. In the literature, the synclinal basins formed by tectonic deformations on the shelf are described as primary repositories of sediment, such as in the Waipaoa and Waiapu River (New Zealand), and the Eel River (California) cases (Clarke, 1987; Foster and Carter, 1997; Lewis et al., 2004). Alternatively, with more limited accommodation in narrower shelves, part of the sediments delivered to collisional margins are transferred to adjacent slopes also during high sea level conditions (Milliman and Syvitski, 1992). This is partly the case of the MACM, where the outer-shelf area is covered by a thin veneer of Holocene deposits as found at the top of A17 and A85 cores and radiocarbon-dated to 8232 ± 232 yr cal BP (A17: Fig. 6 and Table 1), not visible in our high-resolution seismic profiles. This condition is likely the result of storms, floods or other exceptional events, in which the sediment fluxes increase.

On the other hand, the outer shelf is characterized by an apparent uniform subsidence, caused by extensional faulting, and southward tilting. Moreover, we note that most of the outer shelf is built by sediment wedges that show similar geometries and internal architecture. Stratigraphic constraints and a simple linear subsidence model at the scale of a few 100 kyr cycles, suggest that these wedges correspond to forced regression deposits formed during phases of low sea level and preserved by subsidence. This leads to the conclusion that the outer-shelf in correspondence of the Kotor and Bar anticlines is subsiding at a rather constant rate of about 1.2 mm/yr, although uplift due to tectonic deformations is observed. In addition, the width and physiography of the outer-shelf are controlled and shaped by progradation of thick sedimentary wedges in correspondence of the Buna/Bojana outflow during the phases of sea level fall and lowstand, more than by tectonic deformations.

The analysis of the stratigraphic architecture of the MACM suggests that significant sediment accumulation occurs only during lowstand, glacial phases at the 100 kyr time scale, while during interglacials, sediment accumulation is significantly lower, as testified by thickness of U1. This agrees to what proposed by Bossuet et al, 1996, i.e., sedimentary fluxes during the last glacial maximum were 3-3.5 times more intense relative to present-day.

Another important aspect concerns the relative position of the stacked lowstand wedges within the sequence (Fig. 3) In particular, from bottom to top, we see that WC is shifted landward relative to WD (landward migrating roll-over point), i.e., they form a backstepping sequence indicating that subsidence rate is higher than deposition rate. Conversely, between WC and WB there is a seaward migration of roll-over points, indicating that deposition prevails over subsidence. Finally, between WB and WA we fall in the previous case of prevailing subsidence. This would suggest a discontinuous sediment supply during the last ~350 kyrs if we assume a steady, rather constant subsidence curve for the margin. Moreover, the different sizes (volumes) of the sedimentary wedges might suggest different sediment supply or different distances from the sources.

6. Conclusion

Marine geological/geophysical analysis of the Montenegro/Northern Albanian Continental Margin indicates that the main factor controlling its present-day physiography is the effect of the 100 kyr scale cyclicity of sea level changes that contributes to build a relatively thick stack of wedge-shaped deposits at the shelf edge preserved by subsidence. This deposit record encompasses four major seismic sequences marked by forced regression units deposited during MIS 10, 8, 6 and 2. Position and assumed ages of buried shorelines of these lowstand phases indicate that the outer shelf subsidence rate was about 1.2 mm/yr during the last ~350 kyrs. Depositional patterns are also controlled by tectonics, that led to the formation of thrust-top or piggyback basins and the Kotor and Bar ridges acting as by-pass or traps for sediments supplied by local inputs. Morphological identification of the LGM paleoshoreline, approximated to the drowned paleodelta front, suggests that the Bar ridge, in the inner shelf, uplifted by several tens of meters during the last ~20 kyrs. Late Pleistocene/Holocene sediment accumulation along the margin is limited in narrow basin elongated along shore in the inner shelf with a maximum thickness of about 35 m and a modern depositional rate of 0.8 to 1.5 mm/yr for the last 150 yrs. The Holocene deposits were also identified as a thin veneer, up to 10-15 cm by the cores, along the upper continental slope.

This work represents a first step towards the knowledge of the recent (Late Quaternary) geological evolution of MACM and deserves further data acquisition and analysis. A more comprehensive study of relationships between tectonics and sedimentation, including the effects of

the earthquakes that struck repeatedly the coastal zone, would gather benefits by acquisition of more penetrative high-resolution seismic reflection images, and by longer cores.

Acknowledgements

We are indebted to officers, crew, and colleagues for their skilful cooperation during Cruises on board R/V Urania, Mariagrazia and Dallaporta. ADRICOSM-STAR Project provided partial funding with the financial support of the Italian Ministry for the Environment, Land and Sea and the coordination of CMCC. Cores A17 and 85 were collected during cruise ALTRO, carried out in the frame of Collaborative project HERMIONE and COCONET. We are grateful to F. Trincardi and V. Maselli for fruitful discussions that improved the sequence-stratigraphic part of this work and M. Taviani for helpful discussion in the paleobiologic interpretation. We thank A. Polonia for the fruitful discussion about the tectonic. This is ISMAR-CNR scientific contribution no. XXXX.

Figures with caption

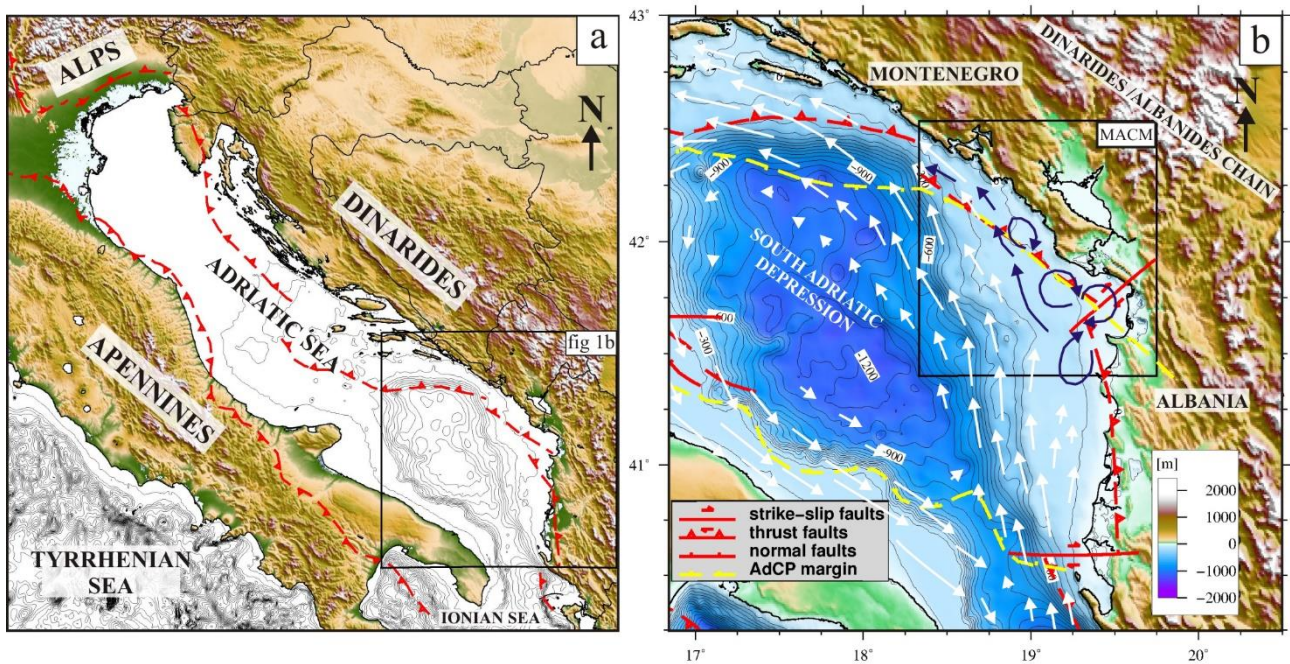


Figure 1. a) the Adriatic Sea between the Alps/Appennines and the Dinaric chains; b) Geodynamic, morphology and oceanographic setting of the South Adriatic Sea, with location of external thrust as limits of the Adria microplate (from Billi et al., 2007; G.M.O.T.M.; Dragičević and Velić, 2002; Vlahović et al., 2005). Blue and white vectors indicate directions and intensity of regional and local currents, from Marini et al. (2010) and Poulain (2001), respectively. Black box indicates the MACM.

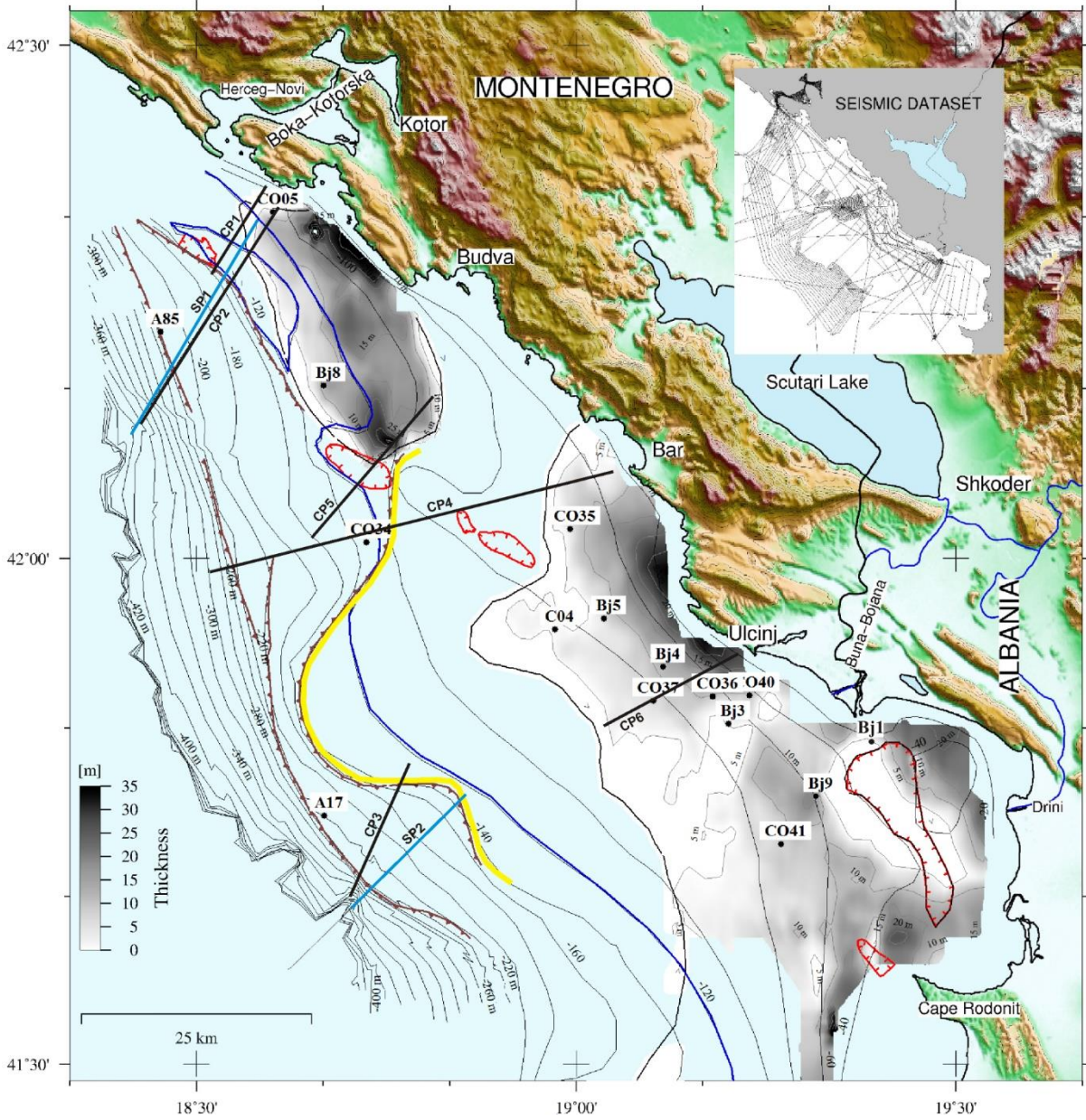


Figure 2. Bathymetric contour map of the MACM with indicated main morphologic features. On grayscale is indicated the isochronopach map of U1 in the inner shelf. Black and blue lines indicate location of seismic reflection profiles displayed in Figs. 3, 4, 5 and 8. Geophysical data coverage is indicated in the inset. Land topography is from GEBCO 08 database.

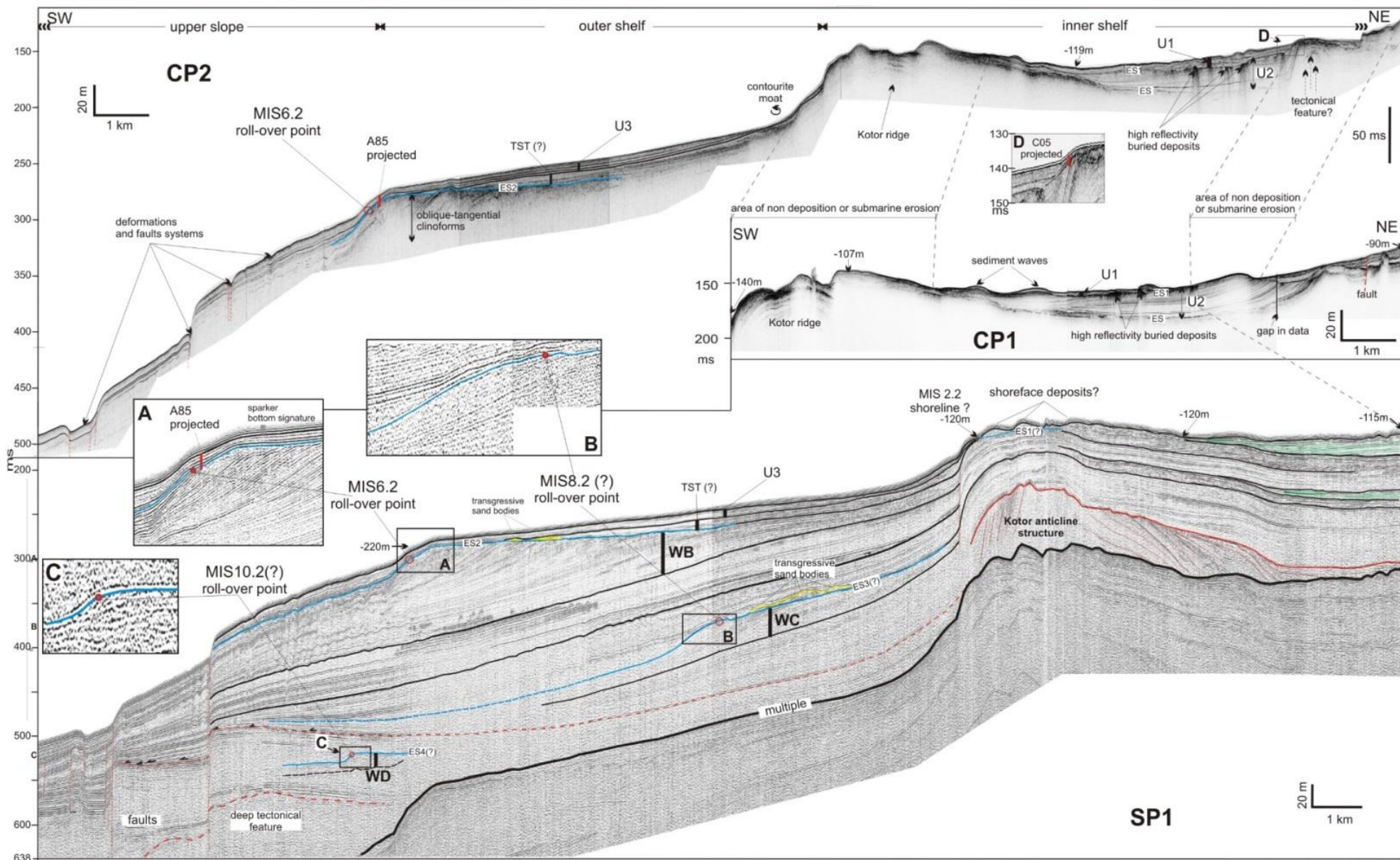


Figure 3. Top: Chirp sonar profiles CP1 and CP2; Bottom: Sparker profile SP1 crossing orthogonally the MACM. Their features are described on the text. Location of profiles is indicated in Fig. 2.

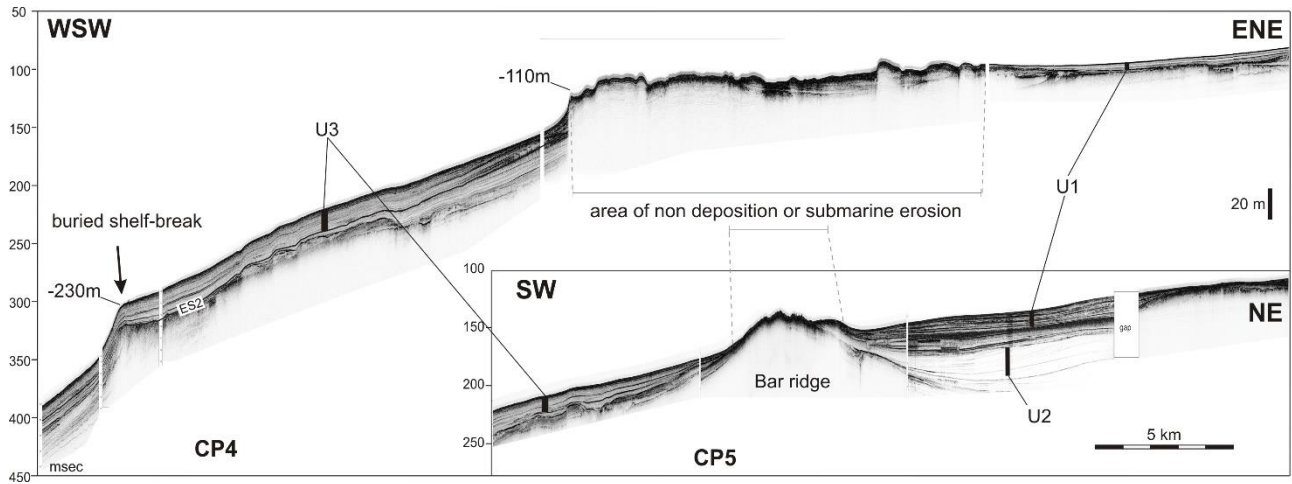


Figure 4. Chirp sonar profile CP4 and CP5 cutting the central area of the MACM, located in Fig. 2.

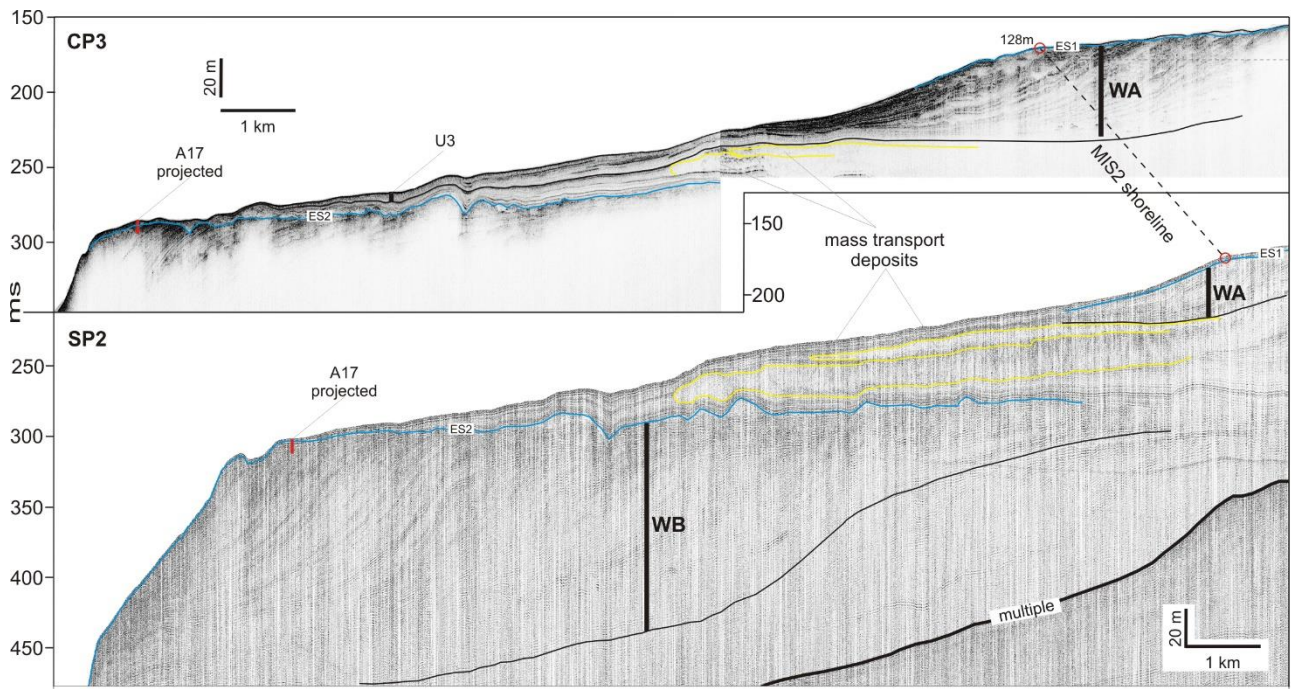


Figure 5. Top: Chirp sonar profiles CP3; Bottom: Sparker profile SP2 crossing orthogonally the MACM. Location of profiles is indicated in Fig. 2.

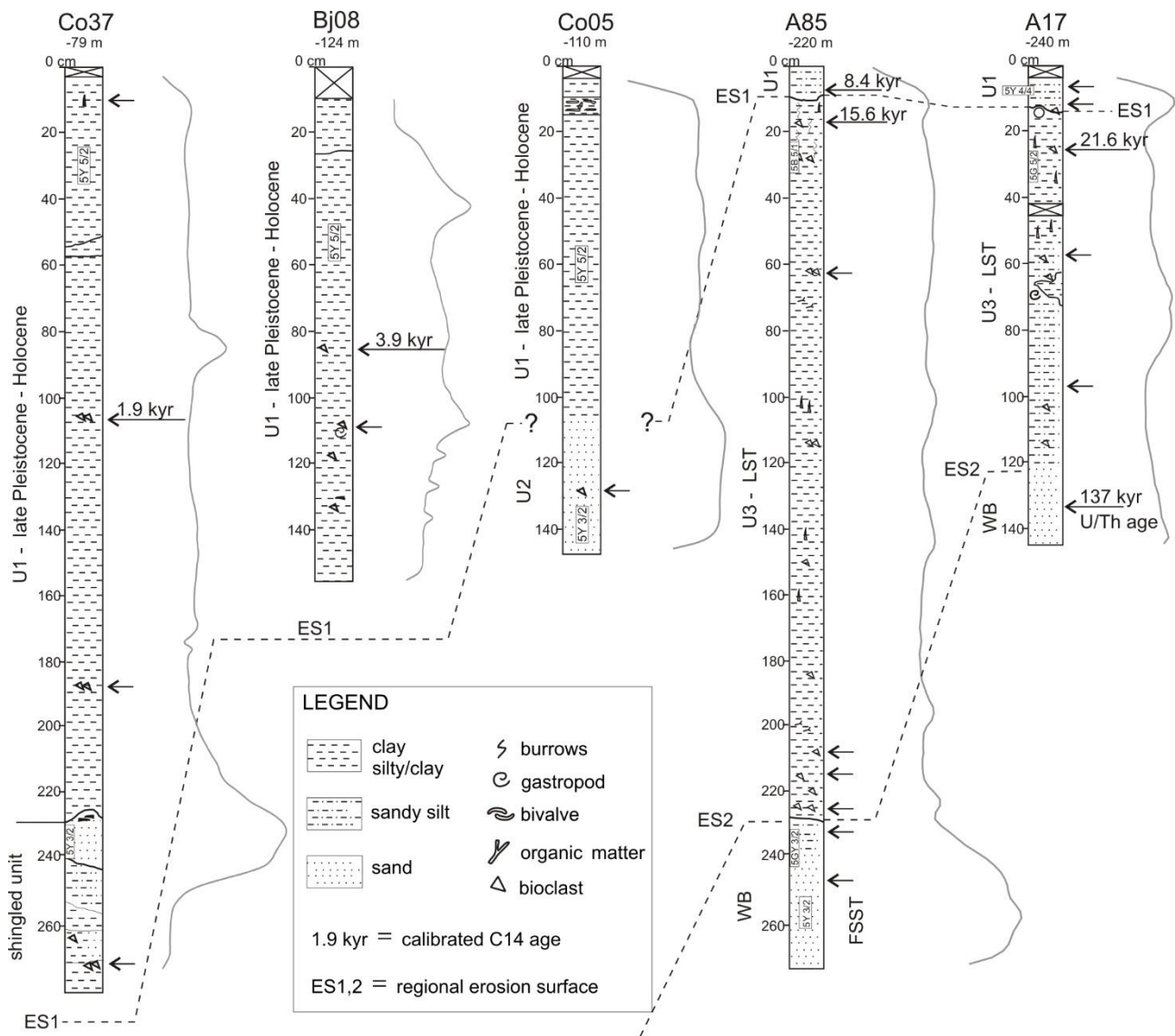


Figure 6. Stratigraphic logs, facies analysis, radioisotope dating and correlation of A85, A17, Co37, Bj08 and Co05 sediment cores.

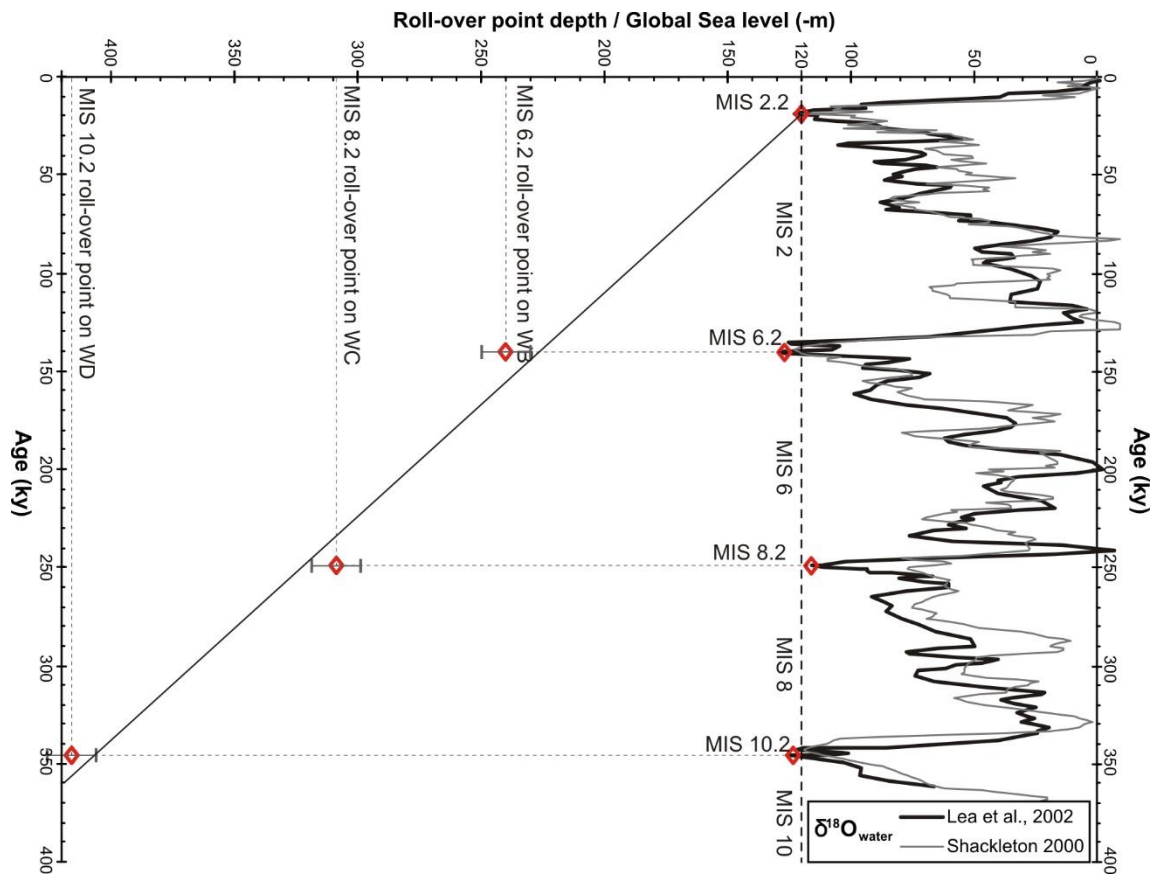


Figure 7. Simple linear regression indicates the subsidence rate estimate. Sea level curves are from Lea et al. (2002) and from Shackleton (2000).

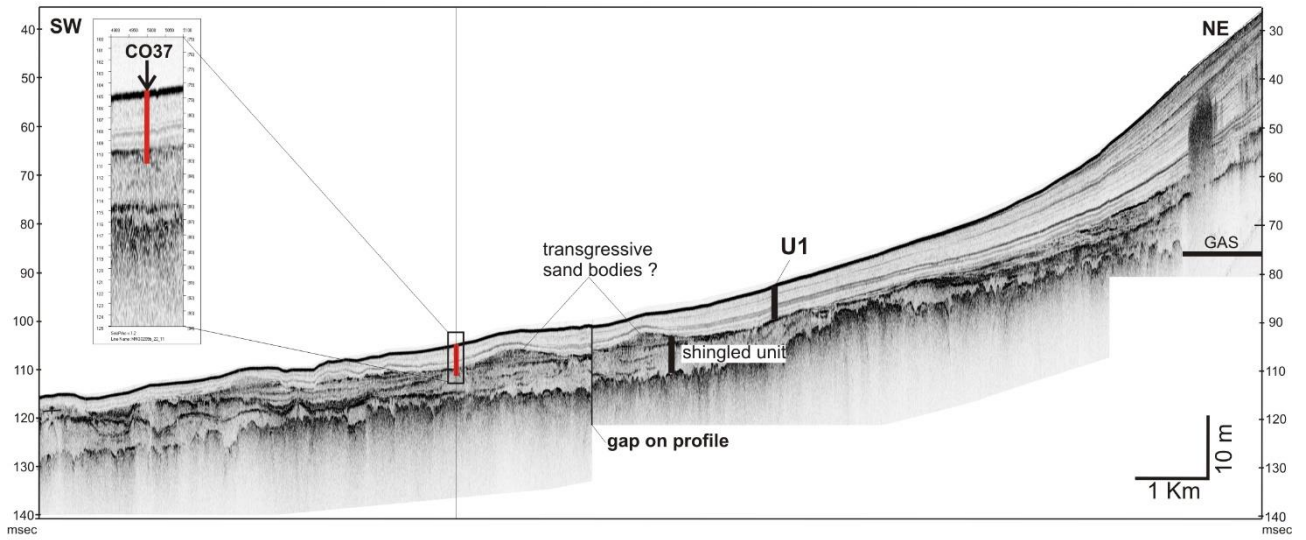


Figure 8. CP6 chirp sonar profile crossing Unit-1 and the underlying shingled unit, located in Fig. 2 with seismo-stratigraphic detail of C037 sampling area.

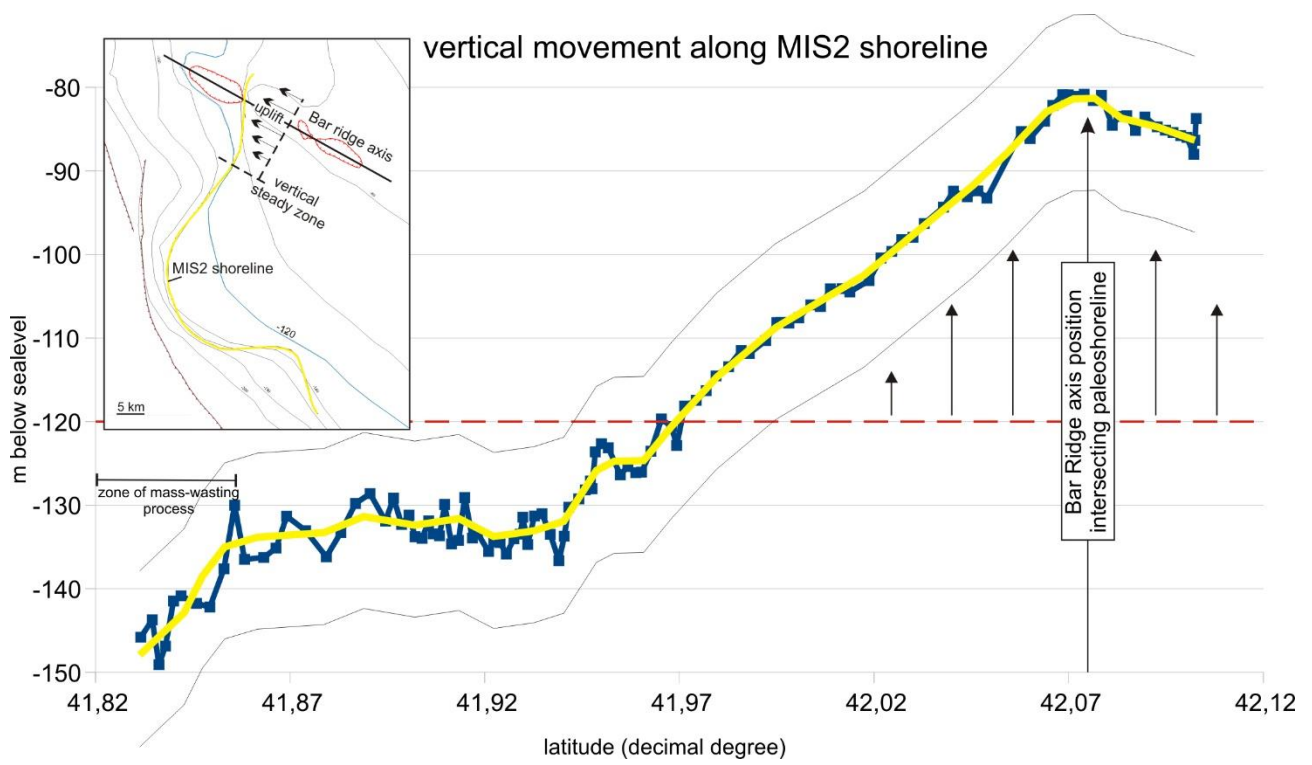


Figure 9. Vertical trend of the drowned lowstand delta front assumed as paleoshoreline during MIS2.

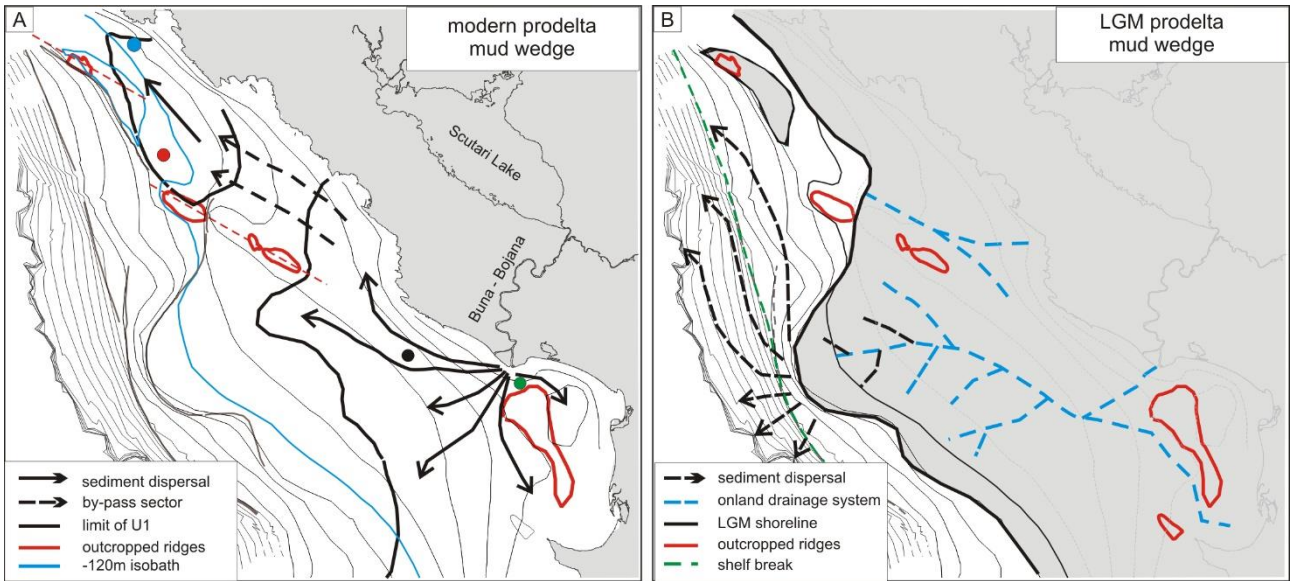


Figure 10. Simplified sketch of modern prodelta mud wedge (A) and during LGM (B). Two zone of depositions are visible, separated by a sill of non-deposition. Sediment dispersal and the onland drainage system vector and lines are pure indicative, see text for more details. Color dots indicates sediment samples analyzed for ^{210}Pb (see Fig. 11).

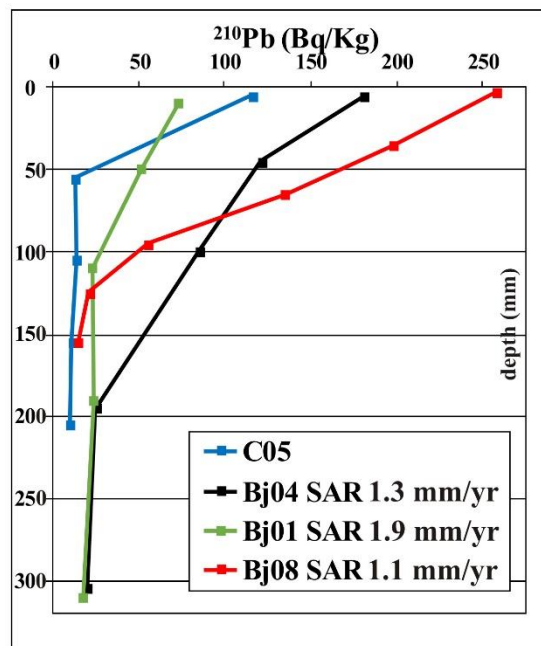


Figure 11. ^{210}Pb excess plots. For location of samples, see Fig.10.

Table 1. Radiocarbon data.

Sample	Depth(cm)	Material	code	yr BP	DR	sigmaR	min yr	max yr	yr cal BP	Err (+/-)
A85	8,5	Benthic forams	Poz-56502	7850 ± 40 BP	61	104	8000	8464	8232	232
A85	16	<i>Pseudamussium peslutrae</i>	Poz-56503	13520 ± 70 BP	61	104	15248	16016	15632	384
A17	28	<i>P. peslutrae</i>	Poz-56507	18370 ± 90 BP	61	104	21262	22073	21667	405
BJ08	83	<i>Neopycnodonte cochlear</i>	Poz-56504	3985 ± 35 BP	61	104	3615	4219	3917	302
C037	105	<i>Acanthocardia paucicostata</i>	Poz-56505	2390 ± 30 BP	61	104	1696	2253	1974	278

Note: from the Poznań Radiocarbon Laboratory in Poznań, Poland. Radiocarbon years (¹⁴C-yr) correspond to the true half-life. Calibrated age ranges reflect the 95.4 % probability window (2σ-error) and were calculated with Calib7.0, using the surface marine calibration curve Marine13 by Reimer et al. (2013).

Table 2. U/Th data.

Sample	Depth (cm)	Labcode Gif	Weight (mg)	²³⁸ U (µg/g)	²³² Th (ng/g)	δ ²³⁴ U _m	(²³⁰ Th/ ²³² Th)	(²³⁰ Th/ ²³⁸ Th)
A17	132	4455	99.55	4.234 ±0.0016	0.501 ±0.004	117.4 ±0.6	21803 ±103.2	0.81367 ±0.00387
A17	137	4456	96.85	4.184 ±0.0018	0.553 ±0.001	107.8 ±0.8	18750 ±38.0	0.80724 ±0.00164

Age (kyr)	δ ²³⁴ U ₍₀₎	Age (kyr)*
137.1 ±1441	173.0 ±1.2	126.350 ±1.5
137.7 ±0.772	159.1 ±1.2	132.200 ±1.1

Note: $\delta^{234}\text{U}_{\text{meas}} = \{[(^{234}\text{U}/^{238}\text{U})_{\text{sample}}/(^{234}\text{U}/^{238}\text{U})_{\text{eq}}] - 1\} \times 1000$, where $(^{234}\text{U}/^{238}\text{U})_{\text{eq}}$ is the atomic ratio at secular equilibrium ($=5.489 \times 10^{-5}$); $\delta^{234}\text{U}_{(0)}$ is the initial value and is calculated by the equation: $\delta^{234}\text{U}_{(0)} = \delta^{234}\text{U}_{\text{meas}} \exp(^{\lambda}234t)$, where t is the age in years; The concentrations of ²³⁸U and ²³²Th were determined using the enriched ²³⁶U and ²²⁹Th isotopes, respectively

*Age calculated using the open-system model (Thompson et al., 2003)

Table 3. Numerical data used for subsidence rate estimate.

MIS	TWT ms	Depth m (@1600m/s)	Location	Age (Rohling, 1998)
2.2	---	120	Kotor Ridge	20 cal-kyr
6.2	299	239.2	WB	135 kyr
8.2	385	308	WC	270 kyr
10.2	522	417.6	WD	340 kyr

References

- Aliaj, S., 1997. Alpine geological evolution of Albania. *Albanian Journal of Natural & Technical Sciences*, No 3, 69-81.
- Aliaj, S., 1998. Neotectonic structure of Albania. *Albanian Journal of Natural & Technical Sciences*, No 4, 79-97.
- Aliaj, S., 1999. Transverse faults in Albanian orogen front. *Albanian Journal of Natural & Technical Sciences*, No 6, 121-132.
- Aliaj, S., 2000. Thrust front along Adriatic collision and seismic potential of its seismogenic nearby zone. *Proceedings International Symposium on Earthquake Engineering (ISEE)*, Montenegro, 85-93.
- Aliaj, S., Adams J, Halchuk S., Sulstarova E., Peci V. and Muco B., 2004. Probabilistic seismic hazard maps for Albania. *13th World Conference on Earthquake Engineering*, Vancouver, B.C., Canada, August 1-6, 2004, Paper No. 2469.
- Aliaj, S., 2008. The Albanian Orogen: convergence Zone between Eurasia and the Adria microplate, in: N.Pinter, G.Gyula, S.Stein and D.Medak (Eds.), *The Adria Microplate: GPS Geodesy, Tectonics and Hazards*. NATO Science Series, IY, Earth and Environmental Science, Vol.61, Springer.
- Andersen, M.B., Stirling, C.H., Zimmermann, B., Halliday, A.N., 2010. Precise determination of the open $^{234}\text{U}/^{238}\text{U}$ composition. *Geochemistry, Geophysics, Geosystems* 11, Q12003, doi:10.1029/2010GC003318.
- Anderson, H. & Jackson, J., 1987. Active tectonics of the Adriatic region. *Geophysical Journal of the Royal Astronomical Society*, 91, 937-983.
- Argnani, A., Bonazzi, C., Evangelisti, D., Favali, P., Frugoni, F., Gasperini, M., Ligi, M., Marani, M. and Mele, G., 1996. Tettonica dell'Adriatico meridionale. *Memorie della Società Geologica Italiana*, 51, 227-237.
- Argnani, A., Rovere, M., & Bonazzi, C., 2006. Tectonics and large-scale mass wasting along the slope of the southern Adriatic basin. *Geophysical Research Abstracts*, Vol. 8, 07261, 2006.
- Artegiani, A., Bregant, D., Paschini, E., Pinardi, N., Raicich, F., Russo, A., 1997. The Adriatic Sea general circulation. Part I. Air-sea interactions and water mass structure. *Journal of Physical Oceanography* 27, 1492-1514.
- Berné, S., Lericolais, G., Marsset, T., Bourillet, J.F., De Batist, M., 1998. Erosional onshore sand ridges and lowstand shore-faces: examples from tide- and wave-dominated environments of France. *Journal of Sedimentary Research*, 68, 540-555.
- Berné, S., Satra, C., Aloïsi, J.C., Baztan, J., Dennielou, B., Droz, L., Dos Reis, A.T., Lofi, J., Méar, Y., Rabineau, M., 2002. Carte morphobathymétrique du Golfe du Lion: notice explicative. Ifremer Brest.

- Bertotti, G., Picotti, V., Chilovi, C., Fantoni, R., Merlini, S. and Mosconi, A., 2001. Neogene to Quaternary sedimentary basins in the south Adriatic (Central Mediterranean): Foredeeps and lithospheric buckling. *Tectonics*, 771-787.
- Billi, A., Presti, D., Faccenna, C., Neri, N., Orecchio, B., 2007. Seismotectonics of the Nubia plate compressive margin in the south Tyrrhenian region, Italy: Clues for subduction inception, *J. Geophys. Res.*, 112, B08302, doi:10.1029/2006JB004837.
- Bossuet, G., Ruffaldi, P., Magny, M., Richard, H., Mouthon, J., 1996. Dynamique et approche quantitative des remplissages fini-et postwürmiens du bassin lacustre de Cerin (Jura, France). *Bulletin de la Société Géologique de France*. 167 (4), 483-494.
- Cattaneo, A., Correggiari, A., Langone, L., Trincardi, F., 2003a. The late-Holocene Gargano subaqueous delta, Adriatic shelf: sediment pathways and supply fluctuations. *Marine Geology* 193, 61-91.
- Cattaneo, A., Correggiari, A., Penitenti, D., Trincardi, F., Marsset, B., 2003b. Morphobathymetry of small-scale mud reliefs on the Adriatic shelf, in: Locat, J., Mienert, J. (Eds.), *Submarine Mass Movements and their Consequences*. Kluwer, Amsterdam, pp. 401-408.
- Cattaneo, A., Correggiari, A., Marsset, T., Thomas, Y., Marsset, B., Trincardi, F., 2004. Seafloor undulation pattern on the Adriatic shelf and comparison to deep-water sediment waves. *Marine Geology*, 213 (1-4), 121-148.
- Cattaneo, A., Trincardi, F., Asioli, A., & Correggiari, A., 2007. The Western Adriatic shelf clinof orm: energy-limited bottomset. *Continental Shelf Research*, 27(3-4), 506-525. doi:10.1016/j.csr.2006.11.013
- Cattaneo, A., and Trincardi F., 1999. The late-Quaternary transgressive record in the Adriatic epicontinental sea: Basin widening and facies partitioning, in: *Isolated Shallow Marine Sand Bodies: Sequence Stratigraphic Analysis and Sedimentologic Interpretation*, edited by K. Bergman and J. Snedden, Special Publications, SEPM Society for Sedimentary Geology, 64, 127-146.
- Cheng, H., Adkins, J., Edwards, R.L., Boyle E.A., 2000a. U-Th dating of deep-sea corals. *Geochimica et Cosmochimica Acta*. 64, 2401-2416.
- Cheng, H., Edwards, R.L., Hoff, J., Gallup, C.D., Richards, D.A., Asmerom, Y., 2000b. The half-lives of uranium-234 and thorium-230. *Chemical Geology*, 168, 17-33.
- Chiocci, F.L., Ercilla, G., Torres, J., 1997. Stratal architecture of Western Mediterranean Margins as the result of the stacking of Quaternary lowstand deposits below glacio-eustatic fluctuation base-level. *Sedimentary Geology*, 112, 195-217.
- Clark, P. U., Dyke, A. S., Shakun, J. D., Carlson, A. E., Clark, J., Wohlfarth, B., McCabe, a M., 2009. The Last Glacial Maximum. *Science (New York, N.Y.)*, 325(5941), 710-4. doi:10.1126/science.1172873.
- Clarke, S.H., Jr., 1987. Geology of the California continental margin north of Cape Mendocino, in: Scholl, D.W., Grantz, A., Vedder, J.G. (Eds.), *Geology and Resource Potential of the Continental Margin of Western North America and Adjacent Ocean Basins. Beaufort Sea to Baja California*. Circum-Pacific Council for Energy and Mineral Resources, Earth Science Series, 6, pp. 337-351.

- De Alteriis, G., 1995. Different foreland basins in Italy: examples from the central and southern Adriatic Sea. *Tectonophysics*, 252, 349-373.
- Del Bianco, F., Gasperini, L., Bortoluzzi, G., Giglio, F., D'Oriano, F., Polonia, A., Ravaioli, M., Kljajic, Z., Bulatovic, A., 2010. The Montenegro-Northern Albanian continental margin: morphotectonic features in a seismically active region. *Rapp. Comm. Int. Mer Medit.* Vol.39 p.20.
- Del Bianco, F., Gasperini, L., Bortoluzzi, G., Giglio, F., Ravaioli, M., Kljajic, Z., 2014. Seafloor morphology of the Montenegro/N. Albania Continental Margin (Adriatic Sea - Central Mediterranean), manuscript in preparation.
- Dragasevic, T., 1974. Recent structure of Earth's Crust and Upper Mantle in Yugoslavia. *Zbornik: Metalogenija i koncepcije geotektonskog razvoja Jugoslavije (Collection: Metallogeny and Concepts of Geotectonic History of Yugoslavia)*. Faculty of Mining and Geology, Belgrade, 59-72 (in Serbian).
- Dragasevic, T., 1983. Oil geologic exploration in the Montenegro offshore in Yugoslavia. *NAFTA*, 34, 397-404.
- Dragičević, I., Velić, I., 2002. The Northeastern Margin of the Adriatic Carbonate Platform. *Geologia Croatica*, 55/2, 185-232.
- Fontugne, M., Shao, Q., Frank, N., Thil, F., Guidon, N., Boeda, E., 2013. Cross-Dating (Th/U-¹⁴C) of Calcite Covering Prehistoric Paintings at Serra da Capivara National Park, Piauí, Brazil. *Radiocarbon*, 55 (2-3), 1191-1198.
- Foster, G., Carter, L., 1997. Mud sedimentation on the continental shelf at an accretionary margin Poverty Bay, New Zealand. *N.Z. Journal of Geology and Geophysics*, 40, 157-173.
- Frank, N., Turpin, L., Cabioch, G., Blamart, D., Colin, C., Tressens-Fedou, M., Bonhomme, P., Jean-Baptist, P., 2006. Open system U-series ages of corals from a subsiding reef in New Caledonia: Implications for Holocene sea level rise, and subsidence rate, *Earth and Planetary Science Letters* 249, 274-289.
- Frignani, M., Langone, L., 1991. Accumulation rates and ¹³⁷Cs distribution in sediments off the Po river delta and the Emilia-Romagna coast (northwestern Adriatic Sea, Italy). *Continental Shelf Research*, 11, 525-542.
- Frignani, M., Langone, L., Albertazzi, S., Ravaioli, M., 1993. Cronologia di sedimenti marini. Analisi di ²¹⁰Pb via ²¹⁰Po per spettrometria alfa. IGM-CNR Technical Report No. 28, Bologna, 24 pp.
- Frignani, M., Langone, L., Ravaioli, M., Sorgente, D., Alvisi, F., Albertazzi, S., 2005. Fine-sediment mass balance in the western Adriatic continental shelf over a century time scale. *Marine Geology*. 222-223, pp. 113-133. doi:10.1016/j.margeo.2005.06.016.
- Garziglia, S., Sultan, N., Cattaneo, A., Ker, S., Marsset, B., Riboulot, V., Voisset, M., Adamy, J., Unterseh, S., 2010. Identification of shear zones and their causal mechanisms using a combination of cone penetration tests and seismic data in the Eastern Niger Delta, in: Mosher, D., et al. (Ed.), *Submarine Mass Movements and Their Consequences*, 28. *Advances in Natural and Technological Hazards Research*. Springer, 55-65.

- Gasperini, L., Stanghellini, G., 2009. SEISPRHO: an interactive computer program for processing and interpretation of high-resolution seismic reflection profiles. *Computers and Geosciences*, 35, 1497-1504.
- GEBCO, 2008. Gridded Global Bathymetry Data. British Oceanographic Data Centre, Liverpool, United Kingdom.
- Gensous, B., Tesson, M., 1996. Sequence stratigraphy, seismic profiles, and cores of Pleistocene deposits on the Rhone continental shelf. *Sedimentary Geology*, 105, 183-190.
- G.M.O.T.M., 2004. Geodynamic map of the Mediterranean. Commission for the Geological Map of the World.
- Grenerczy, G., Sella, G., Stein, S., Kenyeres, A., 2005. Tectonic implications of the GPS velocity field in the northern Adriatic region. *Geophysical Research Letters*, v. 32.
- Hunstad, I., Selvaggi, G., D'agostino, N., England, P., Clarke, P., Pierozzi, M., 2003. Geodetic strain in peninsular Italy between 1875 and 2001. *Geophysical Research Letters*, 30, 1181. doi:10.1029/2002GL016447.
- Jaffey, A.H., Flynn, K.F., Glendenin, L.E., Bentley, W.C., Essling, A.M., 1971. Precision measurement of half-lives and specific activities of ^{235}U and ^{238}U . *Physical Review C*, 4(5), 1889-1906.
- Jouet, G., S. Berné, M. Rabineau, M. A. Bassetti, P. Bernier, B. Dennielou, F. J. Sierro, J.-A. Flores, and M. Taviani, 2006. Shoreface migrations at the shelf edge and sea-level changes around the Last Glacial Maximum (Gulf of Lions, NW Mediterranean), *Marine Geology*, 234, 21-42, doi:10.1016/j.margeo.2006.09.012.
- Kourafalou, V.H., 1999. Process studies on the Po River plume, north Adriatic Sea. *Journal of Geophysical Research*, 104(C12), 29963-29985.
- Lee, H.J., Syvitski, J.P.M., Parker, G., Orange, D., Locat, J., Hutton, E. W.H., Imran, J., 2002. Distinguishing sediment waves from slope failure deposits: field examples, including the 'Humboldt Slide', and modelling results. *Marine Geology*, 192, 79-104.
- Lewis, K.B., Lallemand, S.E., Carter, L., 2004. Collapse in a Quaternary shelf basin off East Cape, New Zealand: evidence for passage of a subducted seamount inboard of the Ruatoria giant avalanche. *New Zealand Journal of Geology and Geophysics* 47, 415-429.
- Marini, M., Grilli, F., Guarnieri, A., Jones, B. H., Klajic, Z., Pinardi, N., Sanxhaku, M., 2010. Is the southeastern Adriatic Sea coastal strip an eutrophic area? *Estuarine, Coastal and Shelf Science*, 88(3), 395-406. doi:10.1016/j.ecss.2010.04.020.
- Maselli, V., Trincardi, F., Cattaneo, a., Ridente, D., Asioli, A., 2010. Subsidence pattern in the central Adriatic and its influence on sediment architecture during the last 400 kyr. *Journal of Geophysical Research*, 115(B12), B12106. doi:10.1029/2010JB007687.
- Maselli, V., Hutton, E. W., Kettner, A. J., Syvitski, J. P. M., Trincardi, F., 2011. High-frequency sea level and sediment supply fluctuations during Termination I: An integrated sequence-stratigraphy and modeling approach from the Adriatic Sea (Central Mediterranean). *Marine Geology*, 287(1-4), 54-70. doi:10.1016/j.margeo.2011.06.012.

- McCulloch, M., Taviani, M., Montagna, P., López Correa, M., Remia, A., Mortimer, G., 2010. Proliferation and demise of deep-sea corals in the Mediterranean during the Younger Dryas. *Earth and Planetary Science Letters* 298, 143–152.
- Migeon, S., Savoye, B., Zanella, E., Mulder, T., Faugères, J.C., Weber, O., 2001. Detailed seismic-reflection and sedimentary study of turbidite sediment waves on the Var Sedimentary Ridge (SE France): significance for sediment transport and deposition and for the mechanisms of sediment-wave construction. *Marine Petroleum Geology*, 18, 179–208.
- Milliman, J., Syvitski, J.P.M., 1992. Geomorphic/tectonic control of sediment discharge to the ocean: the importance of small mountainous rivers. *The Journal of Geology* 100, 525-544.
- Montagna, P., McCulloch, M., Taviani, M., Remia, A., Rouse, G., 2005. High-resolution trace and minor element compositions in deep-water scleractinian corals (*Desmophyllum dianthus*) from the Mediterranean Sea and the Great Australian Bight, in: Freiwald A, Roberts JM (Eds), 2005, *Cold-water Corals and Ecosystems*. Springer-Verlag Berlin Heidelberg, 1109-1126.
- Oluic, M., Cvijanovic, D., Prelogovic, E., 1982. Some new data on the tectonic activity in the Montenegro coastal region (Yugoslavia) based on the landsat imagery. *Acta Astronautica* 9(1), 27-33.
- Plint, A.G., 1991. High-frequency relative sea-level oscillations in the Upper Cretaceous shelf clastics of the Alberta foreland basin: possible evidence for glacio-eustatic control? In: Macdonald, D.I.M. (Ed.), *Sedimentation, Tectonics and Eustasy*, International Association of Sedimentologists. Special Publications, 12, 409–428.
- Posamentier, H.W., Allen, G.P., James, D.P., Tesson, M., 1992. Forced regressions in a sequence stratigraphic framework: concepts, examples and exploration significance. *American Association of Petroleum Geologists, Bulletin* 76, 1687–1709.
- Piper, D.J.W., Aksu, A.E., 1992. Architecture of stacked Quaternary deltas correlated with global oxygen isotopic curve. *Geology*, 20, 415-418.
- Pondrelli, S., A. Morelli, G. Ekström, S. Mazza, E. Boschi, and A. M. Dziewonski, 2002. European- Mediterranean regional centroid-moment tensors: 1997-2000, *Physics of the Earth and Planetary Interiors*, 130, 71-101.
- Posamentier, H.W., Jervey, M.T., Vail, P.R., 1988. Eustatic controls on clastic deposition I - conceptual framework, in: Wilgus, C.K., Hastings, B.S., Kendall et al (Eds), 1988, 42, 109-24.
- Rabineau, M., Berné, S., Olivet, J.L., Aslanian D., Guillocheau, F., Joseph P., 2006. Paleo sea levels reconsidered from direct observation of paleoshoreline position during Glacial Maxima (for the last 500,000 yr). *Earth and Planetary Science Letters*, 252, 119–137. doi:10.1016/j.epsl.2006.09.033.
- Reimer, P.J., Bard, E., Bayliss, A., Beck, J.W., Blackwell, P.G., Bronk Ramsey, C., Buck, C.E., Cheng, H., Edwards, R.L., Friedrich, M., Grootes, P.M., Guilderson, T.P., Haflidason, H., Hajdas, I., Hatté, C., Heaton, T.J., Hoffmann, D.L., Hogg, A.G., Hughen, K.A., Kaiser, K.F., Kromer, B., Manning, S.W., Niu, M., Reimer, R.W., Richards, D.A., Scott, E.M., Southon, J.R., Staff, R.A., Turney, C.S.M., van der Plicht, J., 2013. IntCal13 and Marine13 radiocarbon age calibration curves, 0–50,000 years cal BP. *Radiocarbon* 54/4, 1869–1887.

- Riboulot, V., Cattaneo, a., Berné, S., Schneider, R. R., Voisset, M., Imbert, P., Grimaud, S., 2012. Geometry and chronology of late Quaternary depositional sequences in the Eastern Niger Submarine Delta. *Marine Geology*, 319-322, 1–20. doi:10.1016/j.margeo.2012.03.002.
- Ridente, D., Trincardi, F., 2002. Eustatic and tectonic control on deposition and lateral variability of Quaternary regressive sequences in the Adriatic basin (Italy). *Marine Geology*, 184(3-4), 273–293. doi:10.1016/S0025-3227(01)00296-1.
- Ridente, D., Trincardi, F., 2006. Propagation of shallow folds and faults in late Pleistocene and Holocene shelf-slope deposits, central and South Adriatic Margin (Italy). *Basin Research*, 18, 171–188.
- Ridente, D., Trincardi, F., Piva A., Asioli, A., Cattaneo, A., 2008. Sedimentary response to climate and sea level changes during the past 400 ka from borehole PRAD1.2 (Adriatic margin), *Geochem. Geophys. Geosyst.*, 9, Q09R04, doi:10.1029/2007GC001783
- Robbins, J.A., 1978. Geochemical and geophysical application of radioactive lead. In: Nriagu, J.O. (Ed.), *The Bio-geochemistry of Lead in the Environment*. Elsevier, Amsterdam, pp. 285–393.
- Rohling, E.J., Fenton, M., Jorissen, F.J., Bertrand, P., Ganssen, G., Caulet, J.P., 1998. Magnitudes of sea level lowstands of past 500,000 years. *Nature* 394, 162–165.
- Skene, K., Piper, D., Aksu, A., Syvitski, J.P.M., 1998. Evaluation of the global oxygen isotope curve as a proxy for quaternary sea-level by modeling of delta progradation. *Journal of Sedimentary Research*, 68, 1077-1092.
- Somoza, L., Barnolas, A., Arasa, A., Maestro, A., Rees, J.G., Hernandez-Molina, F.J., 1998. Architectural stacking patterns of the Ebro delta controlled by Holocene high-frequency eustatic fluctuations, delta-lobe switching and subsidence processes. *Sedimentary Geology*, 117, 11-32.
- Steckler, M. S., 1999. High resolution sequence stratigraphic modeling: 1. The interplay of sedimentation, erosion and subsidence, in *Numerical Experiments*, in: *Stratigraphy: Recent Advances in Stratigraphic and Computer Simulations*, edited by J. Harbaugh et al., Mem. 62, pp. 139–149, Soc. of Econ. Paleontol. and Mineral., Tulsa, Okla.
- Stuiver M., P.J. Reimer, and R. Reimer, 2013. CALIB Radiocarbon Calibration v14.0. Execute Version 7.0 html - <http://calib.qub.ac.uk/calib/>
- Tesson, M., Gensous, B., Allen, G.P., Ravenne, C., 1990. Late Quaternary deltaic lowstand wedges on the Rhone continental shelf, France. *Marine Geology*, 91, 325-332.
- Thomson, W.G., Spiegelman, M.W., Goldstein, S.L., Speed, R.C., 2003. An open-system model for U-series age determinations of fossil corals. *Earth and Planetary Science Letters*, 210, 365-381.
- Trincardi, F., Field, M.E., 1991. Geometry, lateral variability, and preservation of downlapped regressive shelf deposits: Eastern Tyrrhenian margin, Italy. *Journal of Sedimentary Petrology*, 61, 75–90.
- Trincardi, F., Correggiari, A., Roveri, M., 1994. Late Quaternary transgressive erosion and deposition in a modern epicontinental shelf: the Adriatic semi-enclosed basin. *Geo-Marine Letters*, 14, 41–51.

- Trincardi, F., Cattaneo, A., Correggiari, A., Ridente, D., 2004. Evidence of soft sediment deformation, fluid escape, sediment failure and regional weak layers within the late Quaternary mud deposits of the Adriatic Sea. *Marine Geology*, 213(1-4), 91–119. doi:10.1016/j.margeo.2004.10.003
- UNEP 1996. Mediterranean Action Plan (MAP), Implications of Climate Change for the Albanian Coast, Technical Reports series No.98.
- Vail, P.R., Mitchum, R.M. and Thompson, S. III, 1977. Seismic stratigraphy and global changes of sea level, Part 3: relative changes of sea level from coastal onlap. In: C.W. Payton (Ed.), *Seismic Stratigraphic Applications to Hydro-carbon Exploration*. American Association of Petroleum Geologists Memories, 26, 63- 97.
- Verdicchio, G., Trincardi, F., Asioli, A., 2007. Mediterranean bottom-current deposits: an example from the Southwestern Adriatic Margin. *Geological Society, London, Special Publications*, 276(1), 199–224. doi:10.1144/GSL.SP.2007.276.01.10
- Verdicchio, G., Trincardi, F., 2008. Mediterranean shelf-edge muddy contourites: example from Gela and South Adriatic Basins, *Geo-Marine Letters*, 28, 137–151. doi:10.1007/s00367-007-0096-9.
- Vlahović, I., Tišljarić, J., Velić, I., Matičec, D., 2005. Evolution of the Adriatic Platform: paleogeography, main events and depositional dynamics. *Paleogeography, Paleoclimatology, Paleoecology* 220, 333–360.
- Weber, O., Migeon, S., Savoye, B., Zanella, E., Mulder, T., & Fauge, J., 2001. Detailed seismic reflection and sedimentary study of turbidite sediment waves on the Var Sedimentary Ridge (SE France): significance for sediment transport and deposition and for the mechanisms of sediment-wave construction, 18.
- Wessel, P., W. H. F. Smith, 1998. New, improved version of the Generic Mapping Tools released, *EOS Trans. AGU*, 79, 579.

3.4 Present-day sedimentation patterns along the Montenegro/N. Albania Continental Margin from geochemical analysis (Adriatic Sea - Central Mediterranean)

Giglio F., Del Bianco F., Gasperini L., Bortoluzzi G., Albertazzi S., Kljajic Z., Castelli A. and Ravaioli M.

Abstract

Sedimentological and geochemical analyses of seafloor sediments collected at several location along the Montenegro/Northern Albania Continental Margin provide information about present-day transport and deposition of marine sediments, as well as indirect information about prevailing current direction and strength. Sedimentation rates, determined based on short-lived radioisotopes analysis range from 0.08-0.15 cmyr⁻¹, reaching their maximum in correspondence of the Bojana River outflow. ¹³⁷Cs and ²¹⁰Pb curves, determined along the upper parts of the marine sedimentary sequence show continuous sedimentation at the scale of the latest 100-150 years, only in two main sectors of the inner shelf, separated by a narrow corridor of erosion/non deposition. Furthermore, geochemical data, e.g. trace metals, C and N and their stable isotopes, indicate the presence of two main source areas in different mineralogical provinces, i.e. the Albanides and Dinarides Mountain Ranges, related to the drainage basins of the river system. The observed gradients pointing towards north observed in all the parameters analyzed indicate a major role is played by longshore currents in redistributing sediments along the margin from SE to NW.

1. Introduction

Differently from its western counterpart, the eastern Adriatic Shelf lacks recent marine geological studies based on seabed mapping and analysis of seafloor sediments. This is mostly due to political reasons, because most of the countries facing this side of the Adriatic suffered recently political turmoil that culminated in the '90 with the Yugoslavia War. This is also the case of the Montenegro/Northern Albania Continental Margin (MACM), in the southeastern Adriatic coast (Fig.1).

However, in recent years, in the frame of the ADRICOSM and ADRICOSM-STAR projects, several marine geological data were collected along the MACM. These projects aimed at the development and partial implementation of an integrated coastal area, river and urban waters management system, which would consider both observational and modelling components. The area under investigation for ADRICOSM was the Bojana River Delta and the whole Montenegro Adriatic coast: the projects considered transboundary water issues, such as the Bojana River that is managed by both Montenegro and Albania, and the Montenegro coastal area, which is naturally affected by Albanian marine waters (Fig. 1). An important topic of the scientific rationale of the project was to understand the fate of sediments supplied by major river system and transported by longshore currents.

Most of the data available for the MACM to date, were collected during ADRICOSM and the ADRICOSM STAR projects, and the results of marine geological and geophysical investigations were reported in several technical papers and scientific notes, including Bignami et al. (2008), Bortoluzzi et al. (2009a,b; 2010; 2011); on the other side, oceanographic data and modeling are reported and discussed in: Campanelli et al. (2009); Marini et al. (2010); Bellafiore et al. (2011); Campanelli et al. (2013). Moreover, a geomorphological description of the peculiar features observed in the shelf-slope system of the MACM, and a preliminary stratigraphic analysis of the interplay between tectonics and eustatic changes during the Late Quaternary are discussed in Del Bianco et al., 2014a, and b, respectively.

In this work, we used part of the ADRICOSM STAR data set, mainly consisting of geochemical/sedimentological analyses of the seafloor sediments collected along the MACM, to provide information about the present-day transport, the depositional features as well as the indirect hints about oceanography and the dynamic of the water column. The study of sediment cores and the analysis of short life radionuclides activities in the shallow subsurface provided information about sedimentation rates, and gave insights to discriminate areas of active deposition and erosion at a decadal scale. At this time-scale, radionuclides data, especially ^{137}Cs and ^{210}Pb , are reliable time

markers. In particular, ^{210}Pb profiles allow us to obtain an under years chronologies and ^{137}Cs permit to refine the age model in fact concentration of ^{137}Cs in marine sediment has a worldwide maximum centered around 1963 (end of the atomic bomb tests in atmosphere) and a more regional peak in Central Europe caused by the Chernobyl radioactive fallout at the end of April 1986. The sedimentation rates evaluated by these techniques, performed together the classical grain size analyses, give insights about sedimentation processes during the last 200 yr, in this area (Van Welden et al. 2008). Furthermore, geochemical data (e.g. trace metals) provide additional information on sediment sources from different mineralogical provinces, in this case the Albanides and Dinarides Mountain Ranges, and associated drainage basins. Finally, the analysis of organic matter, C, N and their stable isotopes, is a good indicator about the origin of the particulate, either continental or marine (Middelburg and Nieuwenhuize, 1998; Graham et al., 2001; Ogrinc et al., 2005; Tesi et al 2008).

We combined these independent proxies to attempt a first characterization of seafloor sediment distribution along the MACM, and try to evidencing the fate of sediment supplied by local river system to the coast. This would be useful to determine which areas along the coasts are particularly prone to accumulation of pollutants supplied from onshore.

2. The study area

The MACM is a shelf-slope system that shows a relict shelf edge at the depth of about 220m characterized by complex morphologies and variable width of the shelf, along with evidence of large-scale mass wasting (Roure et al. 2004; Argnani et al. 2006; DelBianco et al., A e B). The continental shelf is very narrow from Northern Croatia to Cape Patamuni, south of the Boka Kotorska Bay, near Budva, where it widen up to Cape Rodonit. The political boundary between Montenegro and Albania is marked by the Buna/Bojana River, an emissary of the Scutari Lake, and the second largest river in the Adriatic Sea, with a mean annual discharge of about $700 \text{ m}^3\text{s}^{-1}$ (UNEP, 1996). This river represents the principal source of sediments, together with minor rivers in the Albanian coast N of Cape Rodonit, of our study area. Between 1846 and the end of the 19th century, the present connection of the old Drin River and the Bojana-Buna River was formed (Drinisa/Drinjaca). Since then, the waters of the old Drin River are discharged via the Drinisa and the Bojana-Buna to the Adriatic Sea (Schneider-Jacoby et al. 2006); since then, the Drini was flowing into the Adriatic Sea in Albania, southeast of its present-day mouth. The waters from Drin are nowadays regulated by Electrical power plant dams. Because of karst environment in the Dinaric range, especially in North Montenegro, coastal aquifers may also develop at sea, generating submarine siphons, springs and resurgences, within a geological and hydrogeological setting strongly related to tectonic deformations as well climate and sea level

fluctuations (Fleury et al. 2007). The northward bending of the river plume is consistent with the Coriolis effect (Kourafalou, 1999) and is coincident with the direction of prevailing southeastern Adriatic currents (Artegiani et al., 1997). The South Eastern Adriatic current transports Ionian Surface Water (ISW) along the eastern boundary northward into the Adriatic Sea (Marini et al. 2010). In this way, the Buna-Bojana plume is deflected northward although the direction of dominant local winds is towards south, and could cause that formation of southward currents and localized upwelling (Marini et al. 2010). Marini et al. (2010) describe what they call the South Eastern Shelf Coastal Current (SESC), which characterizes the oceanographic regime of this region.

The Late Quaternary stratigraphy of the MACM shelf-slope system is described in Del Bianco et al., (2014a), while in Del Bianco et al., (2014b) high resolution morphobathymetric data are used to describe the peculiar seafloor morphologies along the margin, mostly inherited by the latest lowstand glacial period. Analysis of seismic reflection data and seafloor reflectivity shows that the continental shelf from Albania to Boka Kotorska Bay displays two inner-shelf depocenters, to the E of Bar, and to the W of Budva, separated by an erosional or non-depositional area (by-pass area).

3. Materials and Methods

Sediment samples were collected during six oceanographic cruises, onboard of R/V Dallaporta, (Star08), R/V Urania, (ADR02_08, 2008; MNG01_09, 2009; MNG03_1, 2010; MNG04_10, 2010) and R/V Mariagrazia (MNG02_09). The technical report of each of these cruises is available online (<http://www.ismar.cnr.it/prodotti/reports-campagne>).

A 40 cm diameter box-corer was used to collect bottom sediment samples that have been consequently sub-sampled using short liners. Grain size analyses were performed with a pre-treatment with H₂O₂ to remove organic matter, dried at 60°C, a subsequent wet sieving at 63 µm to separate silty-clay fraction from sand. The former was further subdivided in silt and clay fractions by using a Micromeritics RX-5000D sedigraph. Sand fractions were sieved every half phi.

Organic carbon and total carbon contents were determined using Fisons Elemental Analyzer NA2000. In order to obtain the organic carbon analysis, the carbonate fraction was eliminated by pre-treatment with 1.5 M HCl. Stable isotopic analyses of Carbon were carried out on the same samples by using a FINNIGAN Delta Plus mass spectrometer that was directly coupled to the FISIONS NA2000 EA.

²¹⁰Pb/²¹⁰Po analysis were performed at ISMAR-CNR Bologna. ²¹⁰Pb was determined using alpha spectrometry through its ²¹⁰Po daughter, and measured by alpha spectrometry with a silicon

barrier detector coupled with a multichannel analyser, according to Frignani and Langone (1991) and Frignani et al. (1993). Supported ^{210}Pb activities were obtained from the constant values at depth in the cores. Excess ^{210}Pb ($^{210}\text{Pb}_{\text{ex}}$) activities were obtained by subtracting supported ^{210}Pb from total activities. If the flux of ^{210}Pb to the site has been constant with time, a CF-CS model (Constant Flux-Constant Sedimentation; Robbins, 1978) is applied to the $^{210}\text{Pb}_{\text{ex}}$ and, the assessment of accumulation rates and chronologies from $^{210}\text{Pb}_{\text{ex}}$ -depth profiles is based on a model calculation discussed by Frignani et al. (2005). The simplified conditions of the conceptual models are not necessary met, and all the assumptions are affected by a degree of uncertainty. For this reason, when the $^{210}\text{Pb}_{\text{ex}}$ profiles were too different from theoretical cases, a crude estimate of sediment accumulation rates (SAR) was carry out. The value of supported ^{210}Pb activity was assumed constant along-core and estimated from the values of the deepest sediment samples, where ^{210}Pb was assumed to be in radioactive equilibrium with its parent ^{226}Ra , i.e., by dividing the depth where assumed background value of ^{210}Pb were reached by 100 years. All concentrations and activities were calculated on a dry weight basis.

4. Results and Discussion

Based on the seafloor reflectivity analysis carried out by Del Bianco et al (2014a and b), that inferred the presence of two main depocenters during the Holocene, starting from the LGM, we concentrated our analysis on a transect of sampling stations located parallel to the coastline from N to S of the study area (Fig.1). Sedimentation rates estimated in the two depocenters (SE of Bar and NW of Budva) are quite similar in a range between $0.08\text{-}0.15\text{ cm y}^{-1}$, and appear almost constant for the last 150 years. The presence of short-lived radionuclides on the first cms in the sedimentary sequence indicates that active deposition occurs on both areas. ^{210}Pb data (Fig.2) show an exponential profile suggestive of a low-energy depositional environment where negligible biological or physical reworking of surficial sediments take place. Conversely, the area between the two depocenters (the Bypass or not-depositional area) exhibits a lack of present-day sedimentation, confirming that the fine sediments in this sector do not accumulate, because are probably reworked by currents with seasonal periodicity. This could be due either by a peculiar current pattern in this area, or/and by the absence of accommodation. The dominant grain sizes are silty clays and clayey silt for the northern and southern depocenters, respectively, indicating a preferred pathway for deposition of fines and ultra-fines sediments.

The distribution of OC and N along the MACM shows that the main input of organic matter is the Buna/Bojana River, with a minor contribution from the Albanian rivers. In particular, this latter

contribution is mostly present to the S and SE of the Buna/Bojana, where we observe the highest deposition rates, in agreement with the isochronopach maps of the Late Pleistocene-Holocene compiled in Del Bianco et al. (2014a) based on seismo-stratigraphic evidence.

Using OC as indicator of organic matter is possible to infer the distribution (transport, sedimentation and reworking) of the particles input from the Buna/Bojana River. The relationship between total organic carbon and total nitrogen ratios and carbon stable isotope of organic matter ($\delta^{13}\text{C}$) are useful to understand the source of organic matter in marine sediments (Middelburg and Nieuwenhuize, 1998; Graham et al., 2001; Ogrinc et al., 2005 Tesi et al 2008). Fig 3 show a plot N/C vs. $\delta^{13}\text{C}$ from measured in surface samples collected along the continental margin. Although this interpretation is mostly qualitative, is could be useful to understand the rough picture of main sedimentary processes presently active along the MACM. This hypothesis is based on observation that photosynthetic processes and carbon sources are different between marine organisms and terrestrial plants. In general enriched values of $\delta^{13}\text{C}_{\text{org}}$ and low ratios C/N suggest the presence of predominantly marine phytoplankton (Lamb et al 2006). While poor $\delta^{13}\text{C}_{\text{org}}$ values and high C/N suggest a vegetable source (C3 plants) from continent and therefore the nearness of shoreline and/or the proximity of a source of organic matter of continental origin. The concentration of OC in the surficial sediment (Fig.3) is maximum close to the river mouth with values of about 0.8-1 % and remain almost high still the by-pass area were the lowest content are measured (less than 0.3 %). In the northern part of the MACM, south the Bokakotorska Bay the percentage of OC rise again up to 0.6-0.7%. This distribution suggest that the highest input of organic particles is, at least for the greatest part, due to the river Buna/Bojana, even if it is possible to observe a contribution from the smaller rivers from Albanians. The particles coming from the outflow of the Buna/Bojana River are moved NNW from the main currents (LIV), along the coastline.

Our data suggest that only a few part of material supplied by the river system is deposited along the Montenegro coast. In fact, it is likely that most part of this material is carried towards N, along the coast of Croatia, and a (minor) portion of these sediments could be transported along the slope towards the central sector of the Adriatic Sea through the canyon system cutting the shelf edge (Del Bianco et al. 2014a). However, a more detailed sediment budget relative to our study area and more in general to the SE Adriatic shelf margin, requires further analysis. Plotting C/N ratio against $\delta^{13}\text{C}$ (Fig.4) enable us to observe that samples from depositional areas of the SE (Fig.1 black dots) and NW (red dots in Fig.1) sectors, form two distinct groups, indicating that organic matter composition is different, ranging from marine to continental riverine. Samples collected from the NW depocenter are characterized by a more marked marine input, while the SE area shows a higher continental supply due to the detrital input from the Buna/Bojana River that dilute the marine signal.

Samples from the bypass area (Fig. 1 green dots), display a stronger continental signal, this could be due to the deterioration of the organic matter, confirming, one more time, that this is residual material.

The peculiar pattern of adjacent depositional and erosional sectors observed along shelf, highlighted by seafloor reflectivity (Fig. 1) validated by radioisotopes analysis of seafloor sediments could be caused by the complex oceanographic regime described by Marini et al (2010). According to this work, the SESC detaches from the coast in correspondence with the Buna/Bojana outflow and forms coastal eddies that expand the offshore extent of the river plumes. This results in a local complexity in the water circulation, which could be responsible for a “patchy” distribution of surficial sediments along the MACM.

5. Conclusions

We used sedimentological and geochemical analysis of seafloor sediments collected at several location along the Montenegro/Northern Albania Continental Margin to describe the present-day transport and dispersal system of this poorly known area in the southeastern Adriatic Sea.

Based on ^{137}Cs and ^{210}Pb curves, we estimated maximum sedimentation rates ranging from 0.08-0.15 $\text{cm}\cdot\text{y}^{-1}$ during the last 100-150 years in the two Late Pleistocene-Holocene depocenters that constitutes mid-shelf basins along the MACM. From the shape of radioisotopes concentration curves we observe active sedimentation, not affected by post depositional processes only in these two well defined areas of the MACM shelf. Between these two areas, dominated by clay or silty clay deposition, a non-depositional zone is observed, constituting a by-pass sector for sediments. The maximum accumulation observed is in correspondence of the Bojana River outflow, although other geochemical proxies such as trace metals, organic matter, C and N and their stable isotopes, indicate the presence of two main sources of sediments in different mineralogical provinces, i.e., the Albanides and Dinarides Mountain Ranges, related to the drainage basins of the river system. The observed gradients pointing towards north observed in all of the analyzed parameters indicate a major role played by longshore currents in redistributing sediments along the margin and suggest that the most of the particles from Buna/Bojana River are moved SE-NW along the Montenegro and Croatian coast.

Figures with caption

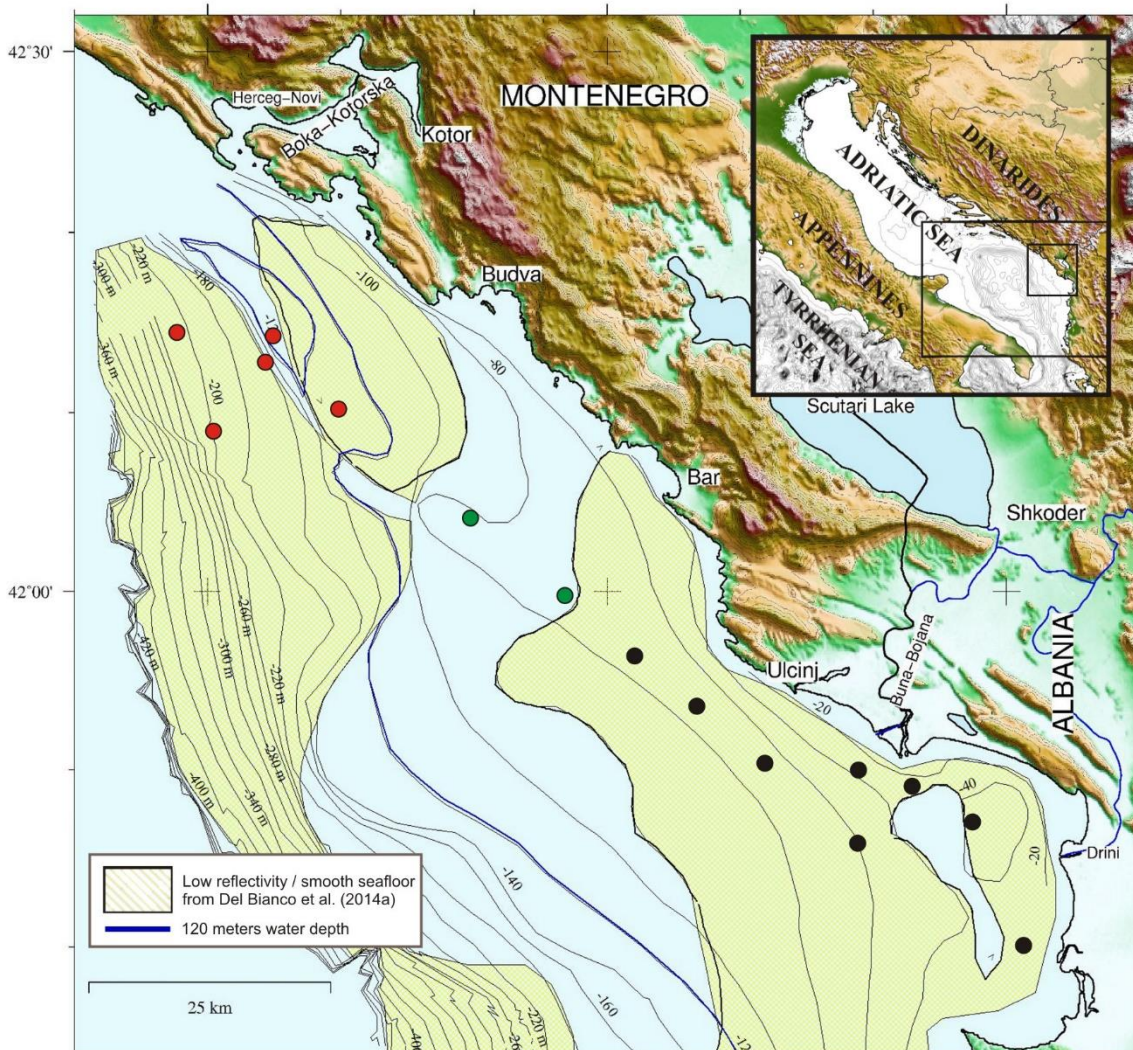


Figure 1. Bathymetric map of the Montenegro/N Albania Continental Margin with indicated: 1) the 120 m isobaths; 2) the seafloor areas characterized by relatively low reflectivity that indicates fine-grained sediments; 3) the analyzed seafloor sediment samples (color circles). From Del Bianco et al. (2014b)

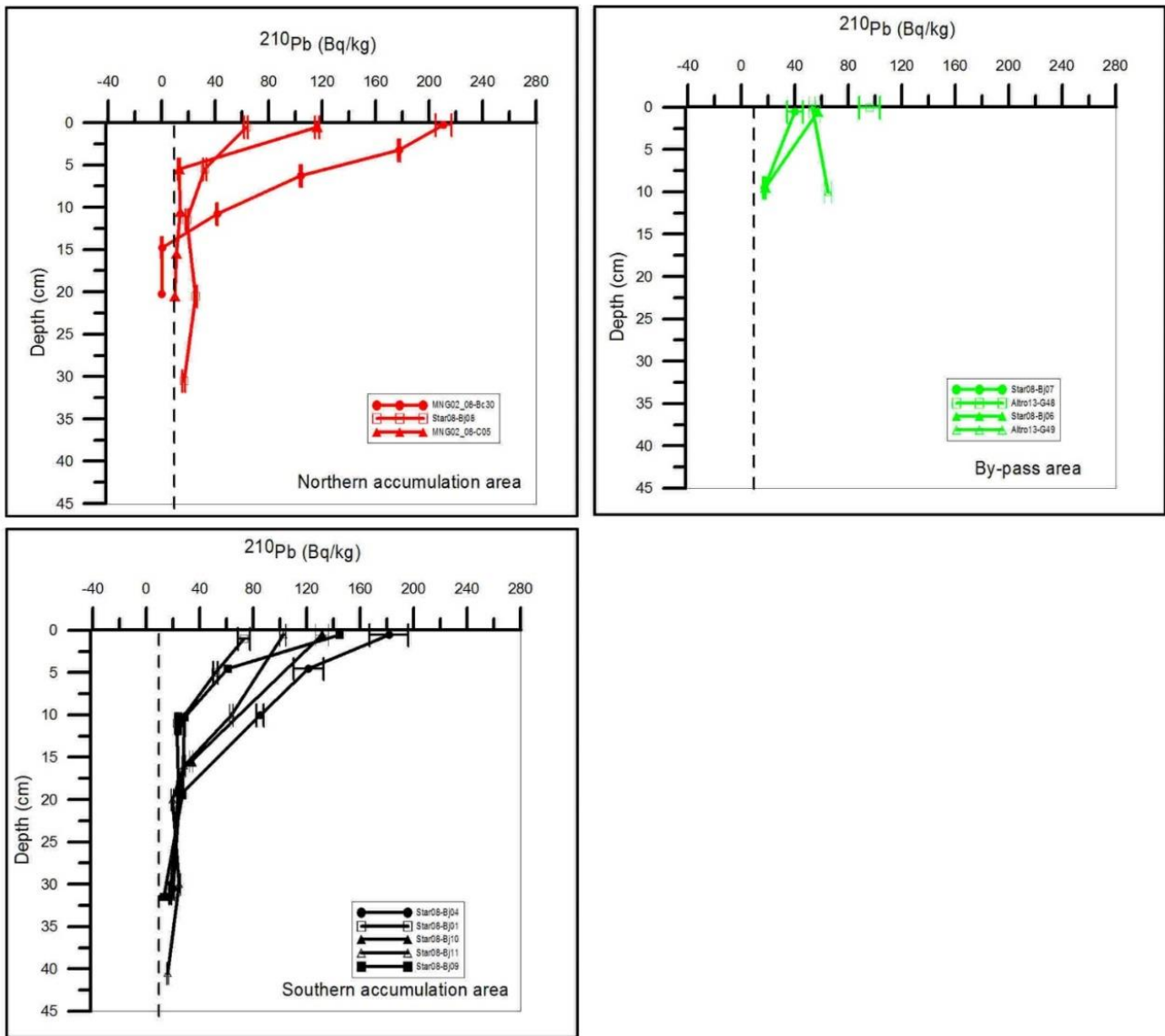


Figure 2. ^{210}Pb vs. depth profiles distributed for the areas: NW depocenter in red, SE depocenter in black and by-pass area in green.

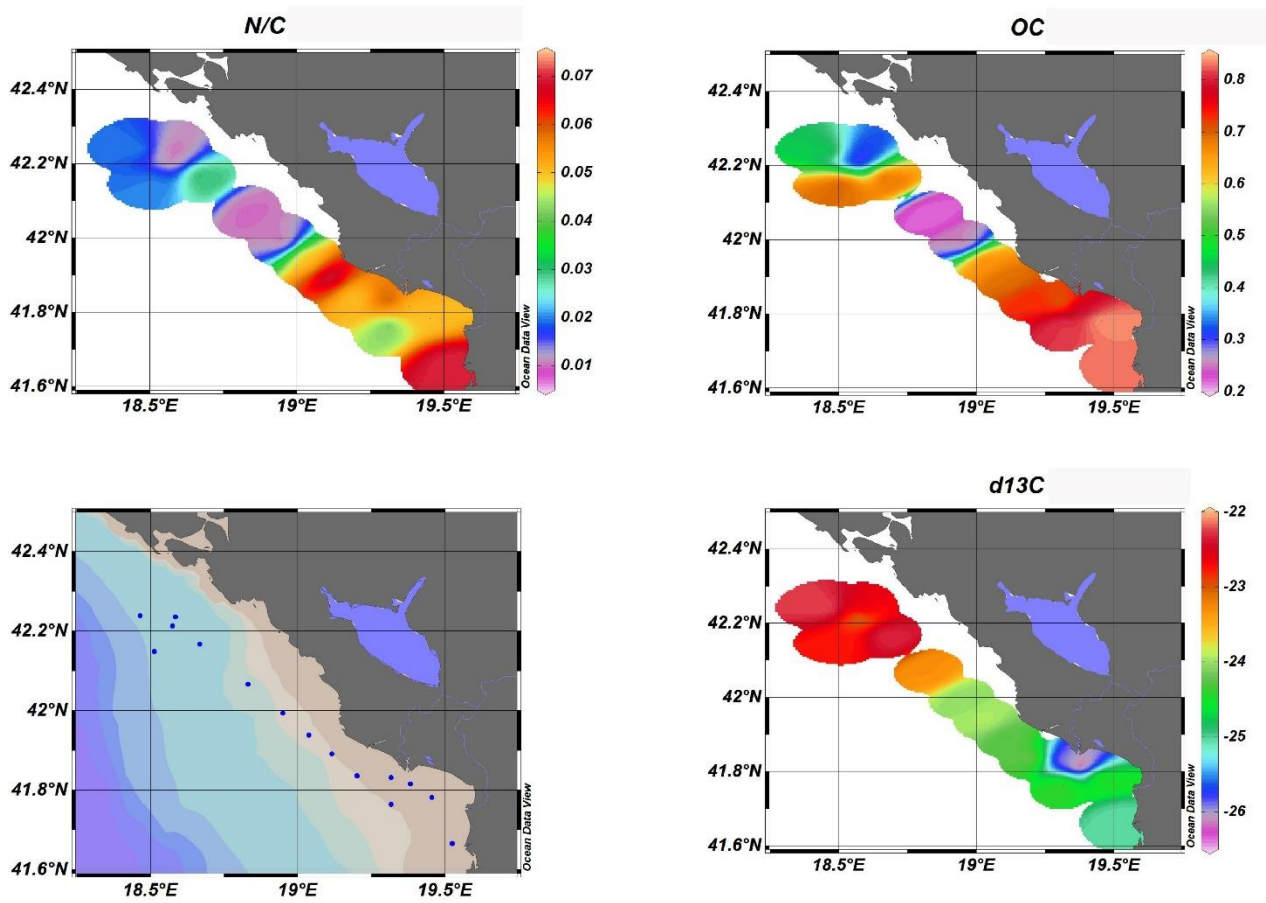


Figure 3. Surface distribution of Organic carbon, $\delta^{13}C$ and N/C ratio along the MACM.

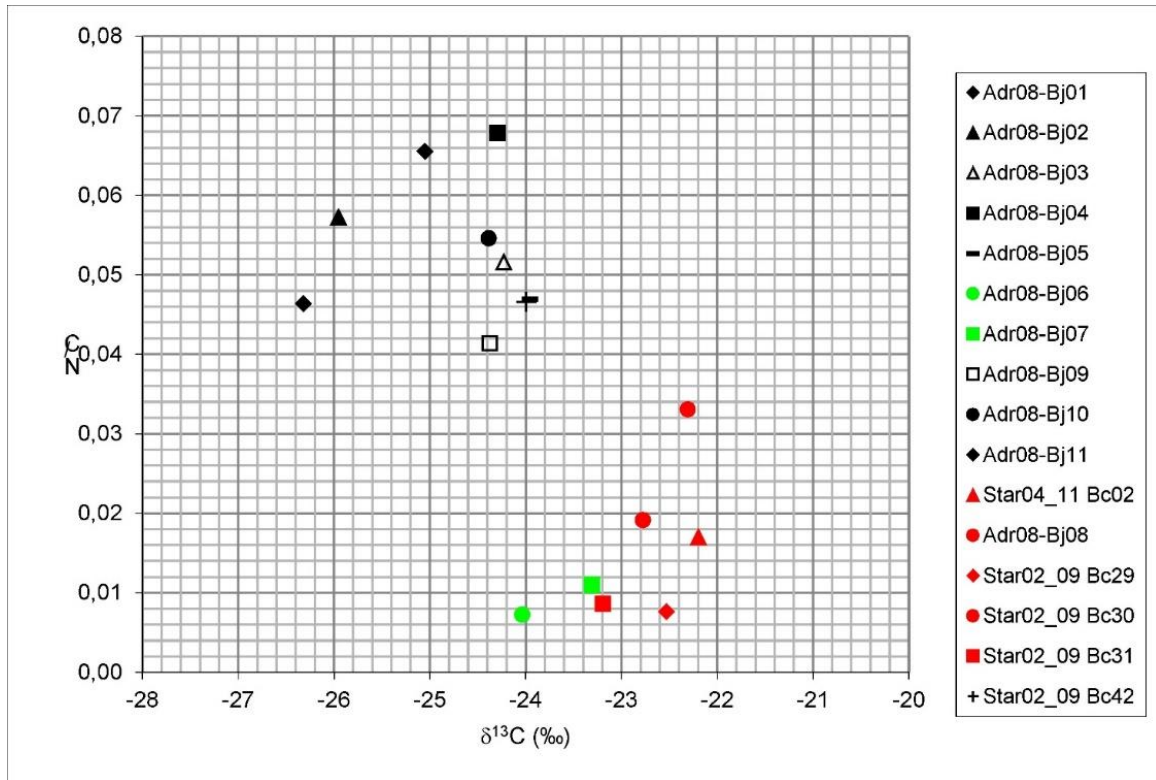


Figure 4 N/C vs $\delta^{13}\text{C}$ plot of surficial sediment samples collected along MACM. Black dots indicate samples from SE area, while red dots samples from NW area and green dots samples collected in the by-pass area between the two inner-shelf depocenters (see Fig.1 for samples location).

References

- Aliaj S., Adams J, Halchuk S., Sulstarova E., Peci V. and Muco B. 2004. - Probabilistic seismic hazard maps for Albania. - 13th World Conference on Earthquake Engineering, Vancouver, B.C., Canada, August 1-6, 2004, Paper No. 2469.
- Aliaj S. 2008 - The Albanian Orogen: convergence Zone between Eurasia and the Adria microplate. - In: N.Pinter, G.Gyula, S.Stein and D.Medak (eds.), The Adria Microplate: GPS Geodesy, Tectonics and Hazards, NATO Science Series, IY, Earth and Environmental Sc., Vol.61, Springer.
- Argnani, A., Rovere, M., & Bonazzi, C. (2006). Tectonics and large-scale mass wasting along the slope of the southern Adriatic basin. *Geophysical Research Abstracts*, Vol. 8, 07261, 2006
- Bellafiore D, A. Guarnieri, F. Grilli, P. Penna, G. Bortoluzzi, F. Giglio, N. Pinardi 2011. Study of the Hydrodynamical Processes in the Boka Kotorska Bay with a Finite Element Model. *Dynamics of Atmospheres and Oceans*. Vol 52 p 298-321
- Bignami F. et al., 2008. – Report on the Oceanographic, Morphobathymetric, Geological and Geophysical activities during Cruise ADR02_08 (17-28 October 2008, R/V Urania) – Adricosm-Star Project - projects.bo.ismar.cnr.it/CRUISE REPORT/2008. - Rapporto tecnico interno ISMAR-BO
- Boore D.M., Sims, J.D., Kanamori, H. e Harding, S., 1981. The Montenegro, Yugoslavia, earthquake of April, 15, 1979: source orientation and strength. *Phys. Earth Planet. Interiors*, 27, 133-142
- Bortoluzzi G., Del Bianco F. et al., 2009a. – Report On The Morphobathymetric, Oceanographic, Geological And Geophysical Investigations During Cruise MNG01_09 (19-27 April 2009, R/V URANIA) - projects.bo.ismar.cnr.it/CRUISE REPORTS/2009/MNG0109 REP/.- Rapporto tecnico interno ISMAR-BO.
- Bortoluzzi G., Del Bianco F. et al., 2009b. – Report On The Morphobathymetric, Oceanographic, Geological And Geophysical Investigations During Cruise MNG02_09 (11-24 July 2009, R/V Maria Grazia) - projects.bo.ismar.cnr.it/CRUISE REPORTS/2009/MNG0209 REP/. - Rapporto tecnico interno ISMAR-BO
- Bortoluzzi et al. (2011), Urania Cruise report. ISMAR-CNR cruise report, Bologna, 2011.
- Bortoluzzi G., F. D'Oriano, F. Del Bianco, V. Maselli, C. Palmiotto, F. Falcieri, K. Marinaccio, D. Radojevic, M. Milic, G. Castelli, E. Çomo, B. Murta. Report on the oceanographical, geological, geophysical activities during Cruise MNG0310 with R/V Urania : Adriatic Sea, 2010-03-02 - 2010-03-12. Projects EMMA (Dr. M. Ravaioli) and ADRICOSM (Prof. N. Pinardi).
- Campanelli, A; Bulatovic, A; Cabrini, M; Grilli, F; Kljajic, Z; Mosetti, R; Paschini, E; Penna, P; Marini, M. Spatial distribution of physical, chemical and biological oceanographic properties, phytoplankton, nutrients and Coloured Dissolved Organic Matter (CDOM) in the Boka Kotorska Bay (Adriatic Sea). *GEOFIZIKA* Vol. 26 Issue: 2 Pgg: 215-228 Published: 2009

- Campanelli A., Cabrini M., Grilli F., Fornasaro D., Penna P., Kljajić Z., Marini M.) Physical, Biochemical and Biological Characterization of Two Opposite Areas in the Southern Adriatic Sea (Mediterranean Sea) *Open Journal of Marine Science*, 2013, 3, 121-131
- CONSOLE R., DI GIOVAMBATTISTA R., FAVALI P. & SMRIGLIO G. (1989) - Lower Adriatic Sea seismic sequence (January 1986): spatial definition of the seismogenic structure. *Tectonophysics*, 166, 235-246.
- Del Bianco F., Gasperini L., Angeletti L., Giglio F., Bortoluzzi G., Ravaioli M. and Kljajic Z. (2014a). The stratigraphic architecture of the Montenegro/N. Albania Continental Margin (Adriatic Sea - Central Mediterranean). Submitted to *Marine Geology*.
- Del Bianco F., Gasperini L., Bortoluzzi G., Giglio F., Ravaioli M. and Kljajic Z. (2014b). Seafloor morphology of the Montenegro/N. Albania Continental Margin (Adriatic Sea - Central Mediterranean). Manuscript in preparation.
- Fleury, P; Bakalowicz, M; de Marsily, G. Submarine springs and coastal karst aquifers: A review. *JOURNAL OF HYDROLOGY* Volume: 339 Issue: 1-2 Pages: 79-92 DOI: 10.1016/j.jhydrol.2007.03.009 Published: JUN 10 2007
- Frignani, M. and Langone, L., 1991. Accumulation rate and ^{137}Cs distribution in sediments off the Po River delta and the Emilia-Romagna coast (northwestern Adriatic Sea, Italy). *Cont. Shelf Res.*, 11: 525–542
- Frignani, M., L. Langone, S. Albertazzi, M. Ravaioli, 1993. “Cronologia di sedimenti marini- analisi di ^{210}Pb via ^{210}Po per spettrometria alfa”. Rapporto tecnico n.28. Consiglio Nazionale delle Ricerche, Istituto per la Geologia Marina, Bologna.
- Graham, M.C., Eaves, M.A., Farmer, J.G., Dobson, J., Fallick, A.E., 2001. A study of carbon and nitrogen stable isotope and elemental ratios as potential indicators of source and fate of organic matter in sediments of the Forth Estuary, Scotland. *Estuarine, Coastal and Shelf Science* 51, 375–380.
- Lamb A.L., Graham P., Wilson, M. J., Leng. A review of coastal palaeoclimate and relative sea-level reconstructions using $\delta^{13}\text{C}$ and C/N ratios in organic material *Earth-Science Reviews* 75 (2006) 29– 57
- Marini, M, Grilli, F; Guarnieri, A; Jones, BH; Klajic, Z; Pinardi, N; Sanxhaku, M. Is the southeastern Adriatic Sea coastal strip an eutrophic area? *ESTUARINE COASTAL AND SHELF SCIENCE* Volume: 88 Issue: 3 Pages: 395-406 DOI: 10.1016/j.ecss.2010.04.020
- Middelburg, J.J., Nieuwenhuize, J., 1998. Carbon and nitrogen stable isotopes in suspended matter and sediments from the Schelde Estuary. *Marine Chemistry* 60, 217–225. Ogrinc et al., 2005
- Roure F., Nazaj S., Mushka K., Fili I., Cadet J.-P. and Bonneau M.; 2004: Kinematic evolution and petroleum systems - an appraisal of the Outer Albanides. In: K.R.McClay, Thrust tectonics and hydrocarbon systems. *AAPG Mem.*, 82, 474-493
- Robins J.A., 1978. “Geophysical and geochemical applications of radioactive lead”, in: *Biogeochemistry of Lead in the Environment*, Ed. Jo. Nriagu, Elsevier, Amsterdam, pp.285-393.
- Schneider-Jacoby M., U. Schwarz, P. Sackl, D. Dhora, D. Saveljic and B. Stumberger (2006): Rapid assessment of the Ecological Value of the Bojana-Buna Delta (Albania / Montenegro). Euronatur, Radolfzell

- Tesi, T., Langone, L., Goni, M.A., Miserocchi, S., Bertasi, F., 2008. Changes in the composition of organic matter from prodeltaic sediments after a large flood event (PoRiver, Italy). *Geochimica et Cosmochimica Acta* 72 (8), 2100–2114.
- Tiberti, MM; Lorito, S; Basili, R; Kastelic, V; Piatanesi, A; Valensise, G. Scenarios of Earthquake-Generated Tsunamis for the Italian Coast of the Adriatic Sea *PURE AND APPLIED GEOPHYSICS* Volume: 165 Issue: 11-12 Pages: 2117-2142 DOI: 10.1007/s00024-008-0417-6 Published: DEC 2008
- UNEP 1996. Mediterranean Action Plan (MAP), Implications of Climate Change for the Albanian Coast, Technical Reports series No.98.
- Van Welden A, C. Beck, J.L Reyss, S. Bushati, R. Koci, F.Jouanne, J-L Mugnier The last 500 year of sedimentation in (Albania/Montenegro): paleoenvironmental and potential for paleoseismicity studies. *J Paleolimnol* (2008) 40:619–633 DOI 10.1007/s10933-007-9186-y

CHAPTER 4

--

DISCUSSION AND CONCLUSIONS

4.1 Discussion

The three scientific papers presented in the previous section analyze different aspects of the MACM geological evolution at very different time-scales. In fact, while morphological maps allowed for indications about LGM paleogeography and the analysis of sparker lines at the shelf edge highlighted the effect of sediment aggradation and progradation, at the 100 kyr scale, geochemical analysis on seafloor sediments enabled us to determine present-day sedimentation rates and sediment dispersal system, mainly controlled by solid transport at the Buna-Bojana outflow and longshore current regime. This “multiscale” approach gives us some hints on how the MACM developed during the Late Quaternary and how the geological features we observe along the margin are diagnostic of the combined effect of natural processes, such as tectonics and eustatic changes.

During the latest phase of sea level highstand, sediment accumulation along the MACM appears limited to narrow inner-shelf basins parallel to the coastline. As shown by the isochronopach map (Fig. 2, § 3.3), the maximum thickness of inner shelf depocenters is < 35 m, corresponding to an average deposition rate of 3-4 mm/yr during the Late Pleistocene-Holocene. These results determined through a seismo-stratigraphic analysis of chirp-sonar and sparker profiles are in agreement with the present-day sediment dispersal regime revealed by geochemical and radio isotopic analysis of surficial sediments. In fact, ^{210}Pb and ^{137}Cs profiles carried out in different sectors of the shelf indicates accumulation rates ranging from 1 to 2 mm/yr for the last ~150 yr, and the presence of wide areas of non-deposition between the two Late Quaternary depocenters observed. We note that, although deposition rate is relatively high, the extent of these basins is very low relative to their western counterparts of Adriatic basin. This could be due to the combined effect of a lower sediment supply and/or to the presence of relatively stronger longshore currents, which cause efficient sediment reworking and dispersal. However, from high-resolution seismic images we observe only part of the post-glacial mud-wedge. In seismic profiles such as that shown in Fig. 2 (§ 3.2), we note a depositional continuity of the Holocene mud-wedge south of our working area. Conversely, according with the direction of prevailing southeastern Adriatic current, the Buna-Bojana plume is deflected northwards (Poulain, 2001; Marini et al., 2010). Unfortunately N of the MACM we lack high resolutions seismic profiles, and could not check whether other inner shelf basin forms. However, a preferential sediment transport direction from SE to NW is also confirmed by geochemical proxies (OC, C/N, $\delta^{13}\text{C}$), suggesting that the most of the particles supplied by the Buna/Bojana River are delivered towards the Montenegro and Croatia coasts.

Furthermore, according to Milliman and Syvitski (1992), in narrow shelves characterized by limited accommodation, part of the sediments is transferred to adjacent outer-shelf or slope. North of

the MACM, starting from the Croatia coast the continental shelf becomes very narrow, and in this could favor sediment deliver towards the slope and the deep basins. In agreement with such hypothesis, we note that the MACM outer-shelf is covered by a thin veneer of Holocene deposits, not visible through our high-resolution seismic reflection data, either the chirp-sonar and the sparker lines, but recognized by direct bottom sampling. Thus, we could assume that sediments reach the outer shelf during episodic events such as storms, floods or other high-energy events.

The role played by the peculiar physiography of the margin, driven by tectonic processes is evident. In fact, we observe tectonic deformations causing folding and uplifting in correspondence of the inner shelf edge, along the Kotor and Bar anticlines, and flexure towards land. This latter effect creates subsidence and accomodation in localized mid-shelf basins, where sediments supplied by the Buna-Bojana and the Drini rivers could accumulate. This is particularly evident in the northern Late Quaternary depocenter (Fig.3, § 3.3), where Unit-1 (Late Pleistocene-Holocene) is confined landward of the Kotor Ridge.

In Fig 4.1, a simplified sketch of this physiographic setting is presented. From the offshore towards the coastline we observe: a main foredeep basin, located in the outer shelf and slope; a structural topographic ridge (the Kotor Ridge); and a thrust-sheet-top or piggy-back basin (Ori and Friend, 1984) in a mid-shelf sector, where the post-glacial mud wedge is mostly confined. This setting is similar to that described by several authors on the Apennines Chain, where a system of inner thrust-sheet-top basins and outer foredeeps is observed (Ricci-Lucchi, 1986 and references therein).

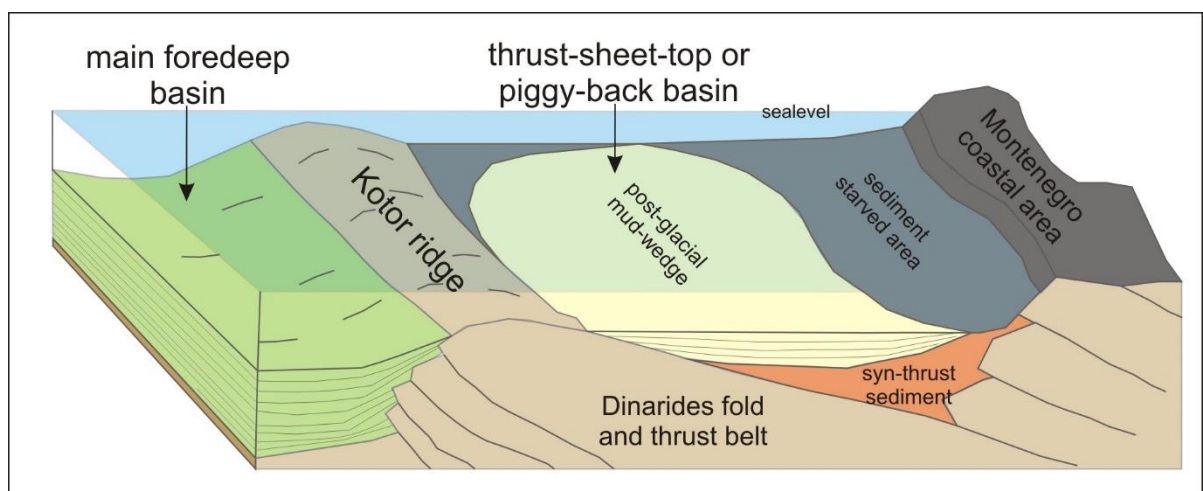


Figure 4.1 Simplified sketch illustrating the depositional setting along the northern continental shelf of the MACM.

On the other hand, seaward of the more external fold and thrust belt, i.e. the Kotor and Bar ridges), the outer shelf is characterized by uniform subsidence, caused by southward tilting and faulting. This is probably due to flexure of the continental lithosphere at the edge of a convergent margin, forming the peripheral foreland (or foredeep) basins developed offshore the MACM. This is in agreement with structural models, constrained by geological and geophysical evidence, suggesting that subsidence processes in the Adriatic region are mainly due to the flexure of a subducted and segmented lithosphere (Royden et al., 1987; Moretti and Royden, 1988). In particular, the so-called South Adriatic Basin (SAB, de Alteriis, 1995) appear generated by flexure of the Adriatic continental lithosphere beneath the Dinarides-Hellenides orogenic belts, and is formed by a deep (4-5 km in the Montenegro) Eocene carbonate basement, filled by Late Tertiary/Quaternary siliciclastic deposits (Frank et al., 1983). In agreement with this reconstruction, we note that most of the MACM outer shelf is built by sediment wedges showing similar geometries and internal architectures relative to the deeper and older units observed in the more penetrative seismic lines. Stratigraphic constraints and a simple linear subsidence model at the scale of a few 100 kyr cycles, suggest that these wedges correspond to forced regression deposits formed during phases of sea level lowstand. Consequently, the forced-regression wedges (WA, WB, WC and WD §3.3) including the latest episodes of sea level fall and rise during the Late Quaternary, are probably the upper part of the NE pinch-out of the SAB deposits. We note that our subsidence rate estimate of 1.2 mm/yr for this foredeep basin is coherent with that described for the northern sector of the western Adriatic margin (Maselli et al., 2010 and references therein) in a similar geodynamic setting. This leads to the conclusion that subsidence in the outer shelf of the MACM could be modeled by a linear mechanism of southward tilting, which creates space for sediment accumulation. Under this structural setting, our data suggest that the basin fill take place mostly during sea level fall and/or lowstand phases, if in form of shelf-margin progradation of thick sedimentary wedges. A clear example of this enhanced shelf-margin growth during lowstand phases is represented by the extent of the drowned paleodelta system described in § 3.2. This is classified as a mid-shelf delta formed during the last falling stage and lowstand (Fig. 4.2) and is considered as a “forced-regression” sedimentary unit of the LGM phase (sedimentary wedge WA, §3.3). It represents a widespread deltaic clinothem, if compared to the modern delta of the Buna-Bojana River, and is classified as a lobate delta (Galloway, 1975), whose peculiarity is the high fluvial influence characterized by important sedimentary discharge. Fig. 4.2 shows the comparison between the extent of present-day Buna-Bojana delta and the LGM delta, reconstructed based on seafloor morphology.

Thus, the stratigraphic architecture of the MACM suggests that significant sediment

accumulation occurs only during lowstand glacial phases at the 100 kyr time scale, while during interglacials, sediment accumulation is significantly lower. This is in agreement to what proposed by Bossuet et al. (1996), i.e., that sedimentary fluxes during the last glacial maximum were 3-3.5 times more intense relative to present-day

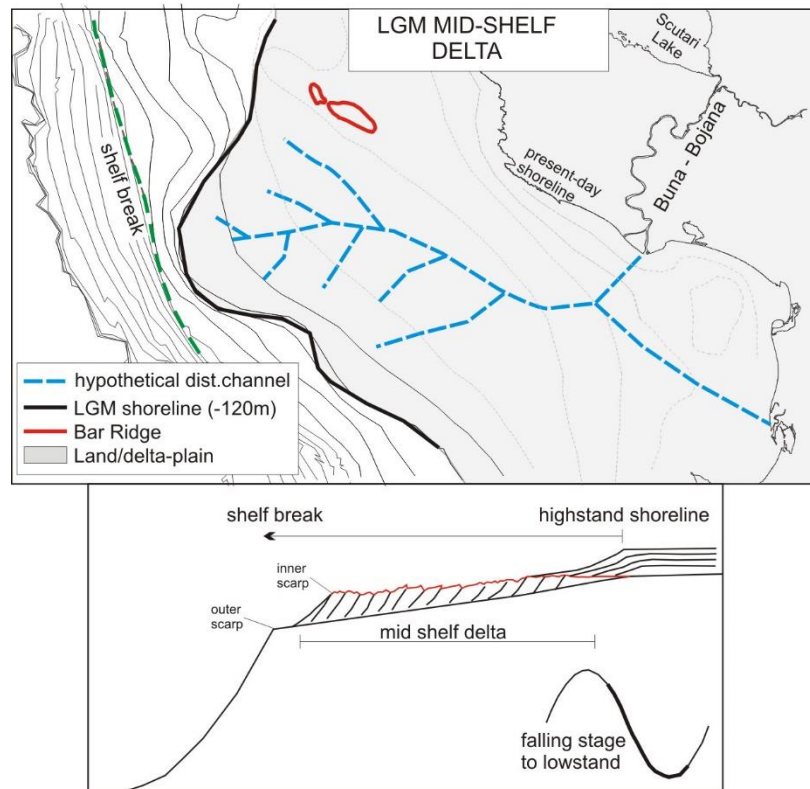


Figure 4.2 Simplified sketch map of the mid-shelf delta during the LGM. From Del Bianco et al. (2014 – § 3.2, this manuscript), modified.

The two morphotectonic ridges observed along the MACM constitutes the surficial expression of buried, deep-seated compressive tectonic structures. Moreover, these features are aligned, and show similar morphologies relative to the system of alternating ridges and troughs that marks the chain front onshore (Fig. 2 – § 3.2). For this reason, the Kotor and Bar ridges could be considered the offshore counterparts of similar tectonic structures observed onshore, which show evidence of ongoing compressive deformations (see Fig.4.1). In the northern sector of the MACM, comparing the modern shoreline position with the -120 m isobaths and plotting these differences vs latitudinal position of reference points (Fig. 4.4) we observe uplift in the northern area, in correspondence of the Bar Ridge. This paleoshoreline was traced following the rollover point between topset and foreset

beds in the clinoforms, although such features could be found in water depths up to 20-30 m (Vail et al., 1977; Steckler, 1999; Cattaneo et al., 2003, 2007), and this introduces a correspondent uncertainty in our estimate. Within this error associated to our estimate, we could reconstruct the position of the MIS2 shoreline at -80 ± 25 m below present-day sea level.

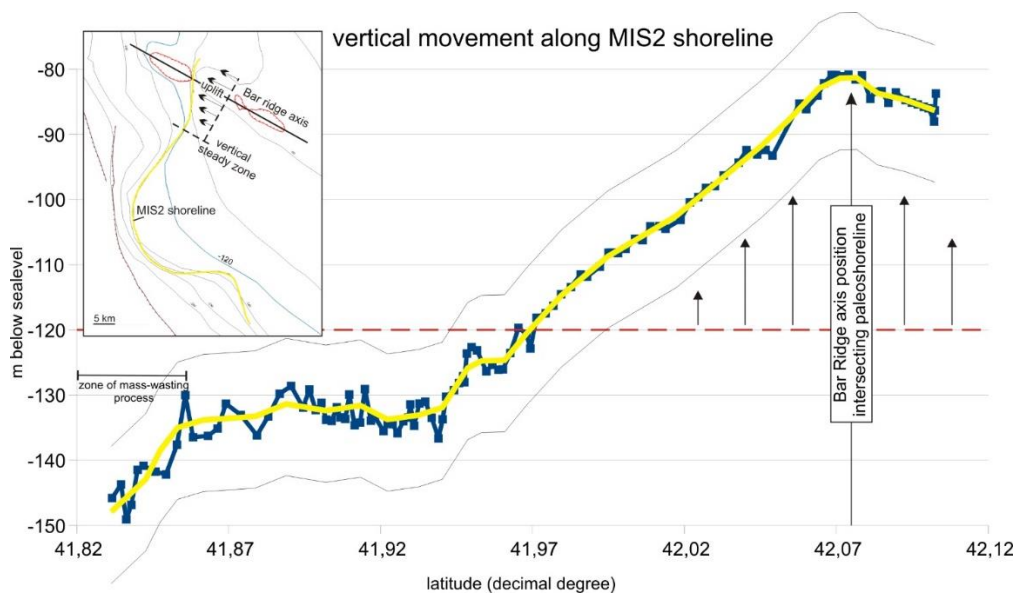


Figure 4.3 Vertical trend of the drowned lowstand delta from assumed as paleoshoreline during MIS2. We note the uplift in correspondence of Bar Ridge area. From Del Bianco et al. (2014 – § 3.3, this manuscript)

Because the minimum eustatic level reached during the LGM was -120 m (Lea et al., 2002), we could thus assume that this sector of the MACM shelf was uplifted by 40 ± 25 m during the last ~20 kyr (Rohling, 1998), that corresponds to 2 ± 1.25 mm/yr. This relatively high uplift averaged is probably related to the Late Quaternary deformation of the seismically active Bar anticline. In fact, if we consider the surface projection of the slip models proposed by Benetatos and Kiratzi (2006) for the recent most two large magnitude events in the area, we note that maximum slip is coincident, or immediately landward, with the Bar Ridge, and show the same NW-SE orientation (Fig. 4.4). These large magnitude (Mw 7.1 and Mw 6.2) earthquakes occurred by April 15, 1979 offshore Montenegro, between Bar and Ulcinj (Fig. 2.6 - §2.1); the main shock of this event occurred along a shallow (7 km deep), low angle (14°) thrust fault, parallel to the coastline and dipping toward NE (Benetatos and Kiratzi, 2006).

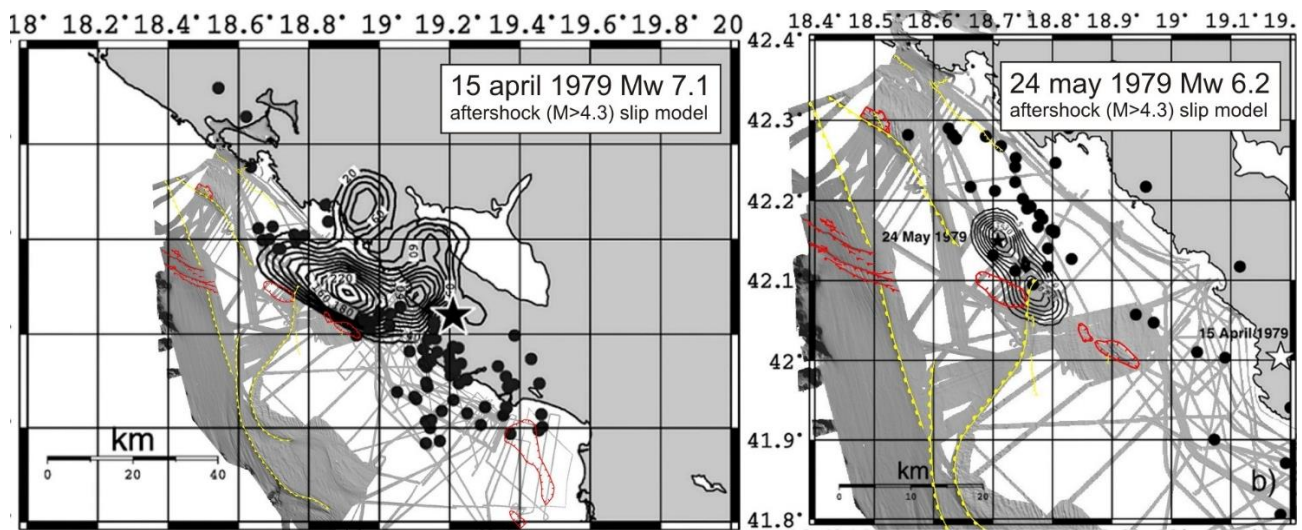


Figure 4.4 Surface projection of slip models for 15 april 1979 (left) and 24 may 1979 (right) earthquakes over morphobathymetric map of the MACM presented in this work. $M > 4.3$ aftershocks (black dots) are also indicated. Modified from Benetatos and Kiratzi (2006).

4.2 Conclusions

During this work the physiography of the MACM was studied through combined interpretation of morpho-bathymetric map and seismic reflection data, as well as the analysis of seafloor sediment samples. The conclusion of the first, more descriptive part of the work, is that MACM is a shelf-slope system characterized by: an inner and an outer shelves, variable in width and characterized by the presence of two tectonically controlled ridges (Bar and Kotor); the presence of a drowned lobate mid-shelf delta formed during the latest phase of sea level fall; an upper continental slope affected by gravity-driven instability and extensional faultings oriented consistently with regional tectonics. The morphology of the seafloor was also studied in detail to determine the presence of relict and active bedforms diagnostic of sedimentary processes. Most part of the continental shelf and upper slope is characterized by the presence of morphologic units that formed during the LGM or the subsequent sea level rise, and are not in equilibrium with sedimentary processes acting at their present depths. The only exception is constituted by an area where elongated ridges created during the latest transgressive/high-stand stage are reworked by bottom-hugging currents.

The second conclusion is that the main factor controlling the MACM physiography is the effect of the 100 kyr scale cyclicity of sea level changes that contributes to build a relatively thick stack of wedge-shaped deposits at the shelf edge preserved by subsidence. This pre-Holocene record

encompasses four major seismic sequences marked by forced regression units deposited during Marine Isotope Stages (MIS) 10, 8, 6 and 2. Position and assumed ages of buried shorelines of these lowstand phases indicate that the outer shelf subsidence rate was about 1.2 mm/yr during the last ~350 kyr. Depositional patterns are also controlled by tectonics, that led to the formation of thrust-top or piggyback basins and the Kotor and Bar ridges acting as by-pass or traps for sediments supplied by local inputs. Identification of the LGM paleoshoreline suggests that the Bar Ridge, in the inner shelf, uplifted by several tens of meters during the last ~20 kyr. Present-day sediment accumulation along the margin is confined to narrow basin elongated along shore, reaching a maximum thickness < 35 m, at depositional rates of 0.8 to 1.5 mm/yr for the last ~150 yr.

Furthermore, a preliminary analysis of geochemical proxies extended to a broader dataset of seafloor samples reveals that the two inner shelf depocenters are not affected by post depositional processes (such as early diagenesis, mixing or bioturbation), and confirms that they are characterized by accumulation rates ranging from 0.8 to 2 mm/yr. Types of sediment presently filling these basins are mainly clayey or silty-clayey. Between these two areas, a non depositional “by-pass” sector displays a lack of modern sedimentation.

This thesis work should be considered a first step towards the knowledge of the recent (Late Quaternary) geological evolution of MACM that deserves further data acquisition and analysis. A more comprehensive study of relationships between tectonics and sedimentation, would gather benefits by acquisition of more penetrative high-resolution seismic reflection images, and longer sediment cores.

As a final remark, I should acknowledge that, due to the lacking of time and the necessity of focusing the thesis work, some interesting scientific topics raised by this work were only introduced, and deserve further analysis. These include the reconstruction of tectonic deformation, and their relationships with co-seismic and post-seismic slip, at least to that related with the most recent large magnitude earthquakes. Another important topic to be analyzed would be the role played by fluids (impressive fluid escape structures were observed along the margin), either in the earthquake cycle, and in the shallow manifestations, such as mud and sand volcanoes, that were observed along the MACM shelf.

Other more specific subjects that will be surely investigated in the future are listed below:

1. The barrier-lagoon systems recognized in shallow seismo-stratigraphic sequences immediately landward of the Kotor and Bar ridges, whose evolution is sensitive to the change of environment of dynamic and sedimentary condition during the LGM;
2. The submerged depositional terraces recognized on the top of the Bar Ridge, which can be

useful to constraint, the vertical tectonic motions of the shelf. It can be important for paleo-sismological reconstruction in this seismically active region;

3. The incised valley discovered above the submerged delta-plain, probably related to the development of the paleodelta during the LGM, whose study might improve the reconstruction of the paleo drainage-systems; in agreement with Zaitlin et al. (1994), such features are key-areas for sedimentary record of sea level variations on continental margins;
4. The Bokakotorska Bay area morphologies, linked to the karst environment of the Dinaric range; in this area, submarine siphons, springs and resurgences were recognized. According to Fleury et al. (2007), the study of such feature could be important to determine the geological and hydrogeological setting strongly related to tectonics and to past (and future) climate and sea level fluctuations.

There were certainly many other scientific aspects which have emerged for the readers of this manuscript, and will have more or less caught their interest according to their inclinations, personal tastes or driven simply by curiosity. Moreover, the curiosity is the basis of all human achievement and all knowledge.

Quoting Albert Einstein:

“It is a miracle that curiosity survives formal education.”

References

- Benetatos C. and Kiratzi A., 2006. – Finite-fault slip models for the 15 April 1979 (Mw 7.1) Montenegro earthquake and its strongest aftershock of 24 May 1979 (Mw 6.2). - *Tectonophysics* 421, 129-143.
- Bossuet, G., Ruffaldi, P., Magny, M., Richard, H., Mouthon, J., 1996. Dynamique et approche quantitative des remplissages fini-et postwürmiens du bassin lacustre de Cerin (Jura, France). *Bullettin de la Société Géologique de France*. 167 (4), 483–494.
- Cattaneo, A., Correggiari, A., Langone, L., Trincardi, F., 2003a. The late-Holocene Gargano subaqueous delta, Adriatic shelf: sediment pathways and supply fluctuations. *Marine Geology* 193, 61–91.
- Cattaneo, A., Correggiari, A., Penitenti, D., Trincardi, F., Marsset, B., 2003b. Morphobathymetry of small-scale mud reliefs on the Adriatic shelf, in: Locat, J., Mienert, J. (Eds.), *Submarine Mass Movements and their Consequences*. Kluwer, Amsterdam, pp. 401–408.
- Cattaneo, A., Trincardi, F., Asioli, A., & Correggiari, A., 2007. The Western Adriatic shelf clinoform: energy-limited bottomset. *Continental Shelf Research*, 27(3-4), 506–525. doi:10.1016/j.csr.2006.11.013
- De Alteriis, G., 1995. Different foreland basins in Italy: examples from the central and southern Adriatic Sea. *Tectonophysics*, 252, 349-373.
- Fleury, P; Bakalowicz, M; de Marsily, G., 2007. Submarine springs and coastal karst aquifers: A review. *JOURNAL OF HYDROLOGY* Volume: 339 Issue: 1-2 Pages: 79-92 DOI:10.1016/j.jhydrol.2007.03.009
- Frank, G., Kriz, J., Vlastic, B., 1983. Results and directions in hydrocarbon exploration of the Adriatic offshore. *Nafta*, 34, 387-396.
- Galloway, W. E., 1975. Process framework for describing the morphologic and stratigraphic evolution of deltaic depositional systems. In Broussard, M. L. (Ed.), *Houston Geological Society, Deltas*, pp.87–98.
- Lea, D. W., Martin, P. A., Pak, D. K., & Spero, H. J. (2002). Reconstructing a 350 ky history of sea level using planktonic Mg / Ca and oxygen isotope records from a Cocos Ridge core, 21, 283–293.
- Marini, M., Grilli, F., Guarnieri, A., Jones, B. H., Klajic, Z., Pinardi, N., Sanxhaku, M., 2010. Is the southeastern Adriatic Sea coastal strip an eutrophic area? *Estuarine, Coastal and Shelf Science*, 88(3), 395–406. doi:10.1016/j.ecss.2010.04.020
- Maselli, V., Trincardi, F., Cattaneo, a., Ridente, D., & Asioli, A., 2010. Subsidence pattern in the central Adriatic and its influence on sediment architecture during the last 400 kyr. *Journal of Geophysical Research*, 115(B12), B12106. doi:10.1029/2010JB007687
- Moretti, I., Royden, L., 1988. Deflection, gravity anomalies and tectonics of doubly subducted continental lithosphere: Adriatic and Ionian Seas. *Tectonics*, 7, 875-893.
- Milliman, J., Syvitski, J.P.M., 1992. Geomorphic/tectonic control of sediment discharge to the ocean: the importance of small mountaneous rivers. - *The Journal of Geology* 100, 525-544

- Ori, G.G., Friend, P.F., 1984. Sedimentary basins, formed and carried piggyback on active thrust sheets. *Geology*, 12 (9), 475-478.
- Poulain, P.M., 2001. Adriatic Sea surface circulation as derived from drifter data between 1990 and 1999. *Journal of Marine Systems*, 29, 3-32.
- Ricci Lucchi F., 1986. Oligocene to Recent foreland basins Northern Apennines. I.A.S., Special Public. No.8, Blackwell, 105-139
- Royden L., Patacca E. and Scandone P. 1987. - Segmentation and configuration of subducted lithosphere in Italy: An important control on thrust-belt and foredeep-basin evolution. *Geology*, 15, 714-717
- Rohling, E.J., Fenton, M., Jorissen, F.J., Bertrand, P., Ganssen, G., Caulet, J.P., 1998. Magnitudes of sea-level lowstands of the past 500,000 years. *Nature* 394, 162–165
- Steckler, M. S., 1999. High-resolution sequence stratigraphic modeling: 1. The interplay of sedimentation, erosion and subsidence, in *Numerical Experiments*, in: *Stratigraphy: Recent Advances in Stratigraphic and Computer Simulations*, edited by J. Harbaugh et al., Mem. 62, pp. 139–149, Soc. of Econ. Paleontol. and Mineral., Tulsa, Okla.
- Vail, P.R., Mitchum, R.M. and Thompson, S. III, 1977. Seismic stratigraphy and global changes of sea level, Part 3: relative changes of sea level from coastal onlap. In: C.W. Payton (Ed.), *Seismic Stratigraphic Applications to Hydrocarbon Exploration*. American Association of Petroleum Geologists *Memories*, 26, 63- 97.
- Zaitlin, B.A., Dalrymple, R.W. and Boyd, R., 1994. The stratigraphic organisation of incised valley systems associated with relative sea-level change. In: R.W. Dalrymple, R.J. Boyd and B.A. Zaitlin., Eds., *Incised valley systems: Origin and sedimentary Sequences*, - SEPM Spec. Pub. 51, 45-60

APPENDIX

A.1 Abstract published* on CIESM

*Del Bianco F. et al. 2010 - The Montenegro-Northern Albanian Continental Margin: Morphotectonic Features In A Seismically Active Region. - Rapp. Comm. Int. Mer Medit. Vol. 39 - page 20.

THE MONTENEGRO-NORTHERN ALBANIAN CONTINENTAL MARGIN: MORPHOTECTONIC FEATURES IN A SEISMICALLY ACTIVE REGION.

F. Del Bianco ^{1*}, L. Gasperini ¹, G. Bortoluzzi ¹, F. Giglio ¹, F. D'Oriano ¹, A. Polonia ¹, M. Ravaioli ¹, Z. Kljajic ² and A. Bulatovic ²
¹ CNR Ismar Bologna, 40129, Italy - fabrizio.delbianco@bo.ismar.cnr.it
² Institute of Marine Biology, 85 330, Kotor, Montenegro

Abstract

During four cruises within the ADRICOSM-STAR project high-resolution CHIRP profiles, morphobathymetric data and bottom samples were collected along the seismically active Montenegro and northern Albanian margin. Preliminary analysis of our data suggest that seismogenic structures are marked at the seafloor by morphological features due to deformation of the sediments and possibly to fluid and gas escape.

Keywords: Adriatic Sea, Continental Margin, Geophysics, Tectonics, Bathymetry

The Montenegro coastal region is characterized by intense seismicity and by the occurrence of large historical earthquakes, such as the Great Dubrovnik Earthquake (M=7, 6 April 1667), the June 13, 1593 event (M=6.5), with epicenter located close to Kotor, and the June 1, 1905 event, with epicentre near Skadar. The last large earthquake affecting the region is the M=7.1 (15 April 1979) whose epicentre was located fifteen kilometers from the Montenegro coast between Bar and Ulcinj (Fig.1). This last event stressed the importance of studying the Montenegro offshore to localize seismogenic features and trying to understand their behaviour in time. The Montenegro offshore and coastal area has been included in the northern segment of the Ionian-Adriatic coastal earthquake belt ([1]). This area constitutes the eastern boundary of the Adria microplate, a block of continental lithosphere presently colliding with the Dinarides chain since the late Miocene ([2], [3]); it constitutes the most external sector of the chain. Along the Adriatic coast of Montenegro, the 200 km-long plate boundary consists of a WNW trending thrust belt (Fig. 1), cut by NS and rarely ENE oriented strike-slip faults which laterally segment the major thrust front ([1], [2], [4]).

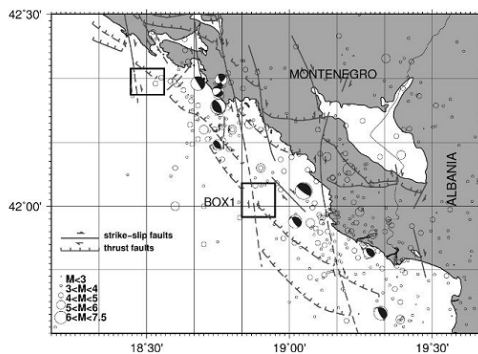


Fig. 1. Structural map of the Montenegro margin ([4] modified). Circles indicate local seismicity and main historical events ([5]). Boxes indicate areas where morphological features possibly related to tectonic deformation were observed

Despite its geological interest and the high seismic hazard, the Montenegro offshore has been poorly investigated in the past, if we exclude extensive multichannel seismic reflection surveys carried out by oil companies, not available to the wider scientific community, and few seismic lines collected during the '90 in the Albania offshore ([3]). During 4 oceanographic cruises, carried out from May 2008 to July 2009 with the Italian CNR research oceanographic ships Urania and Mariagrazia in the frame of ADRICOSM-STAR project (ADRIatic sea integrated COaStal and river basins Management system: Montenegro coaStal ARea and Bojana river catchment), we collected a set of marine geological and geophysical data offshore Montenegro and northern Albania. Our dataset includes high-resolution seismic reflection profiles and multibeam morphobathymetric data, as well as several sediment samples, gravity cores, grabs, and box corers collected in key areas, selected through interpretation of geophysical data. The sediment accumulation in the coastal area is variable along the margin, probably due to the effect of strong alongshore bottom currents. First results from combined interpretation of seismic profiles and sediment samples suggest that wide areas in the shelf are presently starved, and LGM (Last Glacial Maximum) sedimentary features,

such as dunes and sand ridges are present on the seafloor. These features are mostly observed in the bathymetric range 60-120 m and are mainly made of relict coarse sandy material that seems to be cleaned by bottom current reworking.

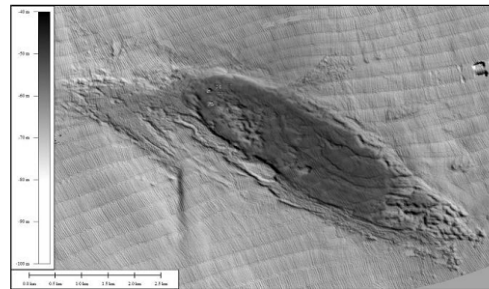


Fig. 2. Morphobathymetric image of compressive deformation along the margin. See figure 1 (box 1) for location

Typical geo-morphological and structural features observed along the margin through integrated analysis of seismic reflection profiles and high resolution bathymetric maps are: 1) hundreds-meter scale bathymetric swells, possibly interpreted as mud volcanoes; 2) elongated, heavily deformed ridges, marking compressive deformation fronts (Fig. 2); 3) rectilinear scarps offsetting the seafloor. All of these features appear aligned with regional tectonic boundaries, described by several authors ([1], [2], [4]) and are thus probably genetically controlled by deep-seated faults. Moreover, a correlation between these features and local seismicity (moderate to large historical earthquakes and recent events) is also observed ([5]). Preliminary analysis of our data suggest that seismogenic structures along the margin, such as thrusts and strike-slip faults, are marked at the seafloor by morphological features due to deformation of the sediments and possibly to fluid and gas escape. This very preliminary results need to be confirmed by further analysis and collection of new data along the margin.

References

- 1 - Alij S., Adams J, Halchuk S., Sulstarova E., Peci V., Muco B. 2004. Probabilistic seismic hazard maps for Albania. 13th World Conference on Earthquake Engineering, Vancouver, B.C., Canada, August 1-6, 2004, Paper No. 2469.
- 2 - Alij S. 2008. The Albanian Orogen: convergence Zone between Eurasia and the Adria microplate. In: N.Pinter, G.Gyula, S.Stein and D.Medak (eds.), The Adria Microplate: GPS Geodesy, Tectonics and Hazards, NATO Science Series, IV, Earth and Environmental Sc., Vol.61, Springer.
- 3 - Argnani A., Bonazzi C., Evangelisti D., Favali P., Frugoni F., Gasperini M., Ligi M., Marani M., Mele G. 1996. Tettonica dell'Adriatico meridionale. *Mem. Soc. Geol. It.*, 51, 227-237.
- 4 - Oluic M., Cvijanovic D., Prelogovic E. 1982. Some new data on the tectonic activity in the Montenegro coastal region (Yugoslavia) based on the landsat imagery. *Acta Astronautica* v 9, No.1, 27-33.
- 5 - Pondrelli S., Salimbeni S., Ekstrom G., Morelli A., Gasperini P., Vannucci G., 2006. The Italian CMT dataset from 1977 to the present. *Phys. Earth Planet. Int.* doi: 10.1016/j.pepi.2006.07.008,159/3-4, pp. 286-303.

A.2 Some concepts about physics of sound in the water media

The development of Marine Geology as a discipline followed the progresses of the marine geophysical (and to a lesser extent, geological) techniques carried out for military purpose during and after the second world war. These progresses included the study of sound propagation in the oceans and the mechanical principles that have allowed us to perform sediment sampling in the deep water. The single class of instruments that better represents the progress of these techniques is that of Multibeam echosounders, that could provide high-resolution morphobathymetrical images of the seafloor at different scales, from the continental margins to the full oceanic depths of thousands of meters. On the other hand, among the instruments able to image the very upper part of the sedimentary sequence using the seismic reflection method, it has to be mentioned the subbottom profiler based on the chirp technology. The combined use of these instruments allows to obtain information about geological processes that shape the continental margins, including tectonic deformation, sediment supply, accumulation and reworking, as well as the effect of eustatic changes.

Sound propagates into the water by a moving series of pressure fronts parallel to the direction of propagation called compressional waves (P-waves) that travel at a given speed that depends on chemical/physical status of the water column. The shear waves (S-waves) do not propagate in water. A series of advancing pressure fronts, representing a travelling sound wave, as shown in Fig 2.1, that propagate as a spherical front. The size of pressure oscillations is the amplitude of the travelling wave, while the time interval between subsequent peaks is the period.

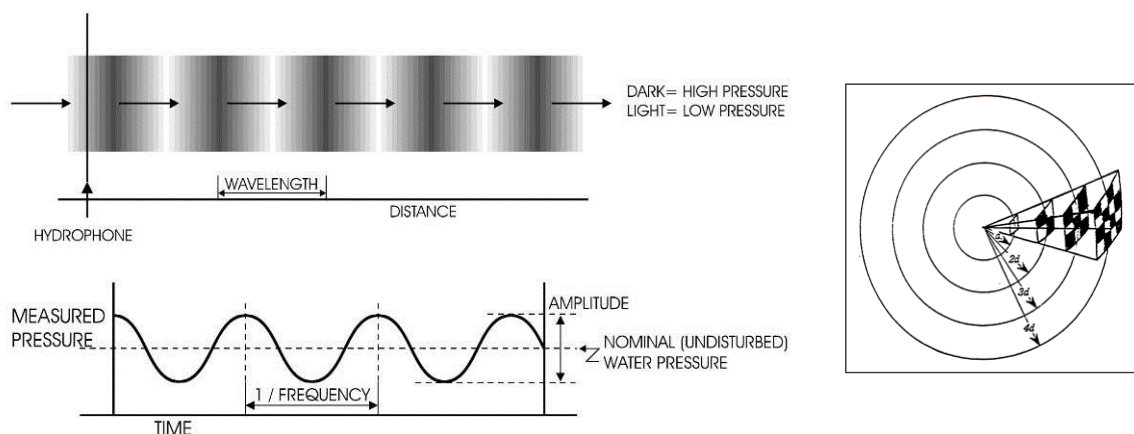


Fig. 2.1. Schematic examples of the propagation of pressure front. From SeaBeam (1999).

The waves moving into the water following a spherical propagation are subjected to the transfer of pressure differences between molecules of water; the effects are:

- 1) geometrical spreading: Loss of energy due to expansion of a spherical waves, it is proportional to $1/r^2$;
- 2) friction (or dissipation) is a loss of acoustic energy into heat, when passing through an acoustic medium;
- 3) attenuation for each cycle of the wave, is the resulting of the decay of sound intensity for different frequency. Generally in the same distance traveled by an acoustic waves, high frequency sound is attenuated rapidly;

When a sound pulse travelling in a given medium encounters another medium with different acoustic properties some fraction of the carried energy is reflected off the surface in a direction that depends on the angle of incidence and some fraction propagates into the bottom with a different angle (Fig 2.2). This last is called refraction phenomenon.

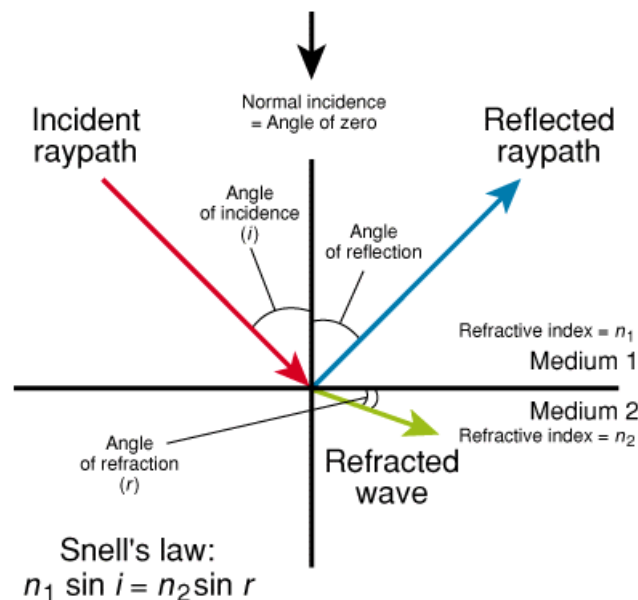


Fig. 2.2. From web glossary of Schlumberger.

The physical difference of the medium can be described by a parameter called acoustic impedance that is a material property:

$$Z_0 = \rho \cdot V$$

Where:

Z_0 is the characteristic acoustic impedance ($[M \cdot L^{-2} \cdot T^{-1}]$; $N \cdot s/m^3$ or $Pa \cdot s/m$)

ρ is the density of the medium ($[M \cdot L^{-3}]$; kg/m^3), and

V is the longitudinal wave speed or sound speed ($[L \cdot T^{-1}]$; m/s)

The amplitude of the reflected wave is predicted by multiplying the amplitude of the incident wave

by the seismic reflection coefficient R , determined by the impedance contrast between the two materials. For a wave that hits a boundary at normal incidence (head-on), the expression for the reflection coefficient is simply

$$R = (Z_1 - Z_0) / (Z_1 + Z_0)$$

where Z_0 and Z_1 are the impedance of the first and second medium, respectively. This parameter determines how much of the energy was reflected and refracted by acoustic discontinuity.

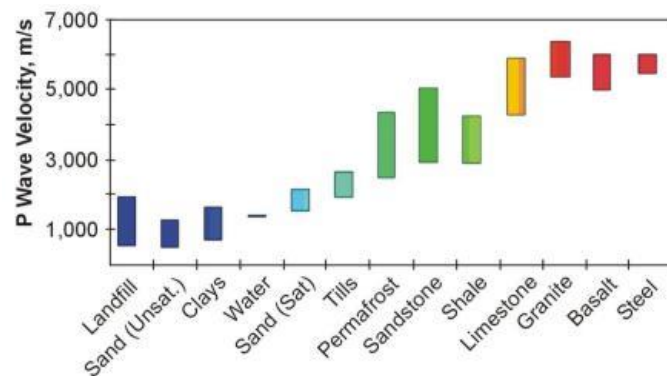


Fig. 2.3. P wave velocity ranges for common materials. From Wightman et al. (2003).

Marine seismic reflection systems consist of a source of acoustic energy and a receiving system, that allows for the digital recording of the signal. These generate a kind of pulse of sound and then listening for the echo of the pulse from the bottom or others interface with different acoustic impedance that generate a reflection.

The time taken by the signal generated at the source to propagate into the medium, reach an acoustic impedance contrast (a reflector) e come back to the receiver at the surface is called the travel time. If the seismic wave velocity of each layer of water, rock or sediment is known, the travel time could be converted into depth to the reflector. For a normal incident seismic wave, the travel time t from the surface to the reflector and back is called the two-way traveltime (TWT) and is given by the formula:

$$t = 2d/V$$

where d is the depth of the reflector and V is the wave velocity in the rock.

The same physical principle that constitutes the basis of seismic reflection theory is used for several purpose in a marine geophysical survey: the characteristic amplitude (energy) and frequency content of the generated wavelet is employed for different target to investigate. In general, depending of the frequency content of the seismic wave, we observe a trade-off between resolution (high-frequencies)

and penetration inside the substratum. Table 2.1 summarize this occurrence for several seismic sources and different targets.

TECHNICS	USED SOURCE	RECEIVER	FREQUENCY	RESOLUTION	PENETRATION	LIABLE TO NOISE
Multichannel seismic reflection	air gun - water gun	hydrophone or array of hydrophone (streamer)	20 -1500 Hz	tens to hundred of meters	several kilometers	high
single channel seismic reflection	sparker - boomer- subbottom - chirp sb	hydrophone	100 - 7000 Hz	meters to decimeters	hundred of meters	medium
single beam echosounders	piezo electric transducers	< the same	100 - 300 kHz	tens to several centimeters	several centimeters	low
multibeam echosounders	array of piezo electric transducers	< the same	100 - 500 kHz	tens to several centimeters	several centimeters	low

Table 2.1

In the next chapters I will describe the multibeam echosounder and single channel chirp sub-bottom investigations that was used to collect data, used in this work.

A.3 Multibeam bathymetry

Single Beam echosounders are the instruments commonly used to measure the depth of submerged areas, either in fresh and marine waters. They consist of an time-gated ultrasonic pulse generator , typically in a range between 10 and 100 kHz, and a receiver, generally based on the same emitting transducer used to detect the reflection from the water-bottom interface and measuring the time interval between emission and detection, which is proportional to the depth. The main assumption is that the emitter/receiver and the insonificated area of sea floor are perfectly on the vertical and the conical beam of emission is narrow enough ($\sim 10^\circ$) to neglect lateral reflections/diffractions of the signal. Acquisition of high-resolution morphobathymetric maps using single-beam echo sounders suffers large amount of time needed to perform survey in relatively wide areas; for this reason, the technical research in this field has been devoted in improve the number of bathymetric measures along relatively wide sectors of seafloor. Starting from 1964 were developed for the US Navy, a technique for multiple narrow-beam depth sounding, initially called Sonar Array Sounding Systems (SASS), employed two separate sonar arrays oriented orthogonal respectively

transmitter and receiver; an arrangement called a Mills Cross Array. A multibeam sonar is an instrument that use this technique with the aid of the modern digital signal processing microprocessor (DSPuP), that allows for an accurate detection of the signal backscattered from the seafloor .

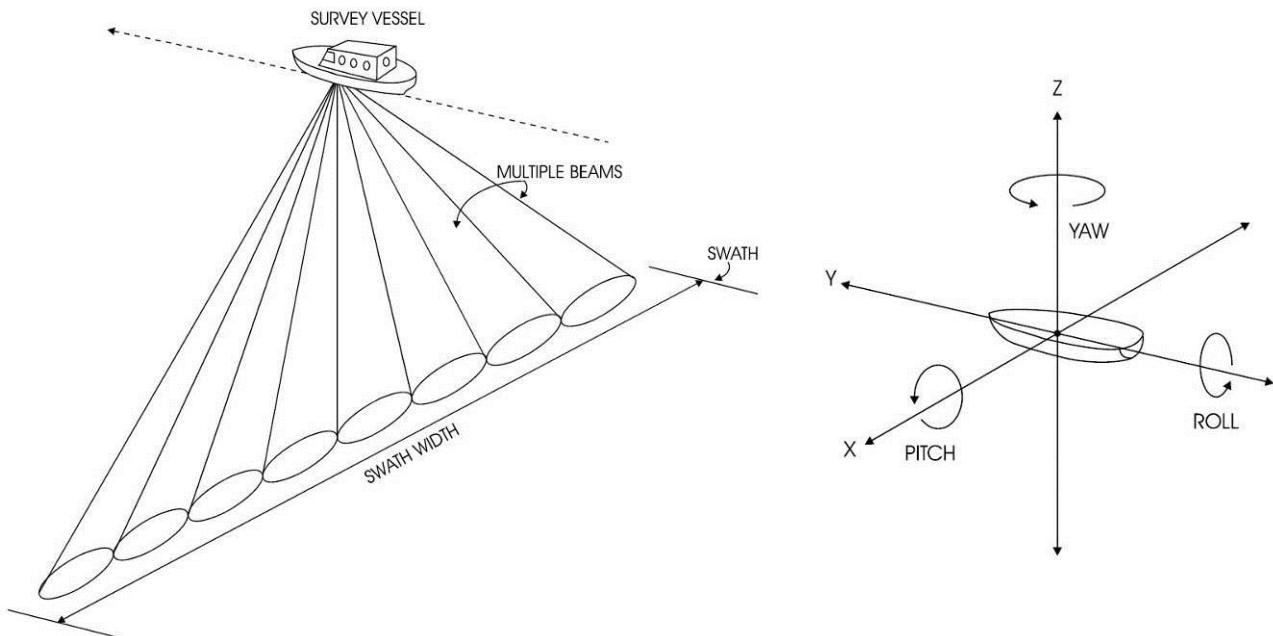


Fig. 2.4 schematic representation of multibeam coverage during a survey. On the right different movement of vessel. From Seabeam (1999).

The multibeam solution is based on the principle that the beams generations is arranged such that they are able to map a contiguous strip of points in a direction perpendicular to the path of the survey vessel, called swath width. The theory behind this system is complex but can be summarize in the following key words:

- 1) projector arrays: a groups of isotropic sources that can be used to transmit non-isotropic waves or sound waves whose amplitude varies as a function of angular location, allowing projected pulse to have a degree of directivity and to generate narrow beams of sound. This is possible for the constructive and destructive interference phenomenon between two neighbouring projectors emitting the same frequency;
- 2) hydrophone arrays: follows the same principles of projector arrays;
- 3) beam steering: is the possibility to alter an hydrophone array to receive preferentially from any of a number of directions, using a delay in the time of receipt;
- 4) motion compensation (beam compensation): consists in a real-time rectify of the vessel movements such as pitch, roll and yaw, that are respectively the rotation about the x, y and z

direction of the vessel (Fig 2.4), using an instrument called MRU (Motion Reference Unit) consisting of a series of very sensitive accelerometers.

A multibeam echosounder allows to produce high-resolution coverage of wide swaths of the ocean bottom in far less ship time.

Another important aspect is related to the exact knowledge of the speed of sound in the water column, because we need to convert the reflection travel times into depth with extreme accuracy, to avoid propagation of errors that in lateral beams can be significant.

A.3.1 Sound propagation in the water

The speed of sound in the water is an increasing function of temperature, salinity and pressure, the latter being a linear function of depth. An example of a simple expression for this dependence, modified from Mackenzie (1981) and Coppens (1981), is the following:

$$c = 1449.2 + 4.6T - 0.055T^2 + 0.00029T^3 + (1.34 - 0.010T)(S - 35) + 0.016Z$$

where

c is the sound speed in m/s

T is the temperature in °C

S is the salinity in part per thousand (ppt)

Z is the depth

This equation is valid for $0 < T < 35^\circ\text{C}$, $0 < S < 40\text{ppt}$, and $0 < Z < 1000\text{m}$

The largest variation in the speed of sound in the water occurs with changes in depth. Obviously the pressure increases with depth causing a uniform increase of about +1.6/1.7 m/s for every 100 m. Furthermore, the ambient temperature changes with depth. A plot of propagation speed (velocity) as a function of depth, is called the *sound velocity profile* (SVP), and is the fundamental tool for predicting how sound will travel (Fig. 2.5). Neglecting salinity, the SVP can be obtained from sampling the ambient temperature at various depths (the pressure contribution never varies). An inexpensive probe to do this is called an expendable bathythermograph (XBT). Another technique usually used on board of oceanographic ship is CTD probe that is a multiparameter sensor. It has a thermocouple to measure temperature, a pressure transducer to measure pressure and consequently depth, and to measure salinity, the CTD actually measures the electrical conductivity of the seawater,

which varies with the amount of dissolved salts. The Fig. 2.5 represent an example of SVP used to calibrate the beam-forming algorithms of on multibeam echosounders:

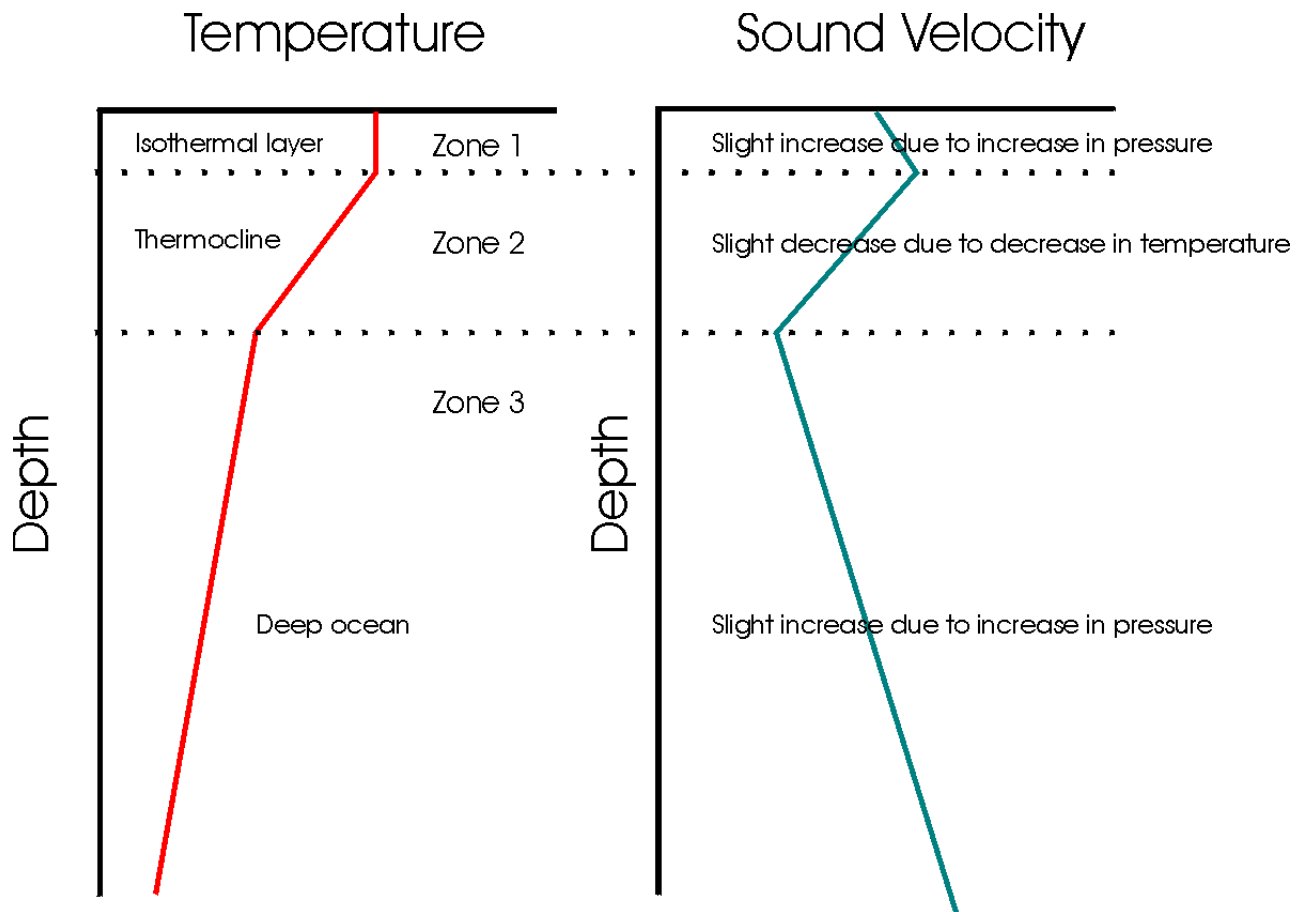


Fig.2.5.: Theoretical drawing of temperature and sound velocity in water column.

A.4 The “Chirp” sub-bottom profiler

Differently from echosounders that use acoustic energy reflected from the seafloor for depth estimates, the subbottom profilers, based on a similar technology of acoustic pulse generation provide a record of acoustic energy reflected by layers at different acoustic impedance beneath the seafloor. The frequencies used to achieve penetration range from some hundreds to thousands of Hz, with lower frequencies providing greater penetration. These instruments are based on the theory developed for seismic reflection exploration. The Sub-bottom profiler represents an instrument intermediate between an echosounder and a seismic source, such as high energy multi or single channel seismic reflection. It allows to perform high resolution imaging of the substratum but with limited penetration. The system is composed of two transducers, one transmitter and one receiver that in some case may coincides, and could be either hull-mounted or towed by the ship or the boat employed for the survey.

This instrument is suitable for a low reflectivity sea floor, constituted generally by unconsolidated sediment because rocky or high consolidated sediment can reflect all the incident pulse preventing its penetration. Usually, under a proper conditions the penetration can reach hundreds of meters.

The last generation of sub-bottom profiler employ a “chirp technology”, also used in telecommunication, that consist in generating acoustic pulse that are calibrated in amplitude and frequency-modulated. This is possible thanks to the modern DAC (digital – analogic converter) and to the real-time DSP (Digital signal processor), widely used today from all the hi-fi audio system.

The operating frequency of acoustic pulse is typically between 2 and 7 kHz, and allow a resolution of 0.5 to 1 meter about. In contrast to the old single frequency pulses (CW) profilers, the time resolution of chirp sonars can be much smaller than the pulse length, higher resolution is achieved using match filtering (cross correlation) of the raw data with the source pulse. Because the resolution does not depend linearly on the transmit duration (and in fact improves with increasing duration), sonars can generate long transmit pulses to achieve high signal levels and greater penetration.

This technology has the following advantages:

- 1) increasing of signal/noise ratio, using a well-known signature emitted;
- 2) higher vertical resolution (up to tens of centimeter) by optimizing the emission band;
- 3) increasing the energy of each sweep without decrease of vertical resolution;
- 4) repeatability of signal allow us to obtain several information by the signal such as reflectivity, use of phases for information about the physical proprieties of the sediment.

References:

Coppens A. B. 1981 - Simple equations for the speed of sound in Neptunian waters (1981) J. Acoust. Soc. Am. 69(3), pp 862-863

Mackenzie K. V. 1981 - Nine-term equation for the sound speed in the oceans - J. Acoust. Soc. Am. 70(3), pp 807-812

SeaBeam, 1999. Multibeam Sonar Theory of Operation – L-3 Communication SeaBeam Instruments, 1999

Schlumberger, 2014. The Online Oilfield Glossary. <http://www.glossary.oilfield.slb.com/>

Wightman, W. E., Jalinoos, F., Sirles, P., and Hanna, K. (2003). "Application of Geophysical Methods to Highway Related Problems." Federal Highway Administration, Central Federal Lands Highway Division, Lakewood, CO, Publication No. FHWA-IF-04-021, September 2003